Water Resources Research Center
Annual Technical Report
FY 2004

Introduction

The Maryland Water Resources Research Center (MWRRC) supports Maryland's water research and educational needs by funding high priority research projects and sponsoring educational programs and conferences on current water issues. Most of the funded research addresses problems associated with the Chesapeake Bay, a major economic asset in Maryland. The four projects funded in this annual reporting period concern the Bay. Research funding is directed toward supporting graduate students and young faculty members. We annually support at least one summer graduate student, depending on funding. During this reporting period we supported 6 students (two undergraduates and four graduate students) and two USGS interns.

We sponsor/cosponsor seminars and conferences on campus. The 2004 Water Resources conference addressed "Wastewater Treatment Plants and the Chesapeake Bay: Processes and Problems," which is described in the Technology Transfer section.

The Center acts as a focal point at the University on Maryland water issues with both Federal and State agencies. We solicit proposals through our two annual newsletters and an e-mail list of about 60 scientists on the College Park campus. We convene a panel of outside experts to review and rank the submitted proposals. In addition to the USGS requirements, the principle scientists are notified and are requested to submit a half page progress report in 6 months and a full page in one year. Progress on projects are monitored informally on a regular basis. The Director and Associate Director meet with State and Federal personnel on an annual basis, including the Maryland Department of Natural Resources, the Maryland Department of the Environment, and the U.S. Geological Survey, Maryland, Delaware, D.C. District Office.

Information Transfer Program

On October 22, 2004 a conference was held on Wastewater Treatment Plants and the Chesapeake Bay: Processes and Problems in the Margaret Brent Room,Stamp Student Union Building, University of Maryland, College Park, MD, 20742. It was cosponsored by the Maryland Water Resources Research Center and the Maryland Sea Grant College

Background Municipal wastewater treatment plants have been traditionally designed for the removal of particulate matter and biodegradable organic material. Recent research has shown that other compounds are being discharged in these wastewater effluents that raise environmental concern. Of major concern is the amount of nitrogen and phosphorus being discharged into the Chesapeake Bay. This half-day seminar discussed five current issues in point source discharges and current research on these issues.

Agenda and Speakers

8:30 - 8:40 Welcome + Opening Remarks. Allen P. Davis, Director

8:40 - 9:00 An Overview of Municipal Wastewater Treatment in Maryland. Eric Seagren, Civil and Environmental Engineering, University of Maryland

9:00 - 9:35 Endocrine Disruptors in Municipal Wastewater Discharges. Alba Torrents, Civil and Environmental Engineering, University of Maryland

9:35 - 10:10 A New Look at Dechlorination.. George Helz, Chemistry and Biochemistry, University of Maryland

10:10 - 10:25 Break

10:25 - 11:00 Nutrient Discharges. Clifford Randall, Civil and Environmental Engineering, Virginia Tech, Blacksburg, VA

11:00 - 11:35 Implications of the Flush Tax on Sewage Plants. Clyde Wilber, Greeley and Hansen, Upper Marlboro, MD 11:35 - 12:00 Wrap-up and Discussion

Here are some of the important points raised by the various speakers:

· There has been a profound failure to implement nitrogen removal at wastewater treatment plants during the life of the Chesapeake Bay Program,

· Flush tax revenues will not begin to cover the costs of upgrading the 66 major wastewater treatment plants in Maryland · One pound phosphorus can produce 111 pounds of algae biomass.

· Current dechlorination methods never completely destroy chloramines, which pose a threat to aquatic organisms.

· Dechlorination with thiosulfate or metallic iron could diminish the threat from chloramines.

· Metabolites of endocrine disrupters are being detected downstream from major wastewater treatment plants.

Research Program

Fate of Alkylphenolic Compounds in Wastewater Treatment

Basic Information

Title:	Fate of Alkylphenolic Compounds in Wastewater Treatment
Project Number:	2003MD28B
Start Date:	3/1/2003
End Date:	2/28/2005
Funding Source:	104B
Congressional District:	5th District of Maryland
Research Category:	None
Focus Category:	Toxic Substances, Waste Water, Water Quality
Descriptors:	None
Principal Investigators:	Alba Torrents, Clifford Paul Rice

Publication

1. Loyo-Rosales, J. E., Schmitz-Afonso, I., Rice, C. P., and Torrents, A. (2003), Analysis of octyl- and nonylphenol and their ethoxylates in water and sediments by liquid chromatography- tandem mass spectrometry. Anal. Chem. 75(18), 4811-4817.
2. Loyo-Rosales, J. E., Rosales-Rivera, G. C., Rice, C. P., Torrents, A. (2005), Linking laboratory experiences to the real world: The extraction of octylphenoxyacetic acid from water. J. Chem. Educ. In press.
3. Loyo-Rosales, J. E., Rice, C. P., and Torrents, A, Determination of octyl- and nonylphenol ethoxylates and carboxylates in environmental samples by isotope dilution and liquid chromatography/tandem mass spectrometry. Submitted to J. Chromatogr. A.

Final project report

March 2003 – February 2005

Fate of alkylphenolic compounds in wastewater treatment plants and a sub-estuary of the Chesapeake Bay

Alba Torrents
Department of Civil and Environmental Engineering
University of Maryland
College Park, MD 20742

Clifford P. Rice
Environmental Chemistry Laboratory
USDA/ARS
Beltsville, MD 20705

Ph.D. Student: Jorge E. Loyo-Rosales

Problem statement and research objectives

A series of recent studies have raised concerns about the presence of persistent organic pollutants in natural waters and the capability of wastewater treatment plants (WWTPs) to remove such chemicals from their effluents. The last decade has also seen an increased interest in pollutants suspected to interfere with the endocrine system, usually known as endocrine disrupters. The hormone-mimicking action of some of these chemicals and their harmful effects were first acknowledged in humans during the late 1940's, but their consequences on wildlife were only recognized decades later (Sonnenschein and Soto 1998). One such compound is 4-nonylphenol (NP), which was found to produce the same effects as estradiol in a line of cancer cells (Soto et al. 1991). NP is a precursor in the synthesis of the nonylphenol ethoxylates (NPnEOs), one class of alkylphenol ethoxylates (APnEOs, where n represents the number of ethoxylate units). APnEOs are nonionic surfactants that have been widely used in industrial processes and as detergents in both industrial and household applications for more than thirty years. After being used, the APnEOs are discharged into wastewater and are treated in WWTPs. During wastewater treatment, APnEOs are subject to microbial degradation processes that

produce different metabolites (NP among them), which are ultimately released into natural waters. Several of these degradation products have been shown to possess estrogenic properties and have been found in WWTP effluents at relatively high concentrations, especially in European systems (Bennie 1999). Although typical concentrations of NP and APnEOs in North American fresh waters are typically below the limit for the onset of endocrine-disruption endpoints, there is still concern for harmful effects in water bodies heavily impacted by WWTP effluent where their concentrations are higher, and for the occurrence of possible additive effects with other estrogenic compounds. Besides, their ubiquity in natural waters has been extensively documented in North America and Europe (Bennie 1999). A recent survey (Kolpin et al. 2002) of organic wastewater contaminants in 139 American streams found NP in 50% of the samples and, together with the nonylphenol mono- and diethoxylates (NP1EO and NP2EO respectively), was one of the pollutants found in the highest concentrations. The toxicity concerns, the ubiquitous presence in water bodies, and the high production volume of these compounds compelled the TSCA Interagency Testing Committee to add NP, 4-octylphenol (OP) and some of their ethoxylates to the US Environmental Protection Agency's Priority Testing List ("Interagency" 2000). The APnEOs have also been signaled as a current pollution issue in the Chesapeake Bay and were highlighted in a recent workshop on emerging contaminants organized by the Scientific and Technical Advisory Committee of the Chesapeake Bay Program on October 18, 2002 at Solomons Island. Currently, little information exists on the presence of these compounds in the State of Maryland or the Chesapeake Bay itself. A recent study by Robert Hale at the Virginia Institute of Marine Science (Hale et al 2000) analyzed water and sediment in 67 separate sites in the Commonwealth of Virginia, and found high levels of NP, not only in wastewater treatment plant effluents, but in other outfalls as well, including stormwater discharges. They observed that some of these outfalls discharge into relatively small streams, where NP could have greater effects on biota due to low dilution factors. Previous work by our group also illustrates the presence of NPnEOs and OPnEOs in WWTP effluents and receiving waters in the area (Loyo-Rosales et al. 2002).

The main objective of the present project is to model the distribution and fate of APnEOs and their degradates in a sub-estuary of the Chesapeake Bay and two WWTPs in the area, and to determine the operating parameters in the plants that control the concentrations of these endocrine-active substances in the estuary.

Results

During the first year of the project, our work was focused in the development of the required analytical methods, and the initial development of the theoretical model.

Analytical method development

The analytical methods described in this section have been submitted for publication in the Journal of Chromatography A. As part of this project, we expanded a method previously developed by our group (Loyo-Rosales et al 2003) for the extraction and quantification of nonylphenol (NP), octylphenol (OP) and their ethoxylated derivatives with up to 5 ethoxylate units (APnEO, n = 1 – 5) in water, to include NPnEO with n = 6 to 16. The main limitation was the lack of adequate analytical standards for these compounds because they are not available individually, only as uncharacterized technical mixtures. We attempted to use Marlophen 810 (Chemische Werke, Hüls, Germany), characterized by Ahel et al (2000), but we discovered that this mixture not only contains the NPnEO, but also the OPnEO, rendering it useless for quantitative purposes. Therefore, we used Surfonic N-95 (Schenectady International, Schenectady, NY), which was characterized by Huntsman Corporation (Austin, TX), and we were able to successfully quantify NPnEO (n = 6 – 16). Unfortunately, there are no characterized mixtures of the OPnEOs available; therefore, we are monitoring these analytes only qualitatively.

We also developed an analytical method to quantify the analytes of interest in particulate matter from water based on Soxhlet extraction with methanol and LC/MS/MS analysis. In order to obtain the particulate, one liter of water is vacuum-filtered with two pre-weighed glass microfibre filters (GF/A and GF/F, particle retention 1.6 and 0.7 μm respectively, Whatman Inc., Clifton, NJ; previously baked at 400°C for 4 h to eliminate any possible NP contamination) in a glass filter holder (Millipore Corporation, Billerica, MA). The filtrate is used for water analysis of the APnEO and the filters are allowed to dry overnight in a desiccator under vacuum. Once dry, the filters are weighed again to calculate particulate concentration and then spiked with a ^{13}C-labeled internal standard and Soxhlet-extracted with methanol for 8 hrs. The extracts are then evaporated to approximately 5 mL in a rotary evaporator, transferred to 15-mL glass centrifuge tubes and further reduced to 0.5 mL under a gentle nitrogen stream. After adding 0.5 mL of carbon-free deionized water, the extracts are filtered using an Acrodisc LC 13-mm syringe filter with a 0.2- μm PVDF membrane (Pall Gelman Laboratory, Ann Arbor, MI) into a 2-mL LC vial; the syringe and filter are rinsed with 0.5 mL of a 50:50 methanol/water mixture that is added to the extract. Finally, volume is adjusted to 1.5 mL and the extracts analyzed by LC/MS/MS. Recoveries for this extraction method vary for the different compounds and range from 73 to 100%.

Besides the APnEO, we are also interested in modeling other metabolites, such as their carboxylated derivatives. Due to their ionic nature, these cannot be extracted along with the APnEO, and a separate extraction method was developed for them. In this method, water samples are filtered as described above and part of the filtrate is acidified to pH 2 with HCl, and extracted with dichloromethane (DCM) in a separation funnel. DCM is evaporated and exchanged to approximately 5 mL methanol in a rotary evaporator and treated as above. Recovery was calculated for the three carboxylated metabolites (NP0EC, 93%; NP1EC, 93%; and OP0EC, 94%) for which standards are available. Additionally, we were able to identify carboxylated derivatives with higher molecular weight, and they were monitored qualitatively.

Analysis of the APnEOs in the Back River and WWTPs

During the second year of the project, we conducted a total of eight sampling trips to the WWTPs and the Back River. Blue Plains WWTP was sampled in July and August 2004, and in February and March 2005. Back River WWTP was sampled in September and October 2004, and in February and March 2005. Samples from the Back River were collected by the WWTP personnel in September and October 2004, and in March 2005. All the samples were analyzed for the following compounds: NP, OP, NPnEO (n=1-16), OPnEO (n=1-5) in the dissolved and particulate phases, and NP1EC, NP2EC, and OP1EC in the dissolved phase. Additionally, ancillary measurements were taken, such as temperature, pH, salinity, TOC, DOC, and TSS at every sampling event.

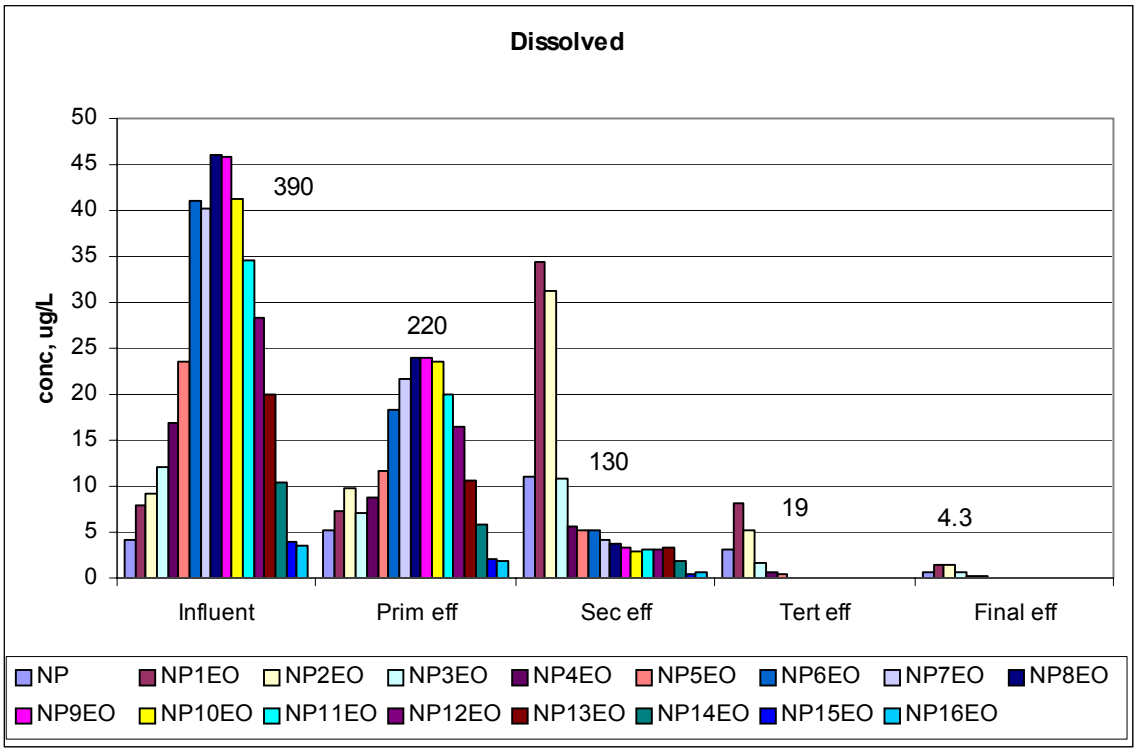

Figure 1. Nonylphenol ethoxylate concentrations in Blue Plains WWTP in the dissolved phase. The numbers above the bars indicate the total concentration (µg/L) of NPnEOs (n=0-16) in each treatment stage.

Although all the samples have been processed, we are still analyzing the data. Figures 1 to 3 are an example of the results obtained for Blue Plains WWTP during the first sampling event in July 2004. Figure 1 shows the concentrations of dissolved NPnEOs (n=0-16) along the different treatment stages. Total dissolved NPnEO (n=0-16) concentration was reduced by approximately 99%, from 390 µg/L in the raw wastewater to 4 µg/L in the final effluent. Moreover, the relative composition of the homologue mixture was enriched in the short-chain APnEOs as the treatment progressed. Such phenomenon is in agreement with previous observations that degradation of the APnEOs proceeds by a shortening of the ethoxylate chain (Ahel et al 1994), which results in the formation of the short-chain APnEOs. As a consequence, removal of NP, NP1EO and NP2EO was lower than total NPnEO removal at approximately 85%.

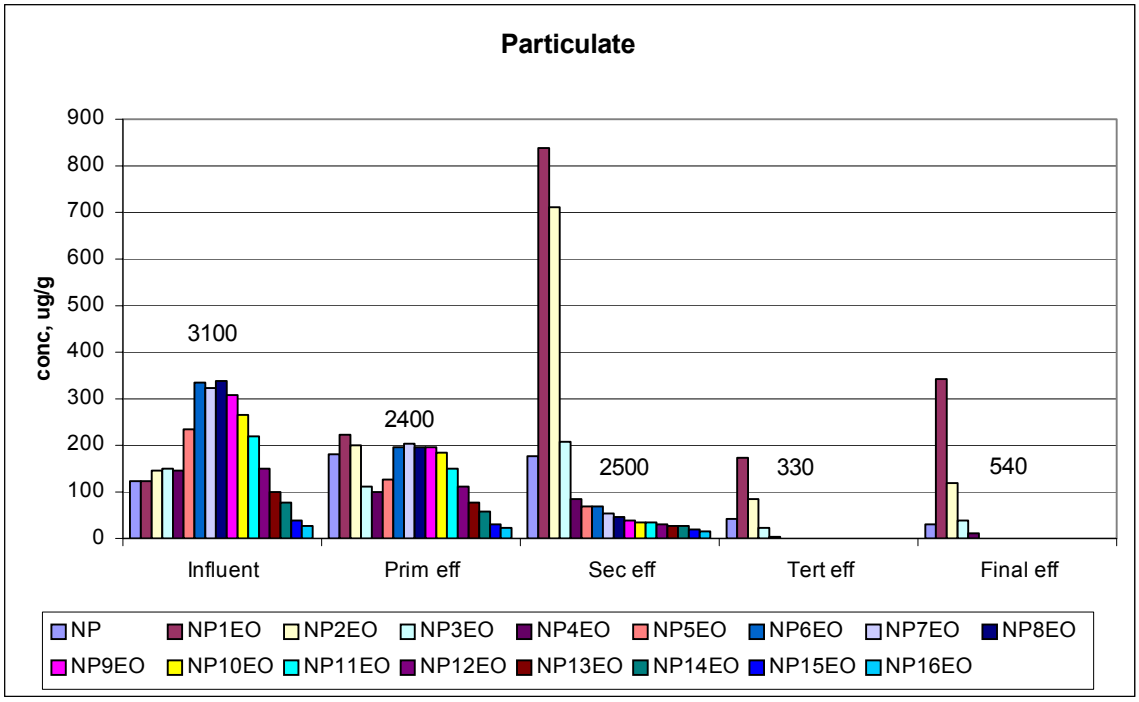

Figure 2. Nonylphenol ethoxylate concentrations in Blue Plains WWTP in particulate. The numbers above the bars indicate the total concentration (µg/g) of NPnEOs (n=0-16) in each treatment stage.

Due to their affinity for organic matter, the APnEOs tend to accumulate in suspended solids. The shorter the ethoxylate chain, the more hydrophobic the compound (Ahel and Giger 1993).

Therefore, the short-chain APnEOs have a greater affinity for the particulate, as Figure 2 exemplifies. The concentration profile of the homologues in the solid phase is similar to the profile of the dissolved compounds, except in that the short-chain APnEOs were present in higher proportions. In fact, in the raw wastewater and the primary influent, more than 60% of the NP, NP1EO and NP2EO occurred in the particulate phase. This situation, combined to a solids removal during the process of more than 99%, was reflected in a 93% removal of the three compounds when considering both the dissolved and solid phases, in contrast with 85% when considering the dissolved phase only.

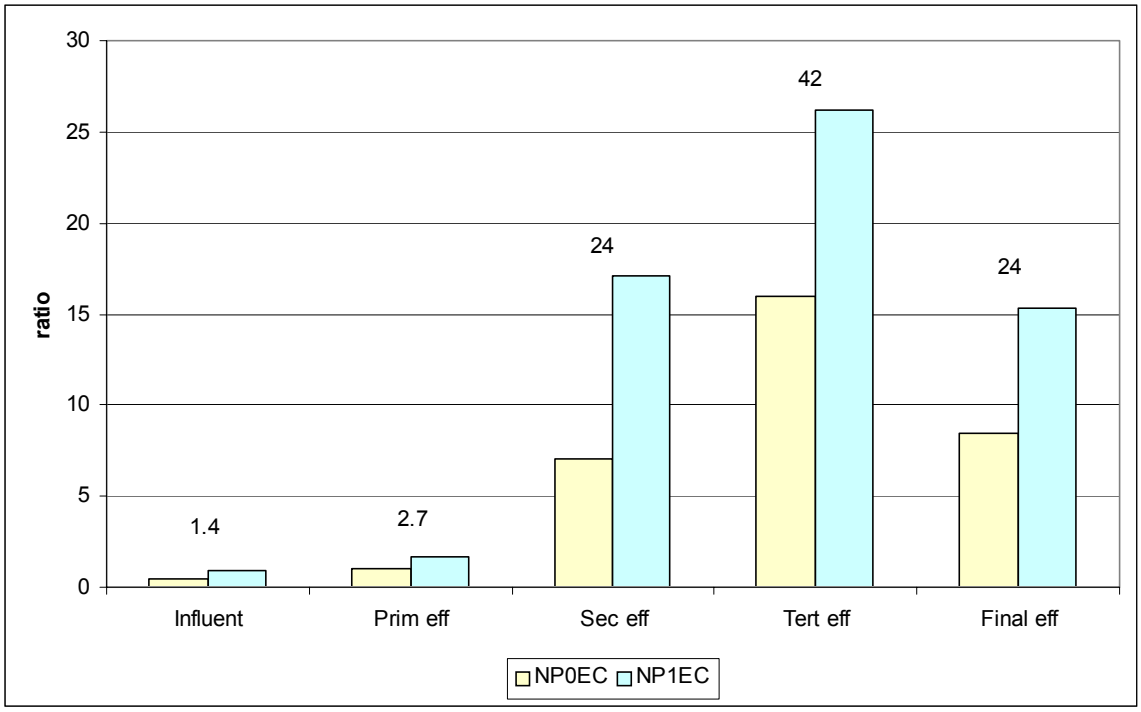

Figure 3. Nonylphenol carboxylate concentrations in Blue Plains WWTP. The numbers above the bars indicate the total concentration (μg/L) of NP0EC and NP1EC in each treatment stage.

In contrast to the APnEOs, the concentration of the APnECs increased along the treatment as can be appreciated in Figure 3. In the final effluent, the amount of APnECs present was approximately six times higher than the amount of ethoxylates, representing 85% of the compounds measured.

We are also investigating the use of the APnEOs as markers of anthropogenic contamination. Although this use has been proposed before, we believe that this concept can be extended beyond using these compounds as wastewater tracers only, but also as an indication of whether the wastewater was treated. As noted above, the initial APnEO mixture degrades in the WWTP to form short-chain APnEOs, NP, OP, and the carboxylated derivatives. In consequence, the ratio of the long-chain APnEOs to the degradation products (i.e. short-chain APnEOs, NP, OP, and APnECs) decreases as degradation occurs.

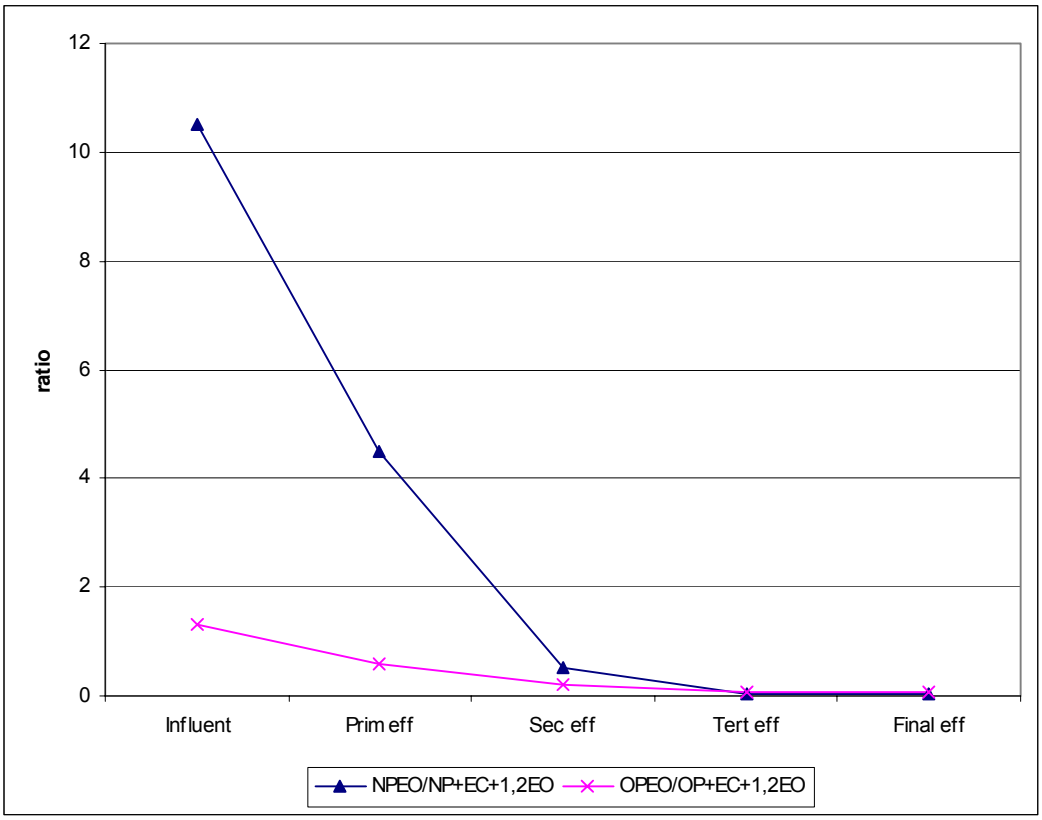

Figure 4. Changes in the ratio of total APEO to degradation products concentrations.

Figure 4 shows the variation in the ratio of the total APnEO concentration to the sum of all the degradation products measured. The ratios range from 11 to 0.04 for the NPnEOs and from 1.3

to 0.05 for the OPnEOs. Therefore, a small ratio indicates a more degraded, or treated, sample. However, this approach would need to be applied carefully because the degradation pathway of the APnEOs in natural waters is reportedly the same as in WWTPs, rendering it difficult to determine if the degradation occurred in the plant or in the stream. This might be especially true in cases when the wastewater source is away from the sampling site, allowing enough residence time for degradation to occur. An additional disadvantage of this approach would be the need to quantify all of the compounds, which makes the determination costly and time-consuming. A possible alternative would be to measure the ratio of individual APnEOs to their respective APnECs, as shown in Figure 5. These ratios change in a very similar way to those obtained using all the metabolites, and only require the quantitation of two compounds.

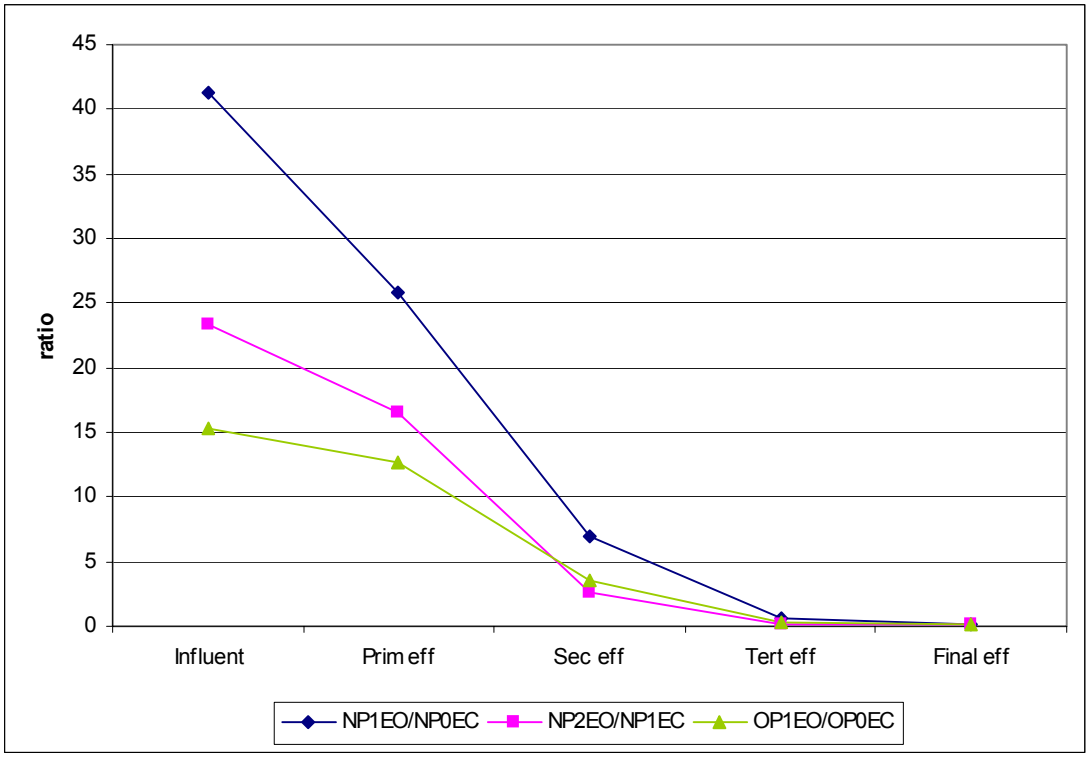

Figure 5. Changes in the ratio of individual APnEOs to their respective APnECs in different wastewater treatment stages.

Theoretical model

For our initial approach, we constructed a model of Back River in a commercial modeling environment (Stella, isee systems, Lebanon, NH). Only NP was considered and the river was divided into four cells (see Figure 6). The first and northernmost cell includes the influent from the two major tributaries, Herring Run and North East Creek and ends before Back River WWTP. The second cell includes the effluent from the WWTP and ends at Muddy Gut. The third cell starts at Muddy Gut and ends at Greenhill Cove. The fourth and last cell runs from Greenhill Cove to the mouth of the river into the Chesapeake Bay. The last two cells receive water only from the preceding cell; no other inputs were considered. This division was based on the location of the influents to the river and specific geographic features; i.e. points where the river turns. Each section of the river was modeled as a well-mixed reactor. The following processes were included in each cell: advection, dispersion, volatilization, photolysis, partition into suspended solids and net deposition into sediments. Advection was modeled as a function of flow rate (Q) and concentration (total concentration of the chemical, including both dissolved and bound species). The flow rate was assumed to be constant and values used were ten times smaller than the actual flow rates to account for tidal flow. Dispersion was modeled as a function of concentration gradients between sections, dispersion coefficient – constant for all sections in the river –, cross sectional area and volume of each section. Volatilization was modeled as a flux out of the water, assuming the concentration of these chemicals is equal to zero in the atmosphere. Photolysis of NP and deposition into sediments were modeled as a first order reaction. Flow diagrams of the model are depicted in Figure 7.

The preliminary results of our model suggest that, after reaching steady state, NP will be present in the water at a concentration of 0.5, 0.7, 0.4 and 0.08 μg/L for cells 1 to 4 respectively. This values are very close to actual concentrations measured in the river in January 2001 (0.3, 0.4, 02 and 0.05 μg/L respectively). The steady-state amount of NP in the water represents approximately 10 % of the total amount entering the Back River over a period of 10 days. Photodegradation appears to be the most important removal process for NP in the water (49% of the NP entering the Back River), whereas deposition into sediments is the second most relevant

process (35%), and volatilization losses are minimal (3%). Even with these losses, 13% of the NP would be transported into the Chesapeake Bay. These results are summarized in Figure 8.

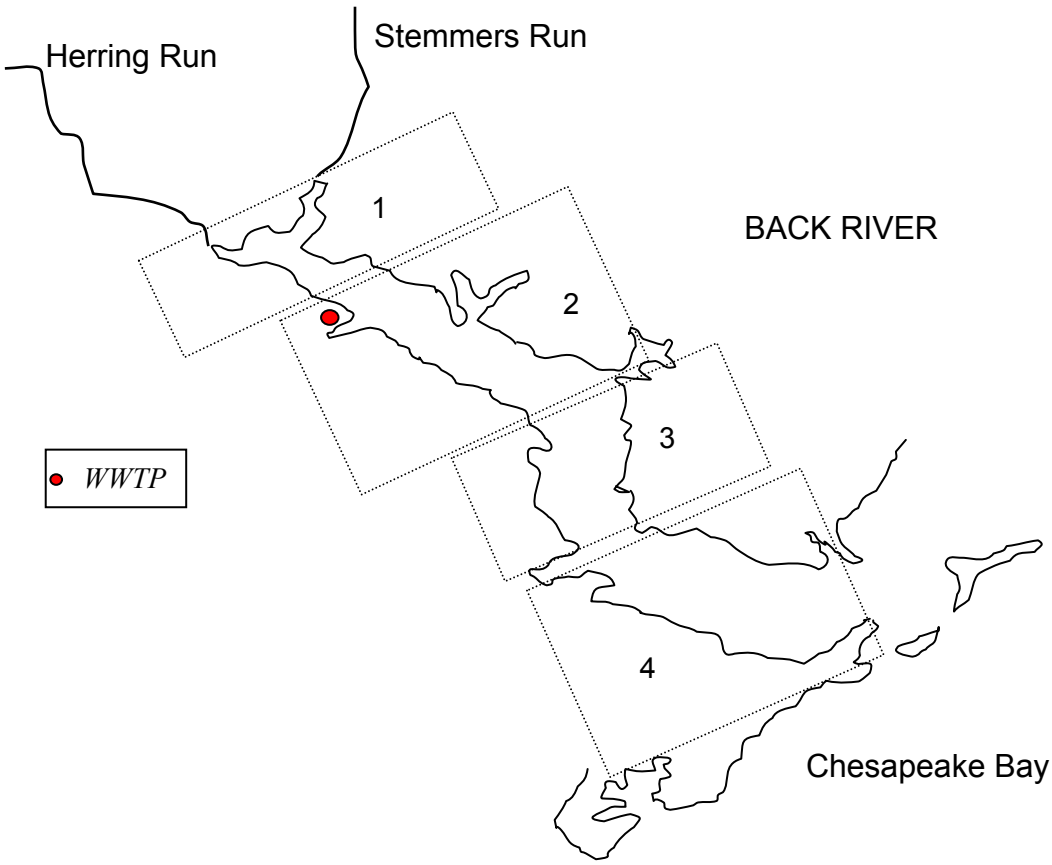

Figure 6. Scheme of the Back River showing the four sections of the model.

Figure 7. Flow diagram for the Stella model of NP distribution in the Back River.

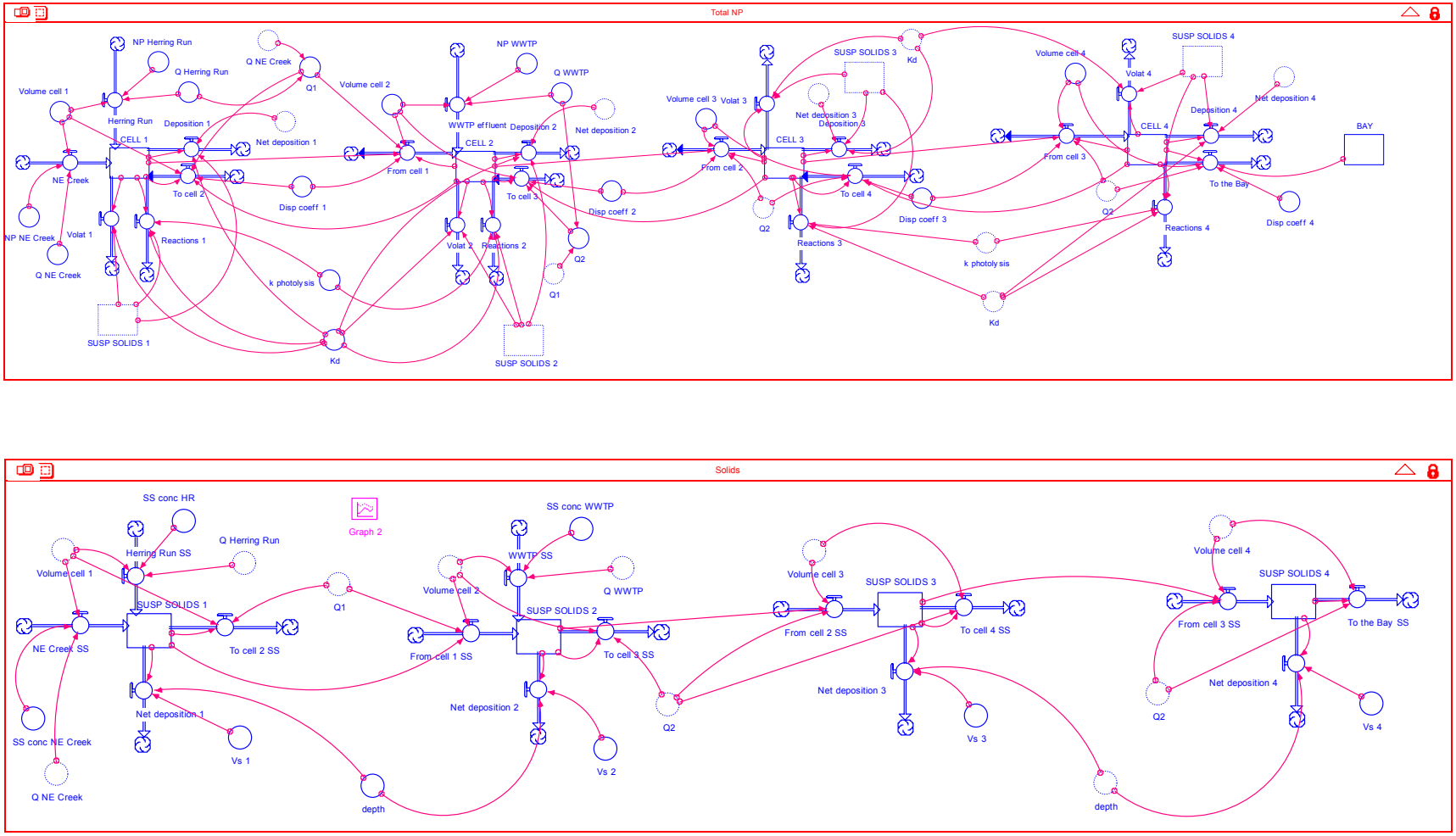

Figure 8. NP distribution in the Back River

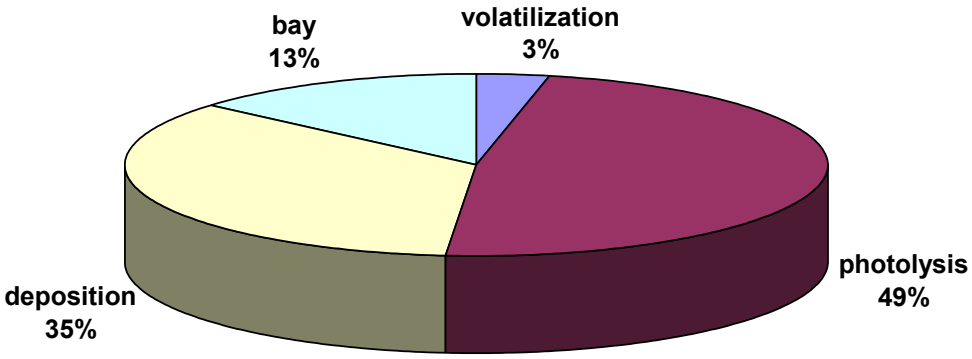

Current and future activities

During the extension to our project we will continue the data analysis and model development, including the addition of the APnEOs and APnECs, and a more accurate characterization of the hydrology of the estuary, specifically the tidal flow.

References

Ahel, M., Giger, W., Molnar, E., and Ibric, S. (2000), "Determination of nonylphenol polyethoxylates and their lipophilic metabolites in sewage effluents by normal-phase high-performance liquid chromatography and fluorescence detection". *Croat. Chem. Acta* 73(1), 209-227.

Ahel, M., Giger, W., and Koch, M. (1994), "Behaviour of alkylphenol polyethoxylate surfactants in the aquatic environment – I. Occurrence and transformation in sewage treatment". *Wat. Res.* 28(5), 1131-1142.

Ahel, M., and Giger, W. (1993), "Partitioning of alkylphenols and alkylphenol polyethoxylates between water and organic solvents". *Chemosphere* 26(8) 1471-1478.

Bennie, D. T. (1999), "Review of the environmental occurrence of alkylphenols and alkylphenol ethoxylates". *Water Qual. Res. J. Canada* 34(1), 79-122.

Hale, R.C., Smith, C. L., de Fur, P. O., Harvey, E., Bush, E. O., La Guardia, M. J., and Vadas, G. G. (2000) "Nonylphenols in sediments and effluents associated with diverse wastewater outfalls" *Environ. Toxicol. Chem.* 19(4), 946-952.

"Interagency Testing Committee" (2000) <http://www.epa.gov/opptintr/itc> Accessed on April 1, 2002.

Kolpin, D. W., Furlong, E. T., Meyer, M. T., Thurman, E. M., Zaugg, S. D., Barber, L. B., and Buxton, H. T. (2002), "Pharmaceuticals, hormones, and other organic wastewater contaminants in U.S. streams, 1999-2000: A national reconnaissance". *Environ. Sci. Technol.* 36(6), 1202-1211.

Loyo-Rosales, J. E., Schmitz-Afonso, I., Rice, C. P., and Torrents, A. (2003), "Analysis of octyl- and nonylphenol and their ethoxylates in water and sediments by liquid chromatography- tandem mass spectrometry". *Anal. Chem.* 75(18), 4811-4817.

Sonnenschein, C., and Soto, A. M. (1998), "An updated review of environmental estrogen and androgen mimics and antagonists". *J. Steroid Biochem. Molec. Biol.* 65(1-6), 143-150.

Soto, A. M., Justicia, H., Wray, J. W., and Sonnenschein, C. (1991), "p-Nonyl-phenol: an estrogenic xenobiotic released from "modified" polystyrene". *Environ. Health Perspect.* 92, 167-173.

Students trained

Jorge E. Loyo-Rosales, a full time PhD student at the University of Maryland, College Park.
Frédérick Adam, an intern from the ESNCR (Ecole Nationale Supérieure de Chimie de Rennes) in France.
Natasha Andrade, a chemical engineering undergraduate student at the University of Maryland, College Park.

Papers

Loyo-Rosales, J. E., Rosales-Rivera, G. C., Rice, C. P., Torrents, A. (2005), "Linking laboratory experiences to "the real world": The extraction of octylphenoxyacetic acid from water". *J. Chem. Educ.* In press.

Loyo-Rosales, J. E., Rice, C. P., and Torrents, A, "Determination of octyl- and nonylphenol ethoxylates and carboxylates in environmental samples by isotope dilution and liquid chromatography/tandem mass spectrometry". Submitted to *J. Chromatogr. A*.

Loyo-Rosales, J. E., Rice, C. P., and Torrents, A., "Fate and distribution of the octyl- and nonylphenol ethoxylates in wastewater treatment plants from the Baltimore-Washington area and the Back River, Maryland". In preparation for *Environ. Sci. Technol.*

Presentations

Loyo-Rosales, J. E., Rice, C. P., Torrents, A.: Endocrine disruptors in municipal wastewater discharges. Platform presentation. Symposium "Wastewater Treatment Plants and the Chesapeake Bay: Processes and Problems". Sponsored by the Maryland Water Resources Research Center and the Maryland Sea Grant College. College Park, MD, October 22, 2004.

Loyo-Rosales, J. E., Rice, C. P., Torrents, A.: Alkylphenol ethoxylates in waters from the Baltimore-Washington area. Poster presentation. Maryland Water Policy Conference – What Does the Future Hold? Organized by the Maryland Water Resources Research Center. College Park, MD, October 24, 2003.

Leaf-scale hyperspectral reflectance models for determining the nitrogen status of freshwater wetlands

Basic Information

Title:	Leaf-scale hyperspectral reflectance models for determining the nitrogen status of freshwater wetlands
Project Number:	2004MD57B
Start Date:	3/1/2004
End Date:	2/29/2005
Funding Source:	104B
Congressional District:	5th & 8th District of Maryland
Research Category:	Not Applicable
Focus Category:	Non Point Pollution, Wetlands, Models
Descriptors:	remote sensing,
Principal Investigators:	David R Tilley, Andrew Baldwin

Publication

Final Report to
Maryland Water Resources Research Center

Leaf-scale hyperspectral reflectance models for determining the nitrogen status of freshwater wetlands

David R. Tilley, Andrew H. Baldwin, Emily P. Jenkins
Biological Resources Engineering, University of Maryland College Park
301-405-8027

Executive Summary

The effects of nitrogen (N) fertilization and species on the hyperspectral leaf reflectance (350 – 1050 nm) of four common emergent freshwater macrophytes (*Acorus calamus, Peltandra virginica, Phragmites australis,* and *Typha* spp.) were determined in a complete randomized experiment. Plants were cultured in a climate-controlled greenhouse and subjected to five levels of N fertilization (0, 1, 2, 5, and 20 mg-N per L), selected to span levels observed in natural and treatment wetlands. An ASD Handheld SpectroRadiometer (Analytical Spectral Devices, Boulder, CO) with a spectral range of 325—1075 nm and a one degree field of view was used to measure plant leaf reflectance in full sun. Prior to fertilization species exhibited a significant ($p<0.05$) effect on leaf reflectance in the visible and near-infrared with all spectral bands between 450 and 1050 nm affected. The majority of the species effect was due to the differences between *Acorus* and both *Peltandra* and *Phragmites*. After 49 d of N fertilization, N, species and their interaction were all significant factors for visible and near-infrared (NIR) response. Grouping *Acorus* with *Peltandra* and *Phragmites* with *Typha* greatly reduced the species effect and heightened the N effect. The reflectance of the invasive species group (*Phragmites* + *Typha*) in the chlorophyll *a* and *b* absorption bands displayed much higher sensitivity to low N additions the non-invasive group (*Acorus* + *Peltandra)*, suggesting that the invasive group had a greater ability to take up N, build chlorophyll and absorb photosynthetically active and NIR radiation. A partial least squares regression model that used the change in reflectance over N fertilization experiment to predict N treatment level had an R^2 of 0.72. The work demonstrated that the capability to detect the response of wetland plants to elevated N availability via leaf reflectance could be used to assess the N levels of natural emergent marshes. This provides a foundation for scaling the technique to aerial or satellite-based hyperspectral radiometers to perform large scale monitoring and assessment of wetland water quality.

1 Introduction

1.1 Problem Statement

The Clean Water Act stipulates that States report the health and quality of all water bodies, including wetlands, in a National Water Quality Inventory Report, but only 4% of wetlands were included in the most recent edition (USEPA 2002a). By 2012 the USEPA's leniency will end and States will be required to report wetland water quality and ecological health (USEPA 2002b). The lack of reporting stems from technical difficulties associated with sampling wetlands and unresolved issues in defining wetland health. Direct sampling of wetland soils and plant tissues provides the most accurate estimate of the N concentration and prevalence for specific locations, but gives limited information on geographical extent of the problem. Remote sensing with hyperspectral radiometry may offer an ability to assess the likelihood of wetland N availability over broad geographical areas, which would vastly improve wetland assessment capabilities.

Nutrients from agricultural runoff and other sources are widely known to cause eutrophication of open-water aquatic systems such as the Chesapeake Bay, stimulating algal growth and causing dieback of submerged aquatic vegetation and declines in fish and shellfish populations (Jaworski et al. 1992; Chesapeake Bay Program 2002). Anthropogenic input of

nutrients to the biosphere is increasingly viewed as a global threat to ecosystems (Vitousek et al. 1997; Fenn et al. 1998). This cultural eutrophication of habitats can alter plant species composition and reduce plant diversity (DiTommaso and Aarssen 1989; Morris 1991). Although Maryland's load of total nitrogen to Chesapeake Bay decreased by 28% from 1986 to 2001 nitrogen loading remains a priority concern for achieving the 2000 Chesapeake Bay Agreement (MDNCWG 2001). Statewide, point source nitrogen loads have decreased from 14,300 MT to 7710 MT (46%) and agricultural loads have dropped from 14,600 MT to 9590 MT (34%). Urban loads, on the other hand, have grown 19%, from 5370 MT to 6390 MT.

Tidal freshwater marshes (TFM) are an extensive type of wetland located along the U.S. coast, often in the upper tidal reaches of rivers flowing into estuaries (e.g., the Patuxent River of Chesapeake Bay) (Odum 1988; Tiner and Burke 1995; Mitsch and Gosselink 2000). TFM's support productive commercial and recreational fisheries, provide recreational opportunities, filter pollutants from land runoff, and add to the biological diversity of the landscape (Odum et al. 1984).

From a water quality management perspective, restoration of wetlands is recommended as a Best Management Practice (BMP) by the State of Maryland for improving Bay water quality (MDNCWG 2001). By 2012 the USEPA will begin enforcing the regulation that all States and Tribes report the water quality and ecological health of wetlands. Thus, not only is there a need to understand the affect of restored and natural wetlands on reducing nutrient and sediment loads to the Bay, we also need to be able to rapidly and easily quantify their nitrogen and phosphorus status. Currently, measuring the nutrient status of wetlands relies on labor-intensive collection and time-consuming water analysis techniques.

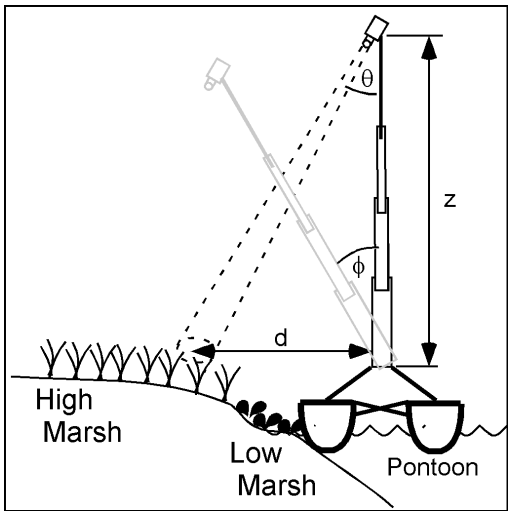

Figure 1.1. Schematic diagram demonstrating measurement positions for the boat-mounted, telescopic spectroradiometer boom.

The emerging field of precision agriculture, whereby satellite, airborne, and handheld spectroradiometers are employed to measure nitrogen status of crops, demonstrates the potential of employing remote sensing technologies to understand the nutrient status of wetland ecosystems. Advancing the capability of wetland remote sensing to quantify the nitrogen status of wetlands can (1) provide a tool for the large scale assessment of water quality in difficult-to-access wetlands, (2) offer a rapid screening method for identifying nitrogen "hot-spots" in a watershed, (3) enable near real-time monitoring in areas suspected of producing significant quantities of non-point source (NPS) pollution, and (4) be used to monitor wetlands used as for nutrient management.

Table 1.1 indicates how Maryland Water Resources Research Center (MWRRC) funding fit into our long-term research and development effort to develop wetland hyperspectral radiometry as a remote sensing tool for assessing the water quality of emergent marshes. Our previous research demonstrated the proof-of-concept of leaf-scale reflectance models for assessing marsh water column N status in brackish treatment marshes (Tilley et al. 2003). The present project focused on advancing reflectance modeling by testing previously developed reflectance indices and exploring the efficacy of the multivariate data analysis technique of Partial Least Squares to assess the availability of N to emergent macrophytes. Simultaneous to the work of this project,

we were developing a boat-borne imaging radiometer system (BIRS, Fig. 1.1) with funds awarded from Maryland Sea Grant College, which evaluated the feasibility of collecting marsh canopy reflectance using BIRS. Now we are seeking further funding to conduct pilot-scale testing of BIRS in a variety of wetlands and to improve the data collection and reflectance modeling methods. Our goal is to have the technology ready in 2 years for full-scale testing in other wetlands by environmental managers and to have a wetland radiometric system operational by 2012 when the U.S. EPA will begin to enforce sections of the Clean Water Act that stipulate States must include wetland water quality in their biennial reports on water quality (303b Reports).

Table 1.1. Tasks required to develop hyperspectral boat radiometry as a commercial tool for assessing wetland nutrient status.

Tasks	Status	Comments
Proof-of-Concept	Completed 2002	Tilley et al. (2003)
Leaf Reflectance Models	2003-2004	This MWRRC project
Boat-radiometer Proof-of-Concept	2004-2005	MD Sea Grant
Pilot-scale testing of boat-radiometer	Near-term	funding TBD
Full-scale testing w/ end users	Mid-term	funding TBD
Commercial Operation	2012	

1.2 Hyperspectral Reflectance and Ecosystem Assessment

Hyperspectral reflectance refers to the ability to measure plant reflectance of solar radiation in hundreds of narrow (1—2 nm) spectral bands. Hyperspectral reflectance data continue to be evaluated for their ability to represent biological and ecological functions and structural properties (see review by Treitz and Howarth, 1999). At the leaf cellular level, reflectance indices have been developed to infer physiological and biochemical attributes (e.g., chlorophyll and carotenoid content, Jago et al. 1999). At the canopy level of terrestrial ecosystems, spectral indices have been developed to infer leaf area index and canopy nitrogen (Boegh et al. 2002), and water use and evapo-transpiration (Szilagyi 2000, Wiegand and Richardson 1990a, 1990b). The reflectance of upland plants are known to respond to various environmental factors—soil nitrogen (Read et al. 2002), soil moisture (Strachan et al. 2002), salinity (Wang et al. 2002), and ozone concentration (Penuelas et al. 1995), demonstrating the versatility of narrow spectral band reflectance indices to detect plant response to environmental stimuli.

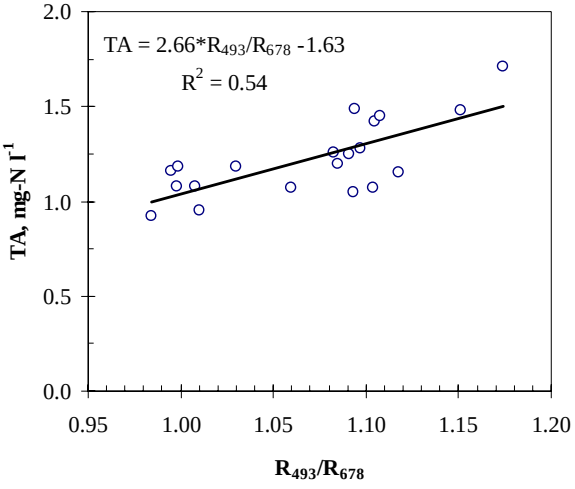

Figure 1.2. A simple reflectance index (R493/R678) was indicative of the wetland's ammonia (TA) concentration over a narrow range.

Although hyperspectral reflectance has been widely used to assess water quality conditions of open-water aquatic ecosystems--classifying the trophic status of lakes (Koponen et al. 2002, Thiemann and Kaufmann 2000) and estuaries (Froidefond et al. 2002), characterizing algal and red tide blooms (Stumpf 2001, Kahru and Mitchell 1998), and identifying and classifying

submerged aquatic vegetation (Williams et al. 2003)--assessment of the ecological health of emergent wetlands based on narrow band spectral reflectance appears limited to plant photosynthetic radiation use efficiency (Penuelas et al. 1997) and redox potential (Anderson and Perry 1996). Thus, quantification of wetland water quality from plant reflectance appears to be a new area of investigation and application (Tilley et al. 2003).

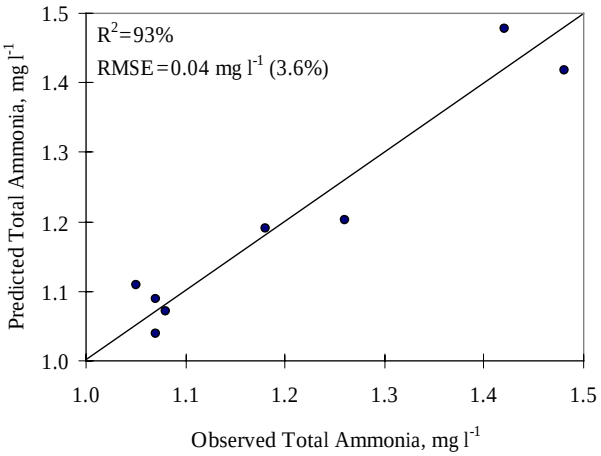

Figure 1.3. A multiple regression equation with PRI and RE of *T. latifolia* as independent variables explained 93% of ammonia variation in the wetland and had a root mean square error (RMSE) equal to 3.6% of the mean ammonia concentration.

During investigations of a brackish (2.5—4.5 ppt) marsh in south Texas, we found the Photochemical Reflectance Index [PRI, defined as $(R_{531}-R_{570})/(R_{531}+R_{570})$], the red edge (RE, defined as the wavelength of maximum slope at the red—NIR transition) and simple reflectance ratios (e.g., R_{493}/R_{678})—determined from handheld spectroradiometric readings of marsh macrophyte leaves (*Typha latifolia* and *Borrichea frutescens*)—to be indicative of marsh water column ammonia concentrations (Tilley et al. 2003; Ahmed 2001). We also found that the normalized difference vegetation index (NDVI) and floating water-band index (fWBI) were responsive to small (1 ppt) changes in salinity (Tilley et al., in review). Others have found the PRI to be positively related to nitrogen, phosphorus, and potassium fertilization rates for annual, deciduous and evergreen upland species (Gamon et al. 1997). Penuelas et al. (1997) determined that the PRI of emergent wetland macrophytes was negatively related to photosynthetic radiation-use efficiency (PRUE), which was similar to non-wetland plants (Gamon et al. 1997).

The red edge (RE), defined as the wavelength of maximum slope at the red—NIR transition, increases with higher chlorophyll content, which is strongly influenced by nitrogen levels. In general, red spectral reflectance is more responsive to nitrogen changes than blue or green spectra due to changes in chlorophyll *a* and *b* (Carter and Miller 1994). Strachan et al. (2002) included PRI along with RE, as necessary members of a multi-index reflectance model developed for classifying nitrogen application rates in corn (*Zea mays*).

Combining individual spectral reflectance bands as simple ratios (e.g., R_{493}/R_{678}) to reduce data noise is a common approach for relating hyperspectral reflectance to biological and ecological properties (Carter and Miller, 1994). Normalization of sensitive wavebands to non-sensitive wavebands minimizes noise and is readily scaled to airborne or satellite platforms. Recently, Read et al. (2002) found a simple blue to red reflectance ratio (R_{415}/R_{710}) as a strong indicator ($R^2 = 0.70$) of leaf nitrogen in cotton (*Gossypium hirsutum*).

Partial least squares (PLS) regression is a type of eigenvector analysis that can reduce full-spectrum data to a small set of independent latent factors (i.e., PLS-components) that explain response in dependent variables, such as the leaf chlorophyll or nitrogen content (Esbensen 2002). PLS regression is related to principal components regression (PCR), which proceeds by first determining the principal components of the independent variable matrix (**X**) without

considering any information contained in the dependent variable matrix (**Y)** and then uses ordinary least squares to relate the principal components to the dependent variables (**Y**). The advantage of PLS regression is that it selects latent components of **X** that explain the most about **Y**. PLS reduces the potential for selecting spectral bands not associated with absorption features, which is a concern with a method such as stepwise multiple linear regression (MLR)—which deals poorly with multicollinearity among spectral bands (Grossman et al. 1996). PLS has become a preferred method for interpreting the hyperspectral reflectance of ecosystems to ascertain biochemical information. Townsend et al. (2003) and Smith et al. (2003) used PLS to develop highly predictive reflectance models of temperate forest canopy nitrogen concentration from airborne and satellite hyperspectral images. We found PLS could estimate the marsh cover occupied by the invasive species *P. australis* (R^2=88%) and the non-invasive dominant species *Polygonum arifolium* (R^2=62%) (Tilley et al. 2004).

1.3 Previous Research

Fig. 1.2 gives an example from our previous work (Tilley et al. 2003) showing that the ratio of leaf (*T. latifolia*) reflectance in a narrow blue band centered at 493 nm and a red band centered at 678 nm explained 54% of the variation in the total ammonia concentration of the wetland's water column. Less leaf reflectance at 678 nm results from higher leaf chlorophyll *a* concentration, which is affected by nitrogen availability. Thus, the technique is a remote sensing method for directly measuring plant reflectance, which infers wetland water quality. We also found that the explanatory power of a multiple linear regression equation containing the Photochemical Reflectance Index (PRI) and red-edge (RE) reflectance indices was highly precise (root mean square error, RMSE = 0.04 mg-N l^{-1}) over a narrow range (1.0—1.5 mg-N l^{-1}) of ammonia (Fig. 1.3).

Our earliest field research on relationships between canopy reflectance and N fertilization conducted on tidal freshwater marshes of the Nanticoke river on Maryland's eastern shore suggested that N supply changes radiation balance. Our initial analysis of canopy reflectance indicates that nitrogen fertilization significantly ($P<0.05$) increased the reflectance in a majority of the near-infrared (NIR) bands, but in none of the visible bands (Fig.1.4). Presumably, the more developed canopy (i.e., higher LAI) of the fertilized sites allows less NIR radiation to reach the soil surface of the wetland where it is effectively absorbed (i.e., not reflected); consequently the canopy of the fertilized plots reflects more NIR. This has interesting ramifications for assessing the global affects of anthropogenic nitrogen fertilization on the energy budgets of wetlands.

1.4 Objectives

In our original proof-of-concept work (Tilley et al. 2003) the range of ammonia concentrations was small (0.9—1.8 mg-N l^{-1}) and we only investigated two emergent macrophyte species. To develop advance wetland hyperspectral radiometry's ability to assess wetland N availability, we needed

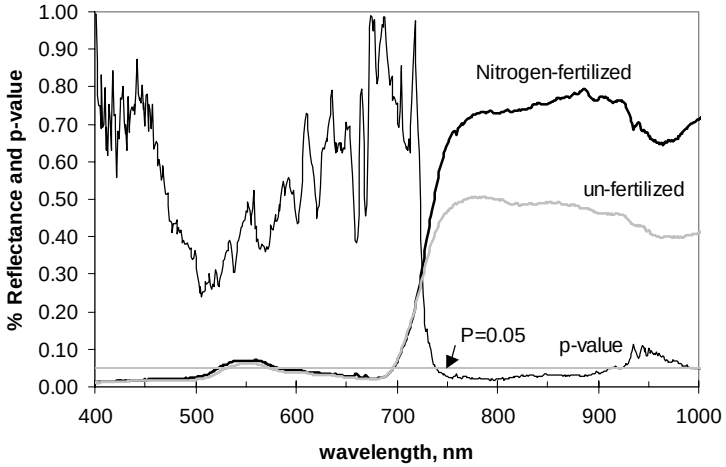

Figure 1.4. Mean canopy reflectance of fertilized and un-fertilized Nanticoke sites and p-value of t-test.

to determine the effect of species on reflectance and we needed to understand the relationship between narrow spectral band reflectance indices and wetland N over a broader range. Presumably, at some high nitrogen concentration N will no longer limit plant growth, which would lead to a saturation of chlorophyll and low reflectance sensitivity, which indicates the limits of the tool as an indicator of wetland N availability.

Therefore, our objective for this project was to test the applicability of previously developed leaf-scale reflectance models over a broader nitrogen range than previously used and to assess the differences among wetland species. A specific objective of our proposed research was to experimentally examine how narrow spectral band reflectance indices (e.g., PRI, RE, R_{678}/R_{493}) and individual spectral bands vary between four common species of wetland plants in their response to a wide range of nitrogen availability. This objective was an integral component of our larger effort to develop BIRS for assessing wetland water quality via remote sensing techniques.

2 Materials and Methods

2.1 Experimental Design

Plant materials were collected in mid-June of 2004 from a tidal freshwater marsh on the Patuxent River near its intersection with U.S. Hwy 301, which is approximately 5 km east of Washington, D.C. Plants with soil residue intact were transferred to 4 L plastic pots containing a peat-perlite mixture. Above-ground tissue was cut back to within 15 cm of the soil surface so plant tissue age would be more uniform. One individual of each potted plant was transferred to one of fifteen 170 L black tubs (i.e., four pots/species per tub) located in the University of Maryland Research Greenhouse Complex. For a period of 21 d following potting and prior to fertilization, plants were irrigated weekly with municipal tap water to flood levels that were 5 cm below the surface of the soil. Each irrigation included emptying the tubs of residual water and refilling to the specified level. Climate conditions within the greenhouse were maintained within ranges indicative of the local summer.

Four species of common wetland emergent macrophytes were used: cattail (*Typha* spp.), common reed (*Phragmites australis* (Cav.) Trin. ex Steud.), arrow arum (*Peltandra virginica* L.) and sweet flag (*Acorus calamus* L.). These species were chosen because they are common in mid-Atlantic freshwater marshes and are large clonal perennials that are easy to collect and grow. Also, cattail and reed are invasive plants of interest to natural resource managers and researchers due to their potential for colonizing disturbed and natural (cattail is native, while exotic genotypes of reed are common in the U.S.). The treatments were 0, 1, 2, 5, and 20 mg-N/L, which were made by mixing municipal tap water with 5-0-1 (N-P-K) fertilizer (4.7% NO^-_3, 0.3% NH_3). In addition to N, all tubs received 2 mg-P L^{-1} and 1.6 mg-K L^{-1} from 0-5-4 fertilizer (5% P_2O_5) to ensure that phosphorus did not limit growth. Treatment began on July 27, 2004, 21 d after plants were potted. Fertilized irrigation water was changed approximately weekly on 8/3, 8/10, 8/18, and 8/27. Each tub was randomly subjected to one of the five nitrogen additions (Table 2.1).

Table 2.1. Summary of experimental treatments for greenhouse study of effects of species and nitrogen concentration on spectral reflectance indices.

		Nitrogen concentration (mg/L)				
		0	1	2	5	20
Species	*Typha*	3 reps	3 reps	3 reps	3 reps	3 reps
	Phragmites	3 reps	3 reps	3 reps	3 reps	3 reps
	Peltandra	3 reps	3 reps	3 reps	3 reps	3 reps
	Acorus	3 reps	3 reps	3 reps	3 reps	3 reps

These levels were selected to span a range from natural marsh concentrations (1-2 mg/L Tilley et al. 2004) up to levels typically seen in treatment wetlands that receive municipal or animal farm wastewater. The design and setup of this study was similar to studies investigating ammonia toxicity in wetland plants (Clarke and Baldwin 2002).

2.2 Radiometric measurements

An ASD Handheld SpectroRadiometer (Analytical Spectral Devices, Boulder, CO) was used to measure plant leaf reflectance. Each pot was taken outside of the greenhouse, and spectroradiometric measurements then taken on clear sky days between 10:00 am and 3:00 pm. Percent reflectance was calculated by dividing canopy reflectance by the reflectance of a calibrated Spectralon white panel (Labsphere, Inc., North Sutton, NH), measurements of which were taken immediately before canopy measurements. We used a 1º field-of-view (FOV) fore-optic positioned at 30º from nadir aimed at the leaf surface from the north side (to reduce shadow) at a distance of approximately 10 cm. The spectroradiometer collected ten sub-samples of each leaf which were later averaged to define the mean reflectance.

2.3 Data analyses

The experimental design resulting from the experimental setup described previously is a 4×5 factorial arrangement of treatments (4 species, 5 N levels per species), with 3 replicates of each treatment combination in a completely randomized design. Analysis of variance (ANOVA) was conducted to examine treatment effects on reflectance indices and spectral band reflectance using SPSS for Windows (SPSS Inc., Chicago, IL). Differences among means were distinguished with Bonferroni's test. Mixed effects two-factor ANOVA, which assumed nitrogen as fixed and species as random, was used to determine whether nitrogen or species affected leaf reflectance response across the full spectrum. Significant differences were defined at the 0.05 probability level. Plots of the p-values for spectral differences were plotted as functions of wavelength to identify patterns in effects. ANOVA and multiple comparison tests were conducted using SPSS for Windows (SPSS Inc., Chicago, IL). We also analyzed effect of N on reflectance by considering N treatment level as a continuous variable in simple linear regression models, which were conducted using SPSS. Spectral reflectance indices included Photochemical Reflectance Index (PRI), a simple reflectance ratio of blue to red (R_{493}/R_{678}), and a standard Normalized Difference Vegetation Index (NDVI).

PLS was used to develop a regression model of hyperspectral reflectance predictive of N availability. We used Unscrambler 9.0 (Camo Process, Oslo, Norway) to conduct PLS. To validate the PLS model we used full-cross validation (i.e., leave one sample out). The number of PLS components to include in the final model was chosen based on the minimum root mean squared error of prediction (RMSEP). The efficacy of the final PLS model to predict N exposure was expressed by the RMSEP and the coefficient of determination.

3 Results and Discussion

3.1 Effect of Nitrogen Fertilization on Hyperspectral Reflectance

3.1.1 Mean reflectance before and after N fertilization

Figure 3.1 shows the mean hyperspectral reflectance of all four species before (July 15, 2004) and after (September 1, 2004) nitrogen fertilization for each of the 5 fertilization levels.

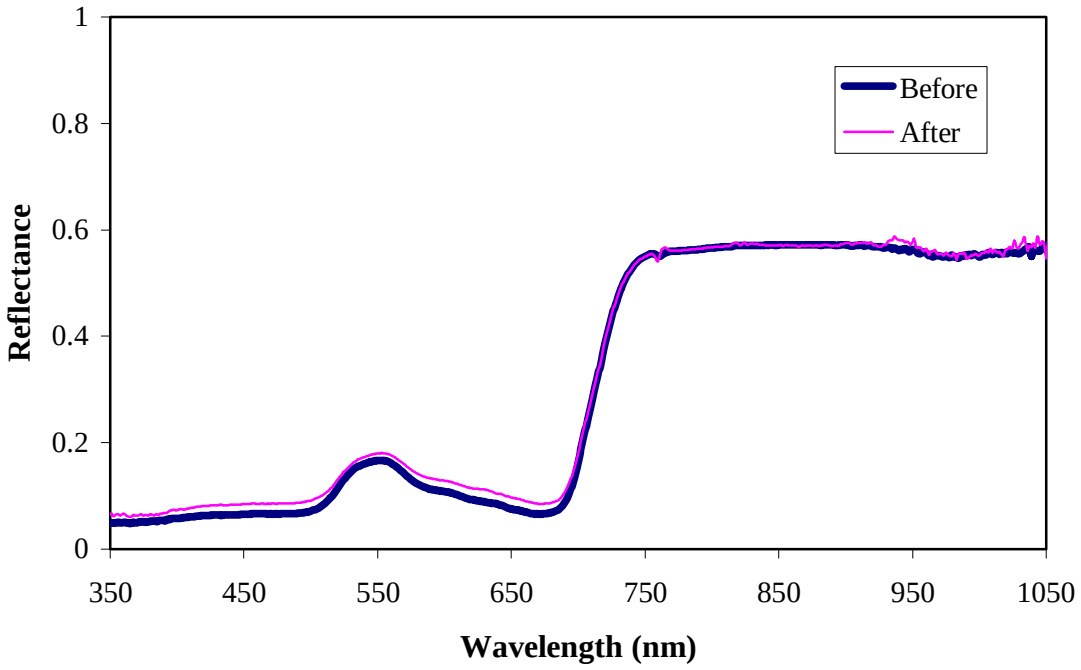

(a)

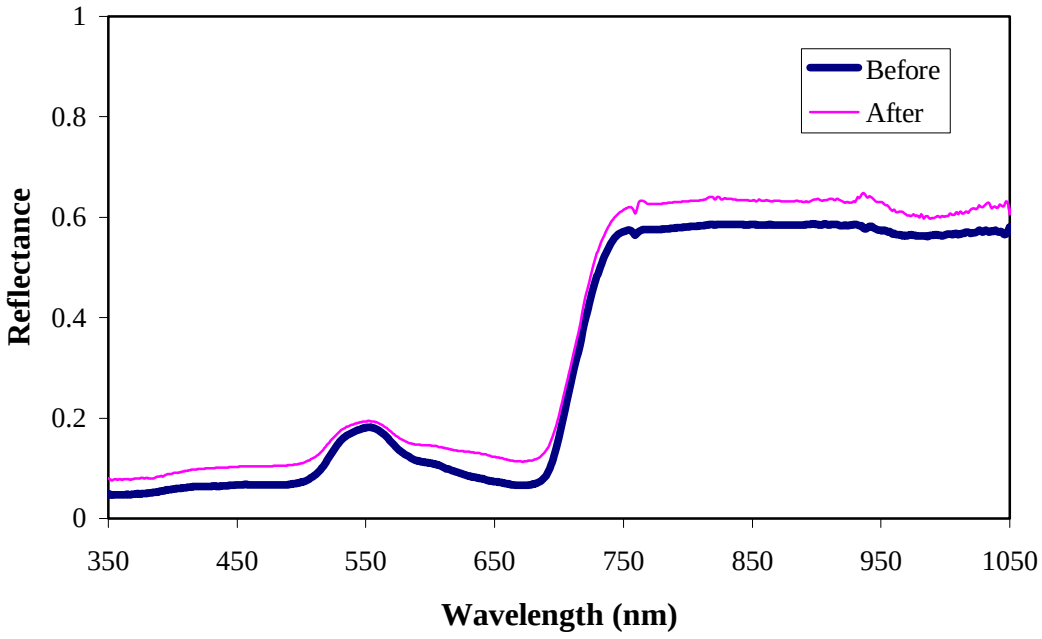

(b)

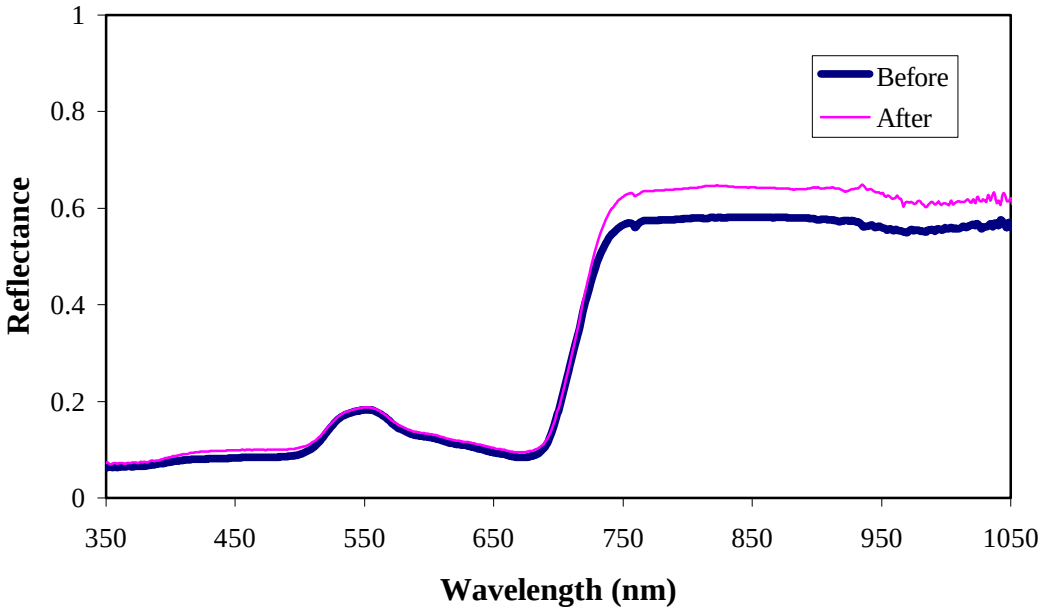
Before
After
Reflectance
Wavelength (nm)
0
0.2
0.4
0.6
0.8
1
350
450
550
650
750
850
950
1050

(c)

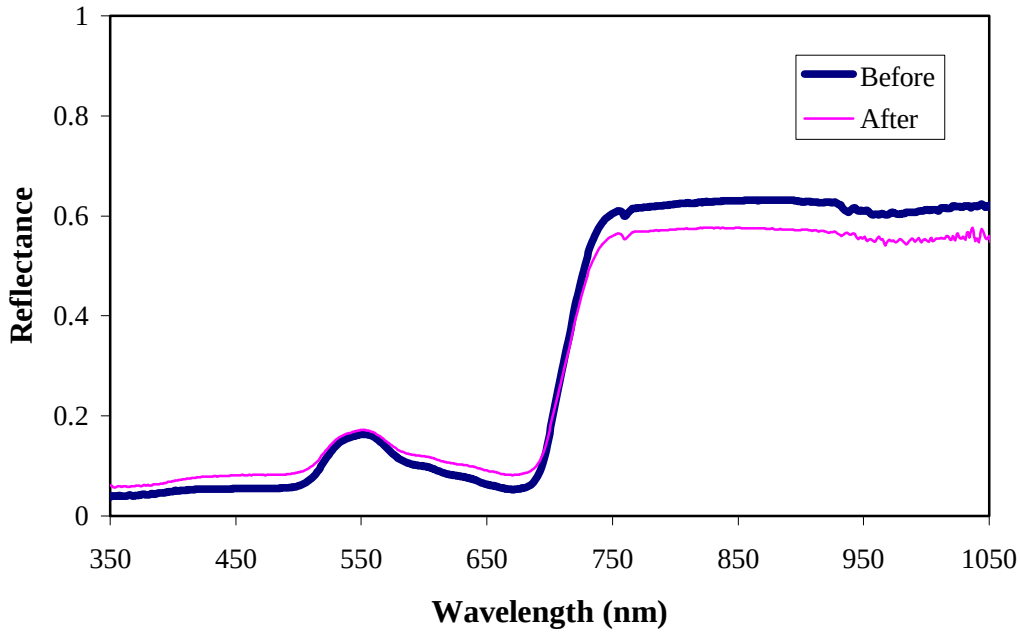
Before
After
Reflectance
Wavelength (nm)
0
0.2
0.4
0.6
0.8
1
350
450
550
650
750
850
950
1050

(d)

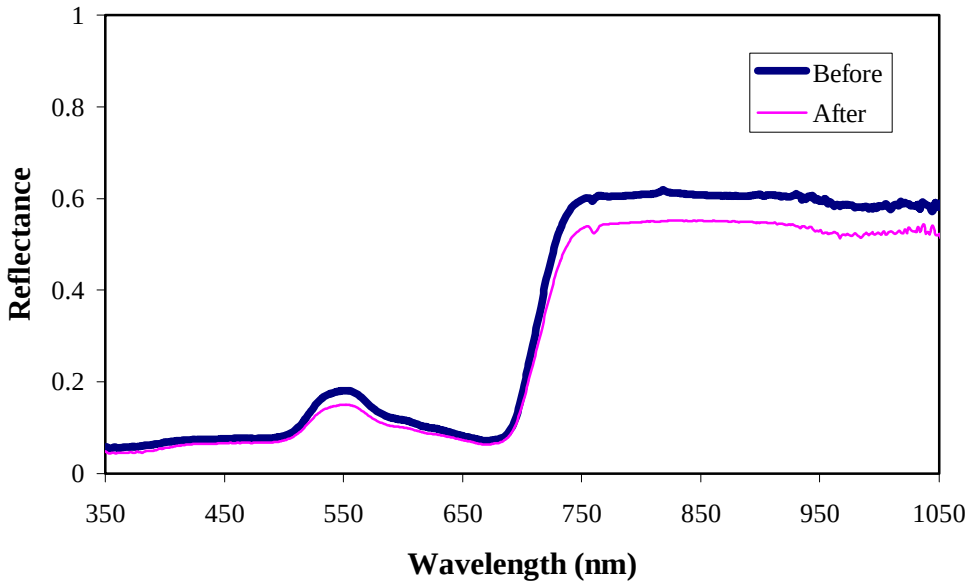

(e)

Figure 3.1. Mean hyperspectral reflectance of four species (3 replicates each) before and 49 days after fertilization for (a) 0 mg-N/L, (b) 1 mg-N/L, (c) 2 mg-N/L, (d) 5 mg-N/L, and (e) 20 mg-N/L treatment levels.

3.1.2 Response of blue, green, red and NIR spectral bands to N fertilization

Figure 3.2 shows the effect of N treatment concentration on mean reflectance at 460 nm, which is a representative blue waveband, when all four species were combine. After 49 d of N fertilization R_{460} was suppressed by higher N availability although p-value was only 0.094.

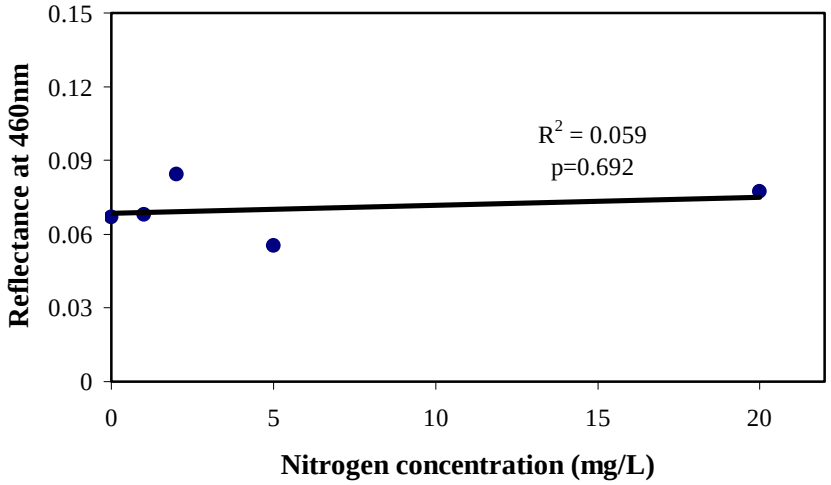

(a)

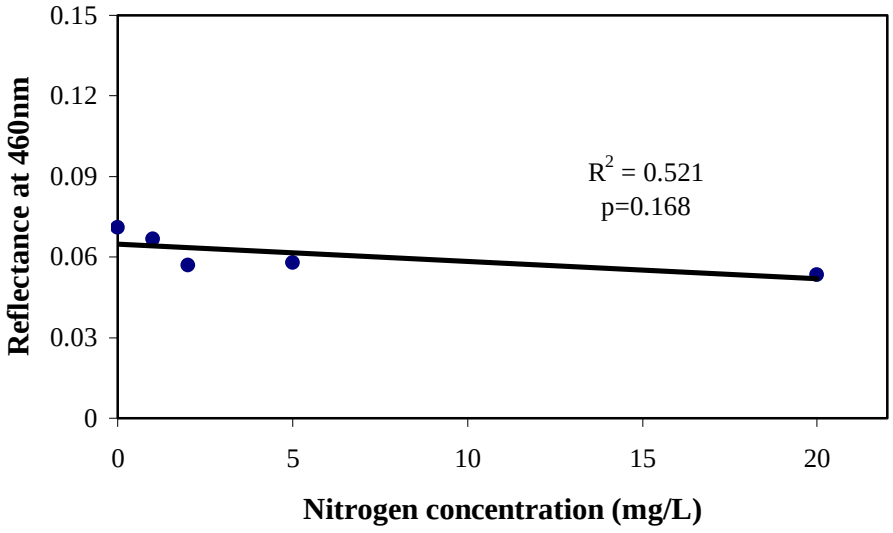

(b)

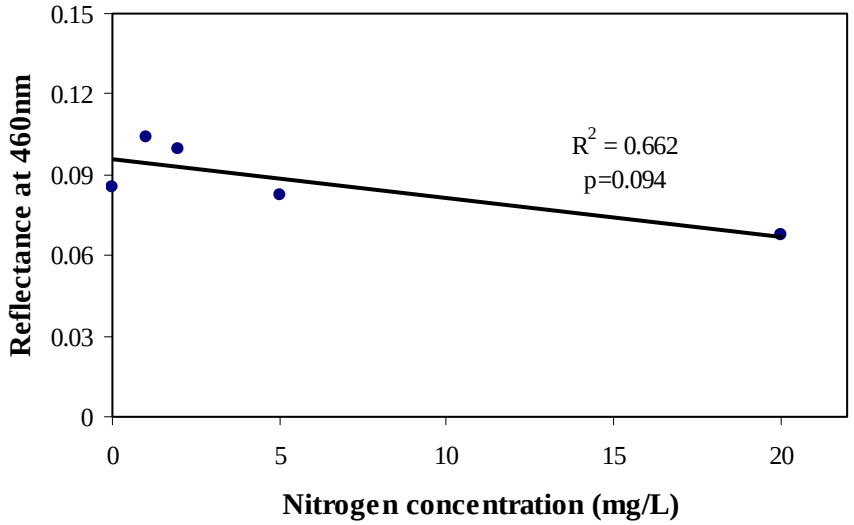

(c)

Figure 3.2. Mean reflectance of four species at the 460nm (blue waveband) across five fertilization levels (0, 1, 2, 5, and 20 mg-N/L) on (a) July 15, 2004 (pre-fertilization). (b) August 9, 2004 (post-fertilization), and (c) September 1, 2004 (post-fertilization). Coefficient of determination and significance of slope (p-value) included.

Figure 3.3 shows the effect of N treatment concentration on mean reflectance at 560 nm, which is a representative green waveband, when all four species were combine. After 25 d of N fertilization R_{560} was suppressed by higher N availability (Fig. 3.3b), which continued after 49 d of N fertilization (Fig. 3.3c).

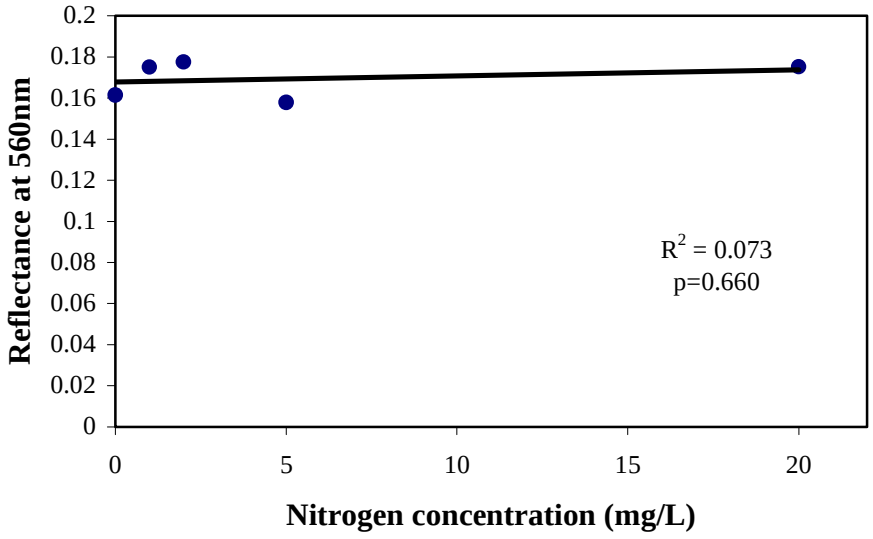
Reflectance at 560nm
0.2
0.18
0.16
0.14
0.12
0.1
0.08
0.06
0.04
0.02
0
0
5
10
15
20
Nitrogen concentration (mg/L)
R2 = 0.073
p=0.660

(a)

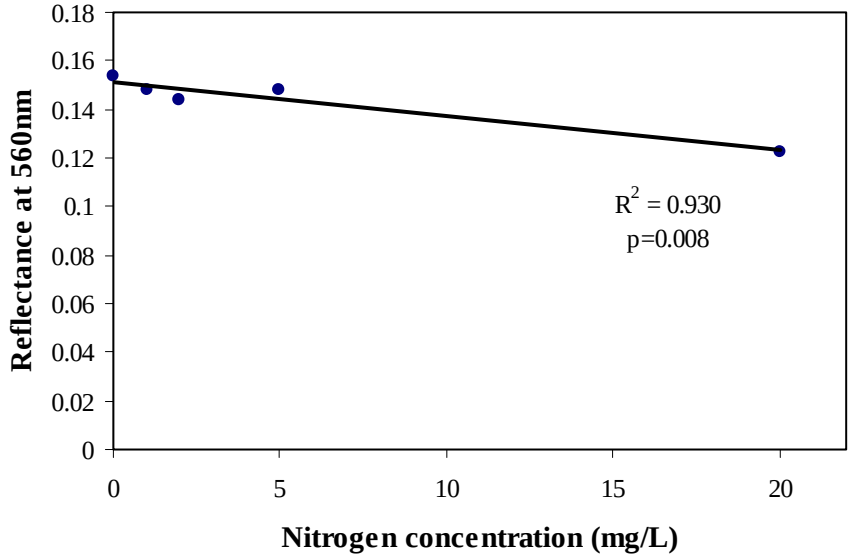
Reflectance at 560nm
0.18
0.16
0.14
0.12
0.1
0.08
0.06
0.04
0.02
0
0
5
10
15
20
Nitrogen concentration (mg/L)
R2 = 0.930
p=0.008

(b)

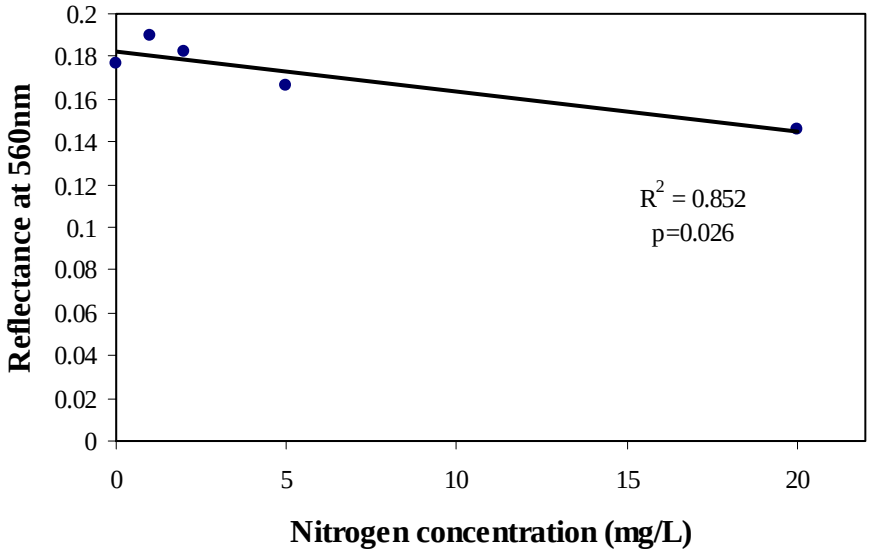

(c)

Figure 3.3. Mean reflectance of four species at the 560nm (green waveband) across five fertilization levels (0, 1, 2, 5, and 20 mg-N/L) on (a) July 15, 2004 (pre-fertilization). (b) August 9, 2004 (post-fertilization), and (c) September 1, 2004 (post-fertilization). Coefficient of determination and significance of slope (p-value) included.

Figure 3.4 shows the effect of N treatment concentration on mean reflectance at 680 nm, which is a representative red waveband, when all four species were combine. After 25 d of N fertilization R_{680} was suppressed by higher N availability, but only moderately significant (Fig. 3.4b). R_{680} was lower at higher N levels after 49 d, but was not significant (Fig. 3.4c)

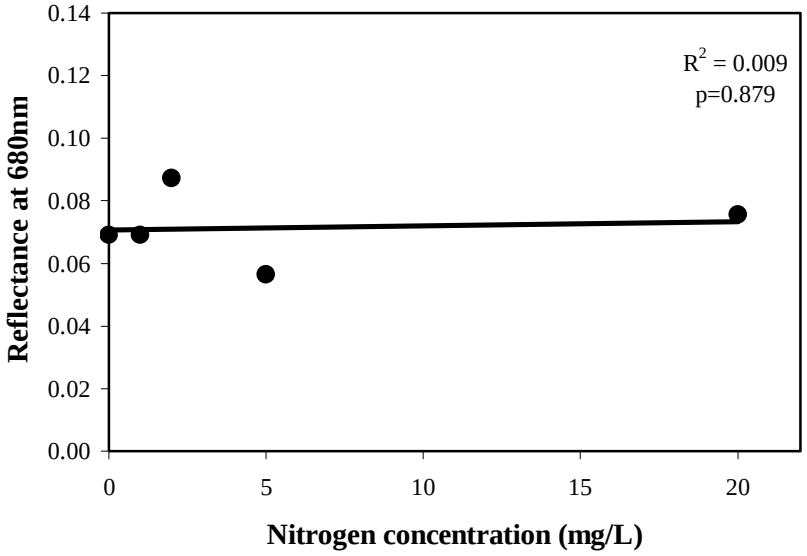

(a)

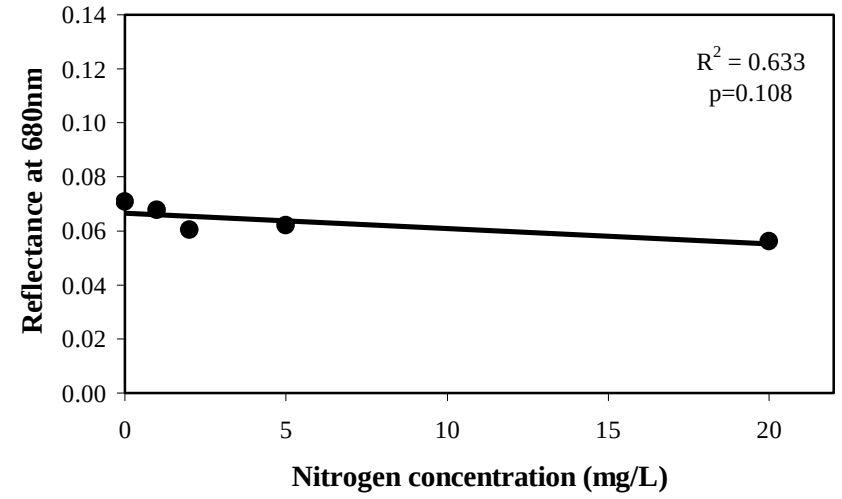

(b)

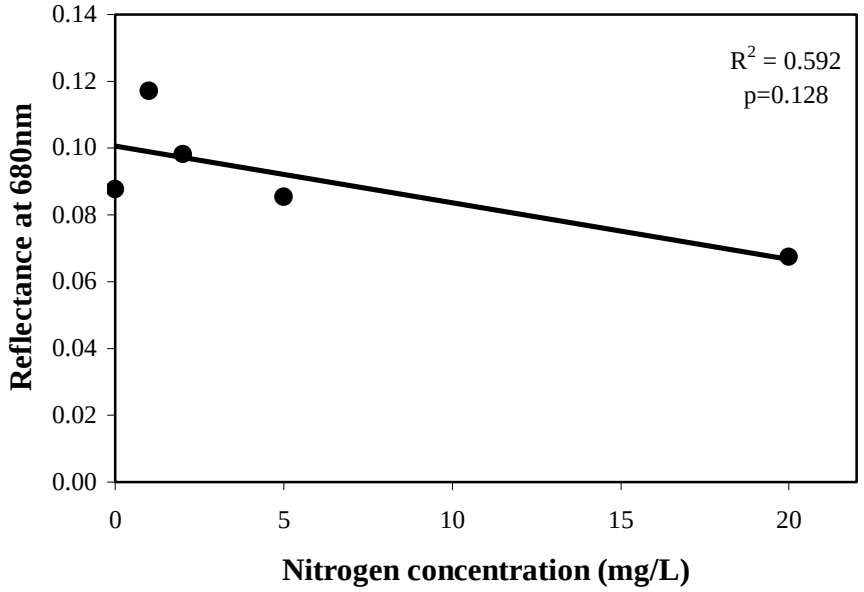

(c)

Figure 3.4. Mean reflectance of four species at the 680nm (red waveband) across five fertilization levels (0, 1, 2, 5, and 20 mg-N/L) on (a) July 15, 2004 (pre-fertilization). (b) August 9, 2004 (post-fertilization), and (c) September 1, 2004 (post-fertilization). Coefficient of determination and significance of slope (p-value) included.

Figure 3.5 shows the effect of N treatment concentration on mean reflectance at 800 nm, which is a representative NIR waveband, when all four species were combine. There was no significant relationship between R_{800} and N availability when all plants were considered together.

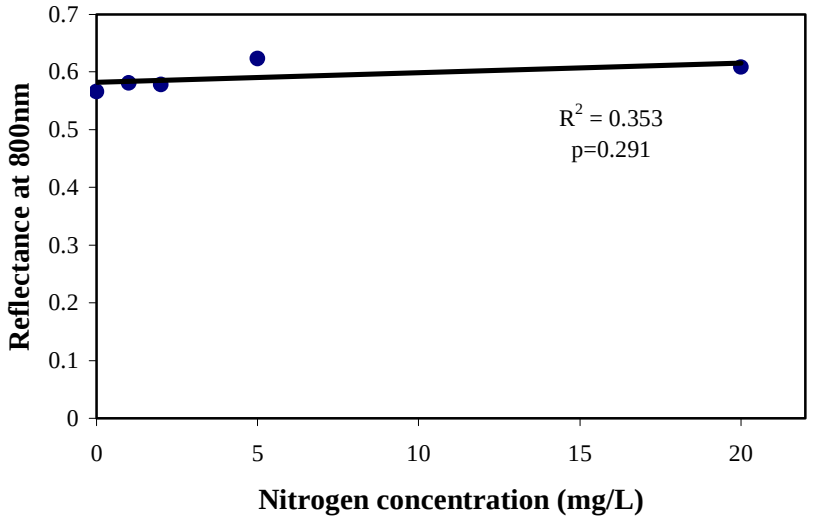
0.7
0.6
0.5
0.4
0.3
0.2
0.1
0
Reflectance at 800nm
R2 = 0.353
p=0.291
0
5
10
15
20
Nitrogen concentration (mg/L)

(a)

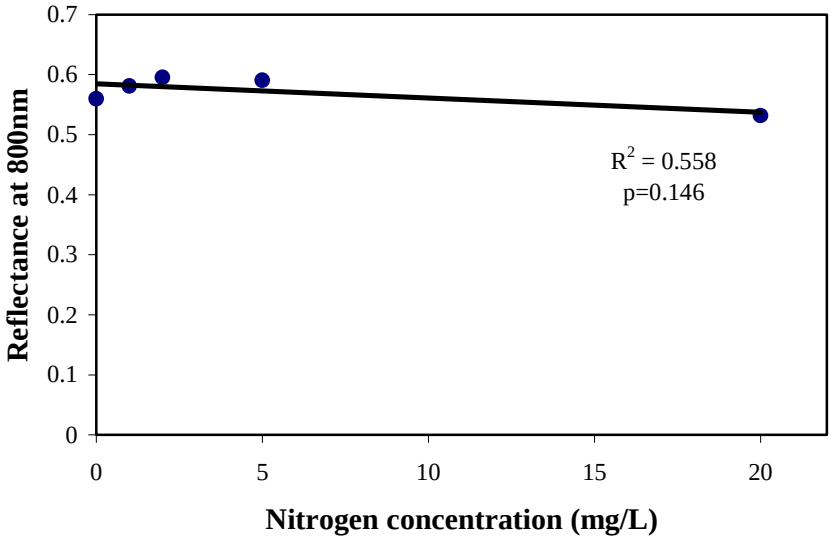
0.7
0.6
0.5
0.4
0.3
0.2
0.1
0
Reflectance at 800nm
R2 = 0.558
p=0.146
0
5
10
15
20
Nitrogen concentration (mg/L)

(b)

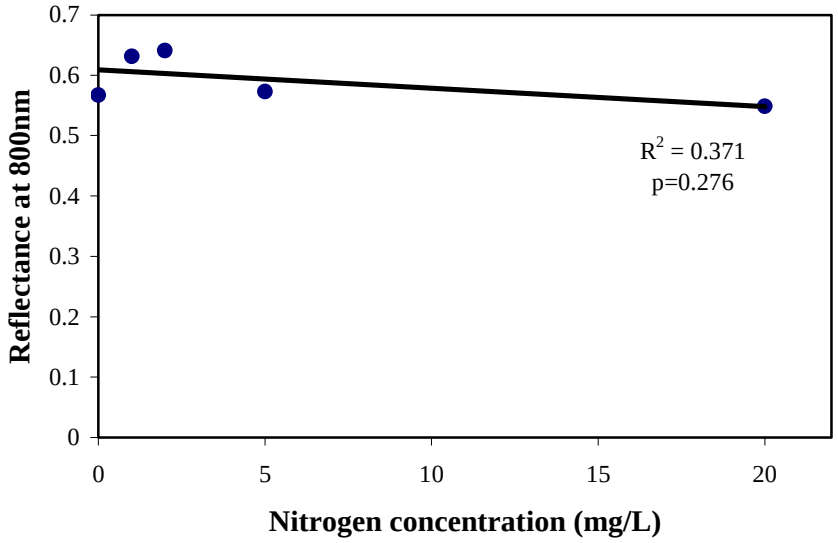

(c)

Figure 3.5. Mean reflectance of four species at the 800 nm (NIR waveband) across five fertilization levels (0, 1, 2, 5, and 20 mg-N/L) on (a) July 15, 2004 (pre-fertilization). (b) August 9, 2004 (post-fertilization), and (c) September 1, 2004 (post-fertilization). Coefficient of determination and significance of slope (p-value) included.

3.1.3 Effect of N on Reflectance Indices

Figure 3.6 shows relationship between N treatment level and the simple reflectance ratio R_{493}/R_{678} before and after fertilization.

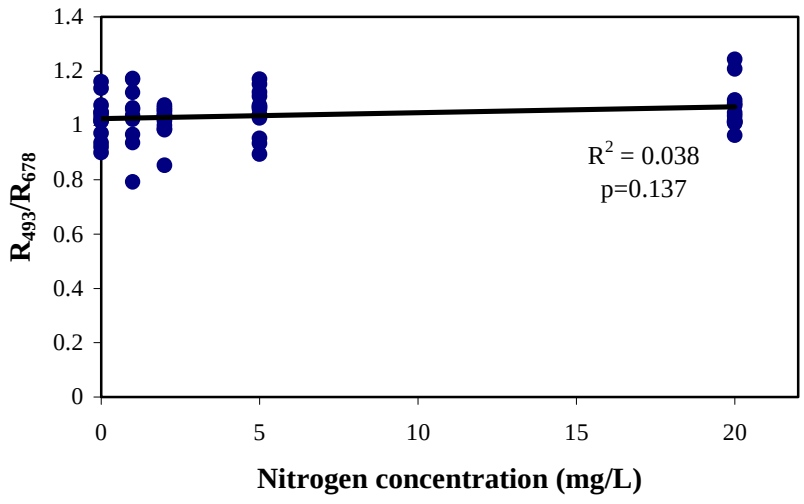

(a)

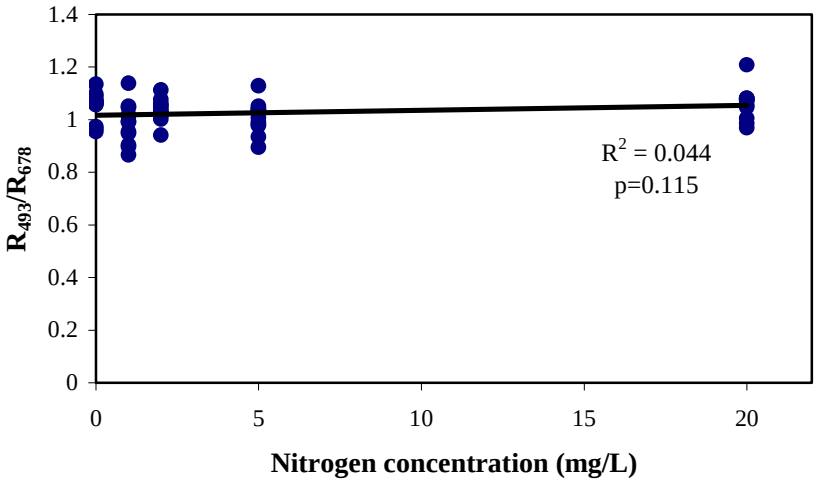

(b)

Figure 3.6. Relationship between reflectance index, R_{493}/R_{678}, and N treatment level (a) before and (b) after fertilization when all four species were combine.

Figure 3.7 shows relationship between N treatment level and the simple reflectance ratio R_{415}/R_{710} before and after fertilization. R_{415}/R_{710} exhibited a significant negative response to N availability after 49 d of N fertilization (Fig. 3.7b).

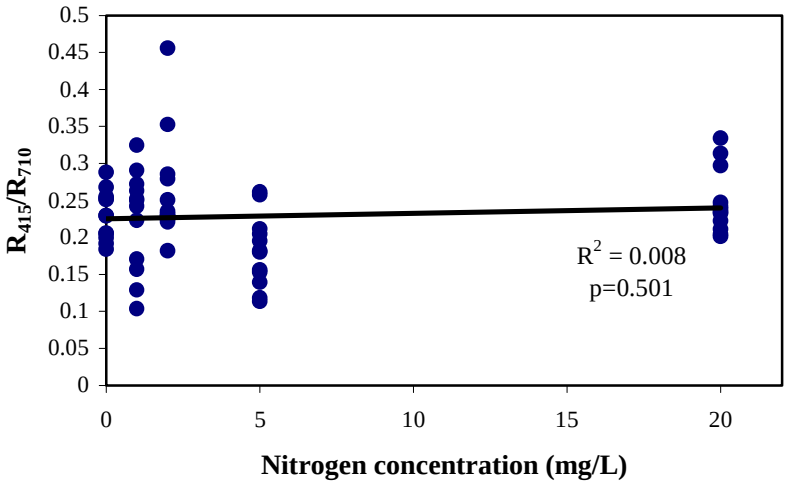

(a)

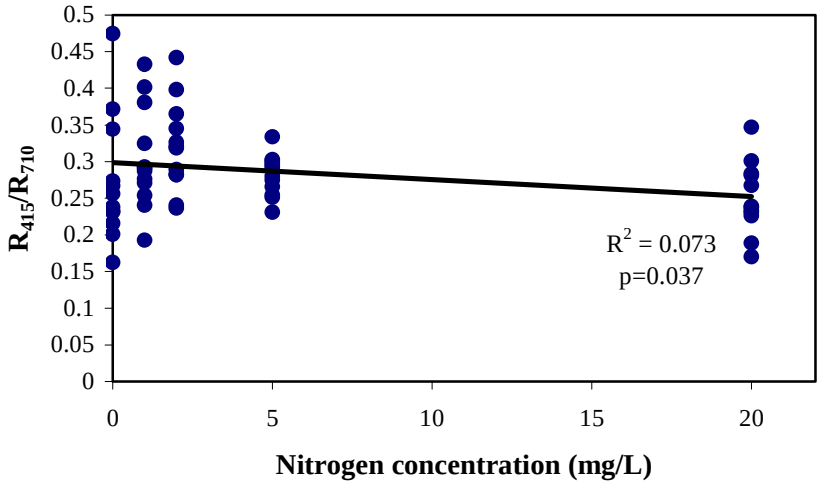

(b)

Figure 3.7. Relationship between reflectance index, R_{415}/R_{710}, and N treatment level (a) before and (b) after fertilization when all four species were combine.

Figure 3.8 shows relationship between N treatment level and the simple reflectance ratio R_{564}/R_{768} before and after fertilization. R_{564}/R_{768} did not exhibit a significant relationship with N availability after 49 d of N fertilization (Fig. 3.8b).

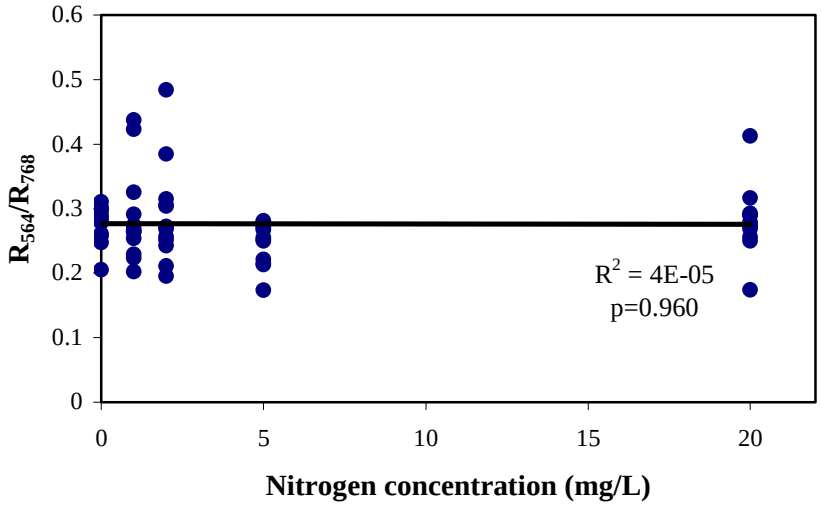

(a)

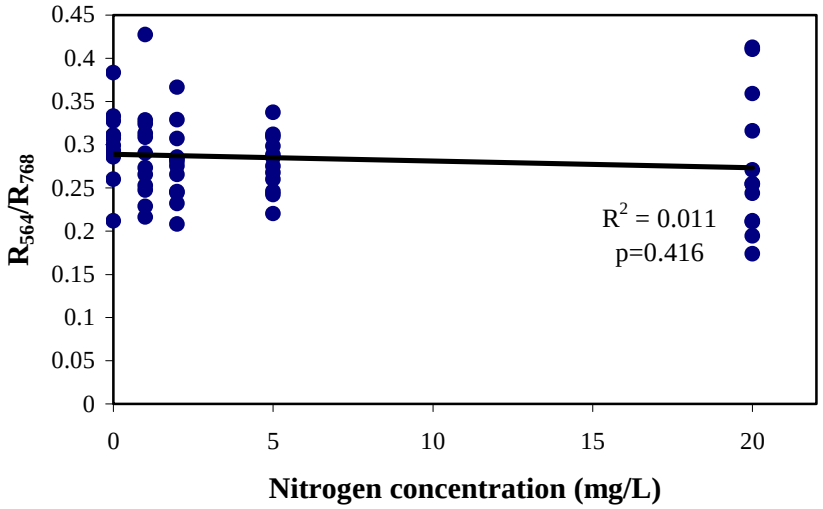

(b)

Figure 3.8. Relationship between reflectance index, R_{564}/R_{768}, and N treatment level (a) before and (b) after fertilization when all four species were combine.

Figure 3.9 shows relationship between N treatment level and the simple reflectance ratio PRI before and after fertilization. PRI exhibited a significant positive response to N availability after 49 d of N fertilization (Fig. 3.9b).

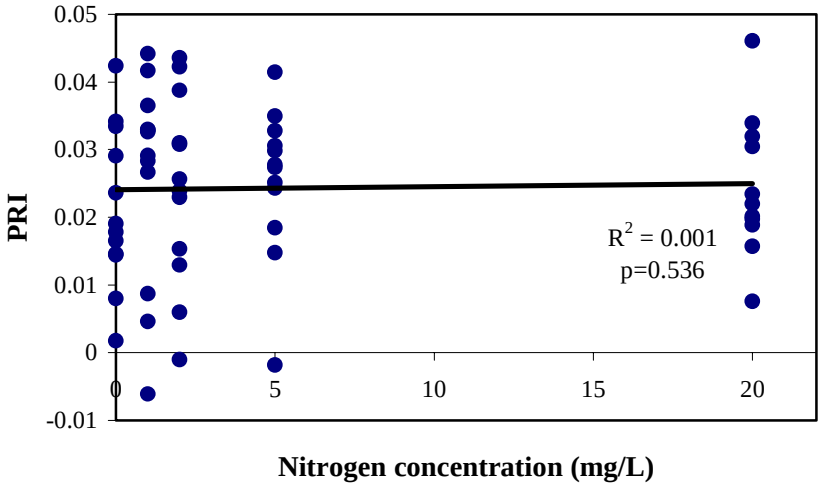

(a)

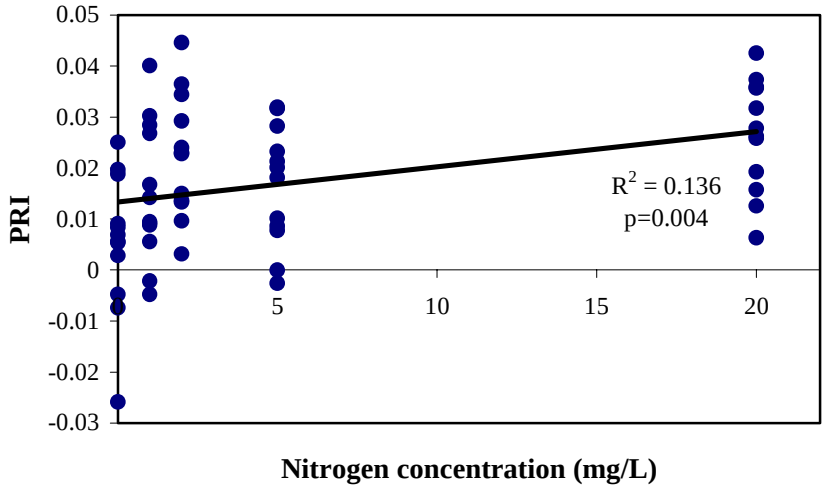

(b)

Figure 3.9. Relationship between reflectance index, PRI, and N treatment level (a) before and (b) after fertilization when all four species were combine.

Figure 3.10 shows relationship between N treatment level and the simple reflectance ratio NDVI before and after fertilization. NDVI exhibited a significant positive response to N availability after 49 d of N fertilization (Fig. 3.10b).

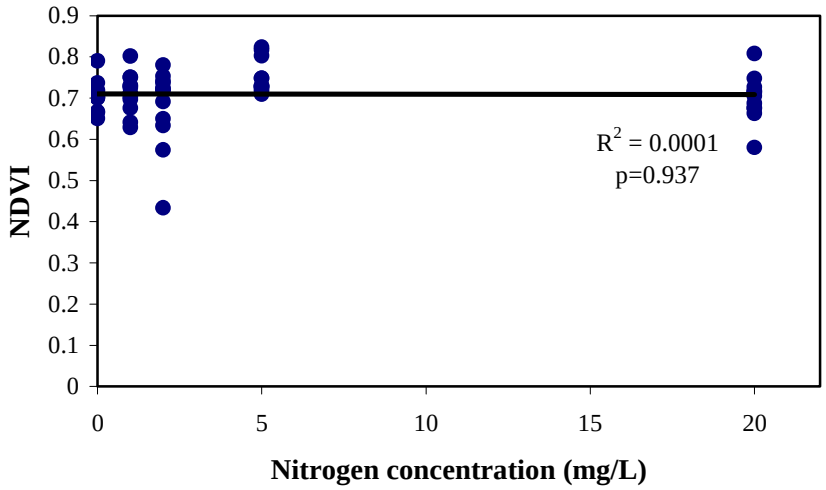

(a)

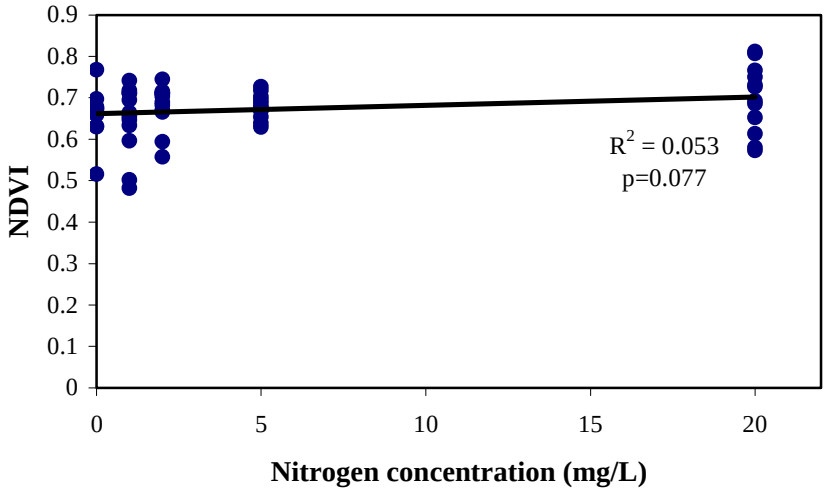

(b)

Figure 3.10. Relationship between reflectance index, NDVI, and N treatment level (a) before and (b) after fertilization when all four species were combine.

Table 3.1 identifies whether chosen reflectance indices were significantly affected by N treatment level according to species. Only R_{493}/R_{678} for *Typha* exhibited a significant relationship to N treatment level before fertilization. All five reflectance indices were significantly affected by N level for at least one species. Likely the sensitivity of the experiment could have been improved by a higher number of replicates for each treatment (species x N level).

Table 3.1. Relationship (R^2 (p-value)) between chosen reflectance indices to N treatment level for each of four species (ns—not significant at p=0.05).

Reflectance Index	*Acorus*	*Phragmites*	*Peltandra*	*Typha*
		Before N fertilization		
R_{493}/R_{678}	ns	ns	ns	0.32 (0.03)
R_{415}/R_{710}	ns	ns	ns	Ns
R_{564}/R_{768}	ns	ns	ns	Ns
PRI	ns	ns	ns	Ns
NDVI	ns	ns	ns	Ns
		After N fertilization (45 d)		
R_{493}/R_{678}	ns	ns	0.39 (0.01)	Ns
R_{415}/R_{710}	ns	ns	0.66 (0.00)	Ns
R_{564}/R_{768}	0.28 (0.04)	ns	ns	Ns
PRI	0.40 (0.01)	ns	ns	Ns
NDVI	0.29 (0.04)	ns	ns	Ns

Figure 3.11 highlights the differences among N treatment levels in the visible waveband after samples were fertilized for 49 d. The highest N treatment had the lowest mean visible reflectance, which supported the contention that higher N availability increases absorption of visible radiation (i.e., photosynthetically active radiation, PAR) by taking up N to increase chlorophyll concentration.

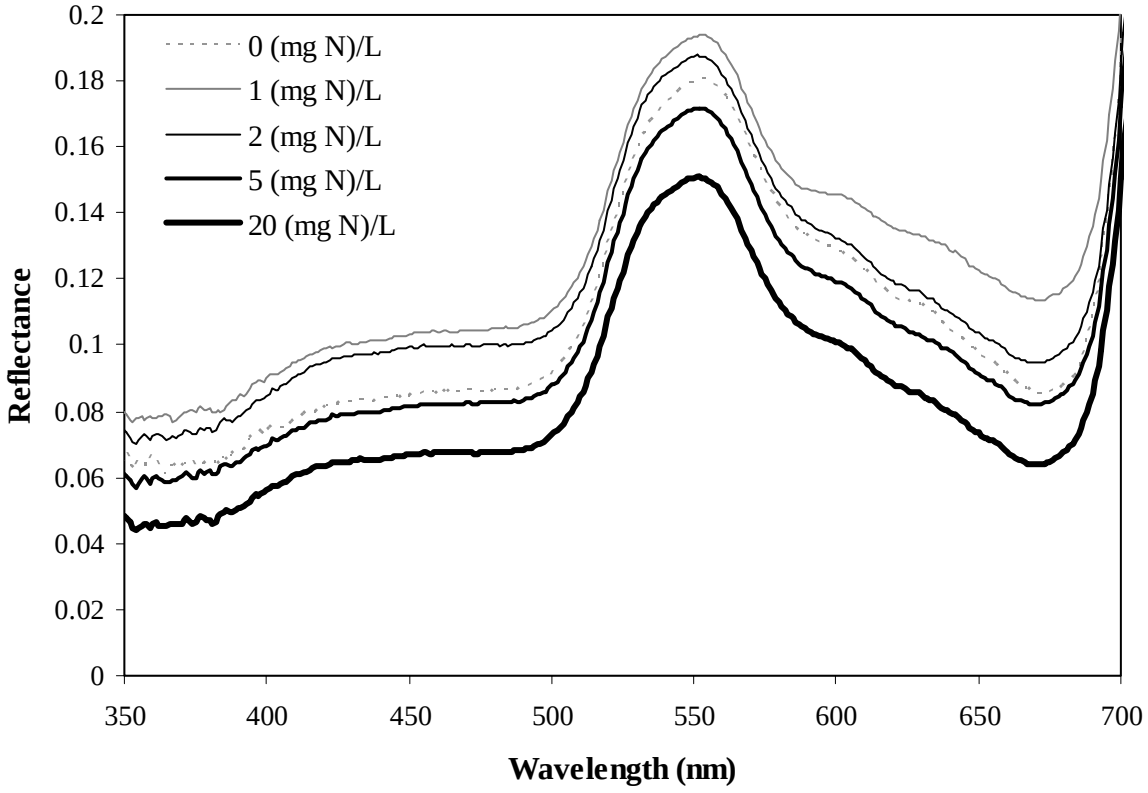

Figure 3.11. Mean visible reflectance on September 1, 2004 of four species for each nitrogen level.

3.2 Species Differences before N fertilization

Fig. 3.12 shows the mean spectral reflectance of the four species on July 15, 2004 after growing in the greenhouse for 21 d without any fertilization. Species had a significant effect on reflectance in all spectral bands except in the UV-blue waveband from 374 to 456 nm (Fig. 3.13). Multiple comparison tests of the species effect revealed that one species (*Acorus*) was responsible for all of the effect (Fig. 3.14a,b,c). The contrast of *Acorus* with *Peltandra* and *Phragmites* exhibited the highest number of significantly different spectral bands, while the *Acorus/Typha* comparison had only a few different bands (Fig. 3.14c). In the 497-658 nm waveband, *Acorus* was 2.7 to 5.5% greater than *Peltandra*, while the difference in the red-edge centered 685-712 nm waveband ranged from 2.8 to 7.1% (Fig. 3.14a). A large portion of the NIR was also greater for *Acorus* compared to *Peltandra*, averaging around 12% (Fig. 3.14a). The significant difference in spectral response between *Acorus* and *Phragmites* covered the entire portion of the spectrum from 492 nm to 1075 nm (Fig. 3.14b). *Acorus* reflected around 15% more in the NIR, 3.1% more in the red, 5.3% more in the green and 2.7% more in the blue than *Phragmites*. Pairwise comparisons between *Peltandra*, *Phragmites*, and *Typha* exhibited no significantly different spectral bands (Fig. 3.14d,e,f).

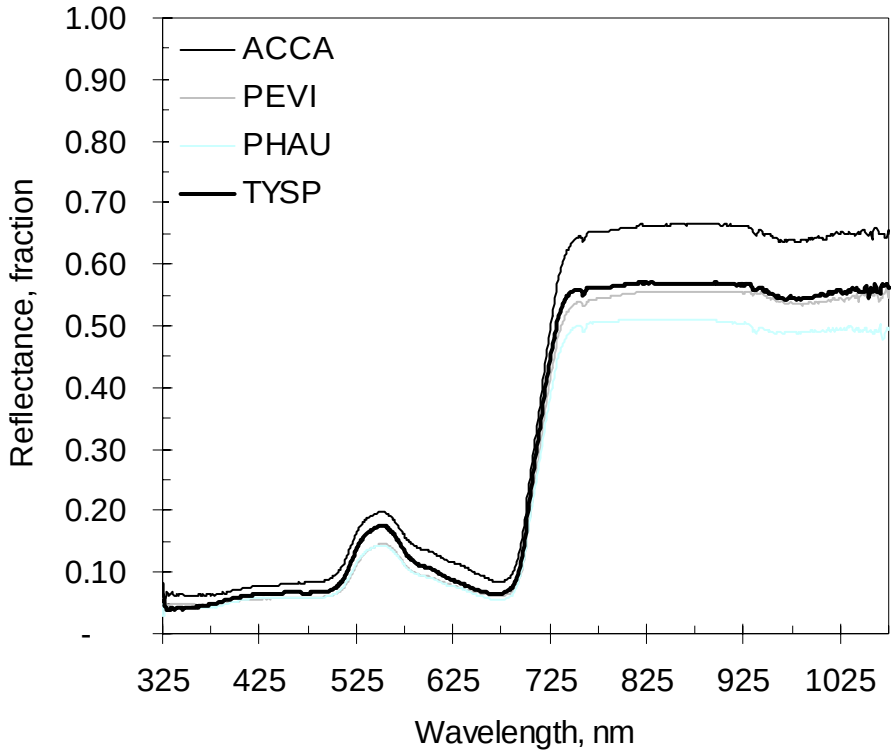

Figure 3.12. Mean reflectance of four emergent freshwater macrophytes prior to N-fertilization (7/15/04). n=15 per species.

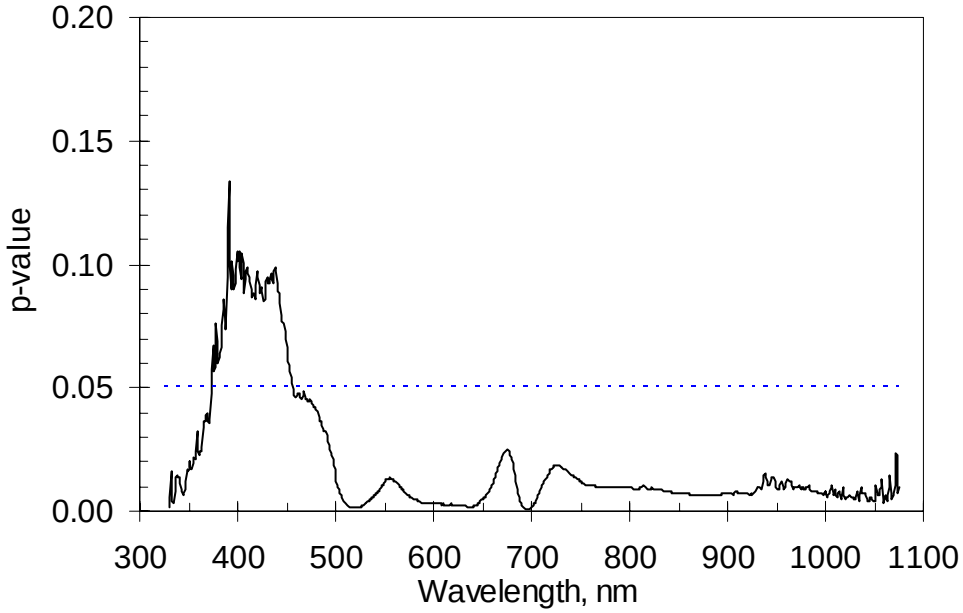

Figure 3.13. Significance of effect of species on spectral reflectance of four wetland species prior to fertilization (7/15/04). Species as fixed factor ANOVA

a) *A. calamus - P. virginica*

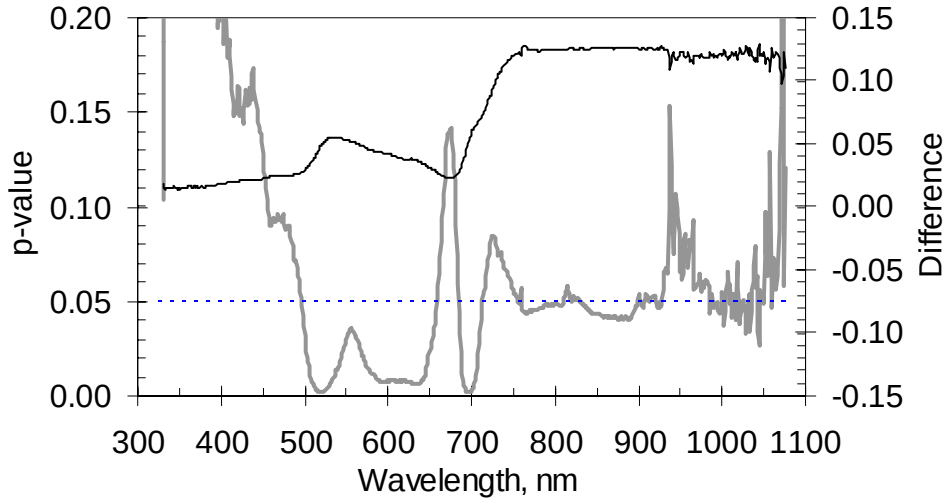

b) *A. calamus - P. australis*

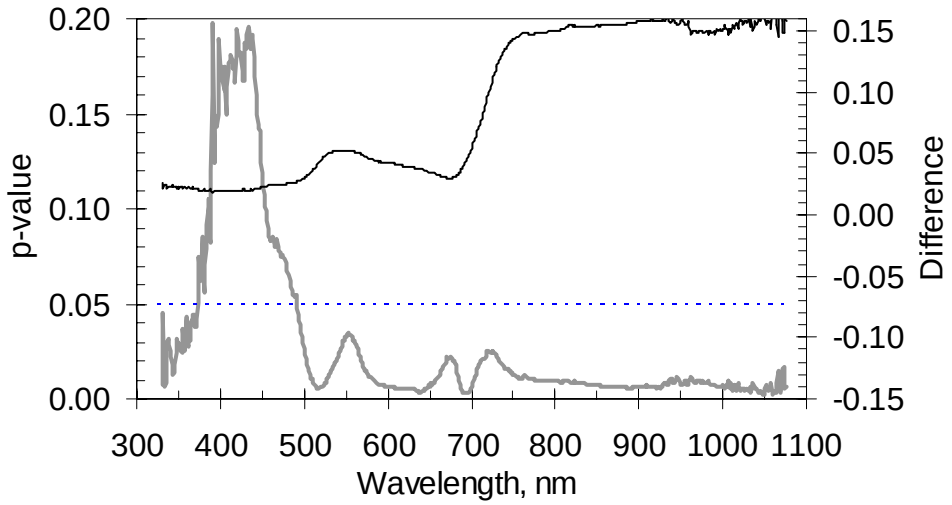

c) *A. calamus - Typha* spp.

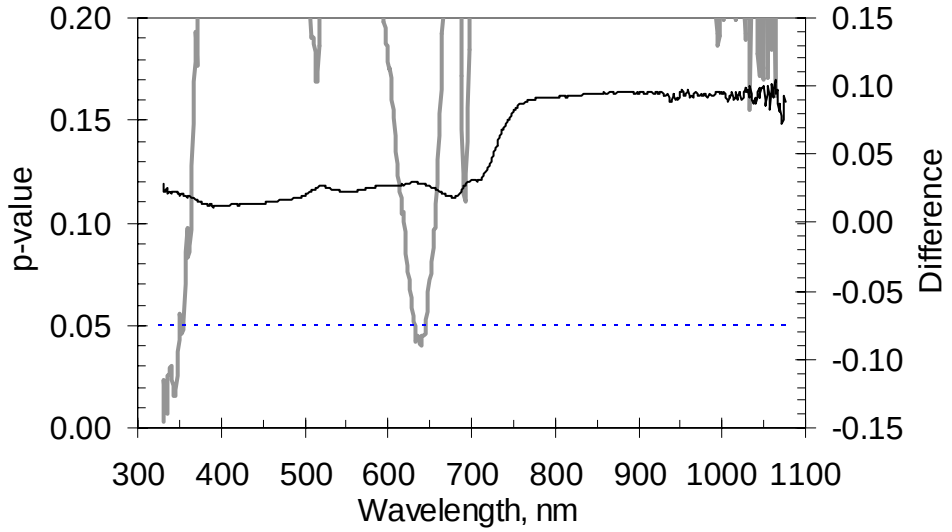

d) *P. virginica - P. australis*

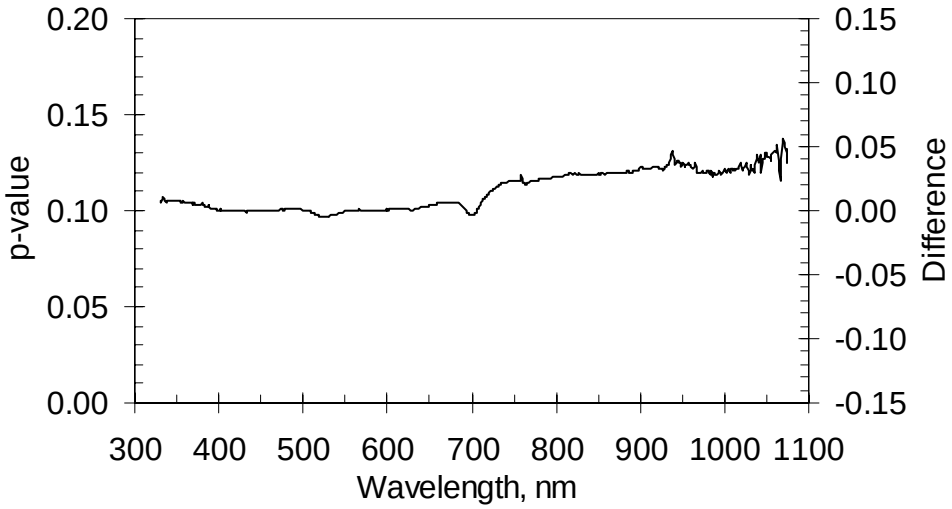

e) *P. virginica - Typha* spp.

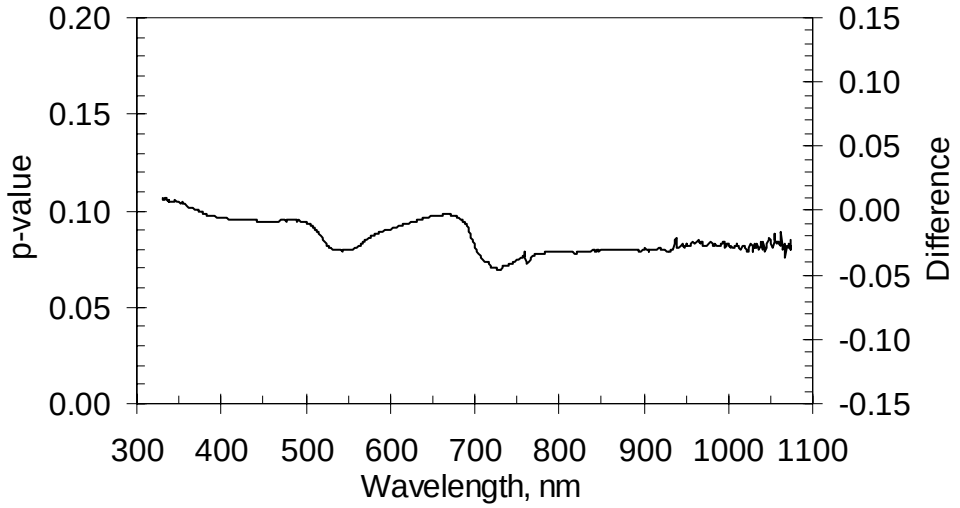

f) *P. australis - Typha* spp.

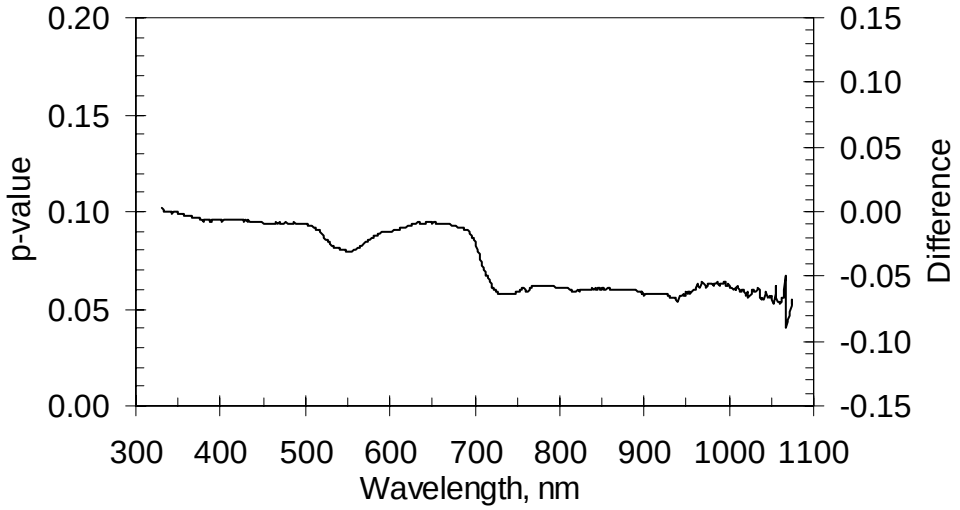

Figure 3.14. Mean difference in spectral reflectance for each two-way species comparison and its significance as estimated with Bonferroni's multiple comparison test for the four wetland species prior to fertilization (7/15/04).

3.3 Effects of N and species on reflectance post-fertilization

Fig. 3.15a shows that nitrogen, species, and their interaction had a significant effect on reflectance across the spectrum 49 d after initiating fertilization. The only exceptions were the effect of N on several NIR bands greater than 1000 nm and the 357 nm UV band, and the interaction effect at the extreme ends of the spectrum. Grouping *Acorus* and *Peltandra* together and *Phragmites* and *Typha* together reduced much of the effect of species and the nitrogen x species interaction (Fig. 3.15b,c). For the *Acorus+Peltandra* group, the main effect of species was non-existent with no spectral bands exhibiting a significant effect (Fig. 3.15b). The effect of the nitrogen x species interaction was reduced greatly with only the blue (400-500 nm) and a portion of red (650-680 nm) wavebands significantly affected (Fig. 3.15b). Nearly all spectral bands showed a significant response to N in the *Acorus+Peltandra* group with a less distinct

response in the NIR. Similarly, the main effect of species for the *Phragmites+Typha* group was removed when the two species were analyzed separately and the nitrogen x species interaction was restricted to the NIR wavebands (Fig. 3.15c). All spectral bands between 400 and 1050 nm were affected by N treatments for the *Phragmites+Typha* group.

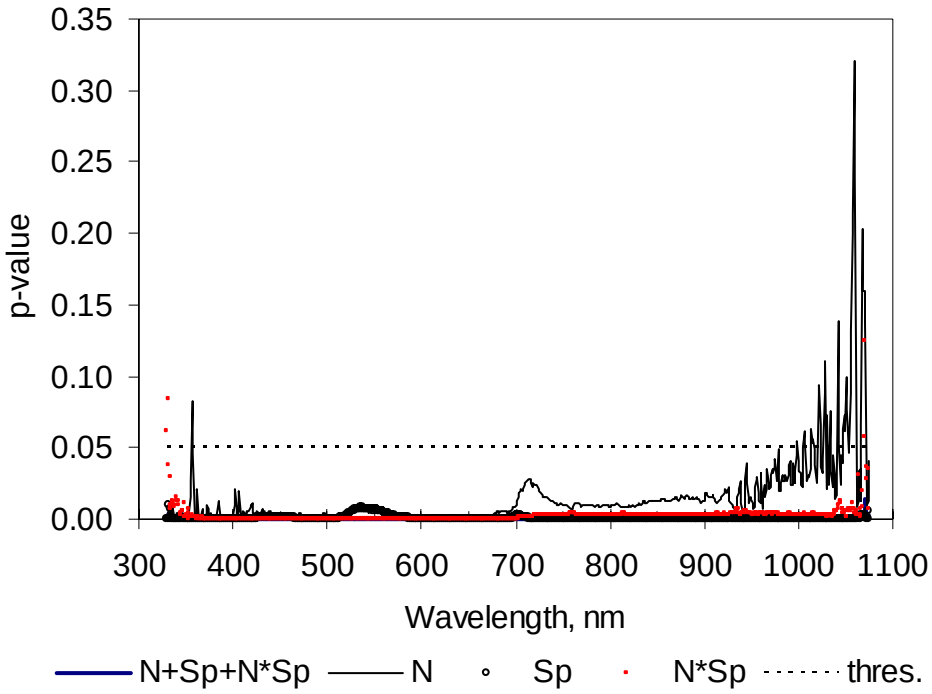

(a)

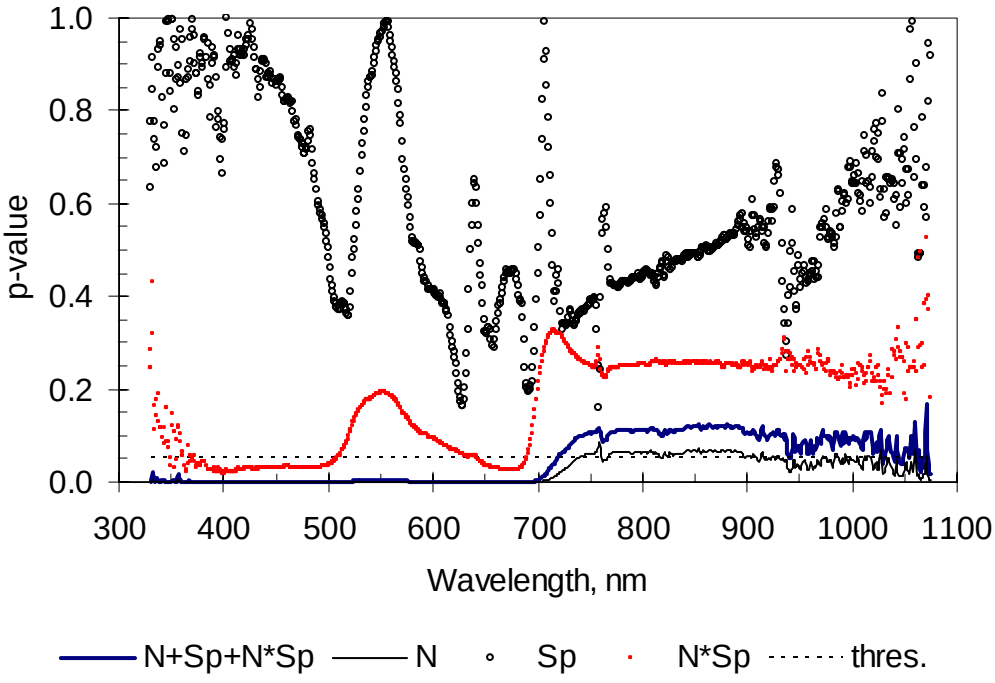

(b)

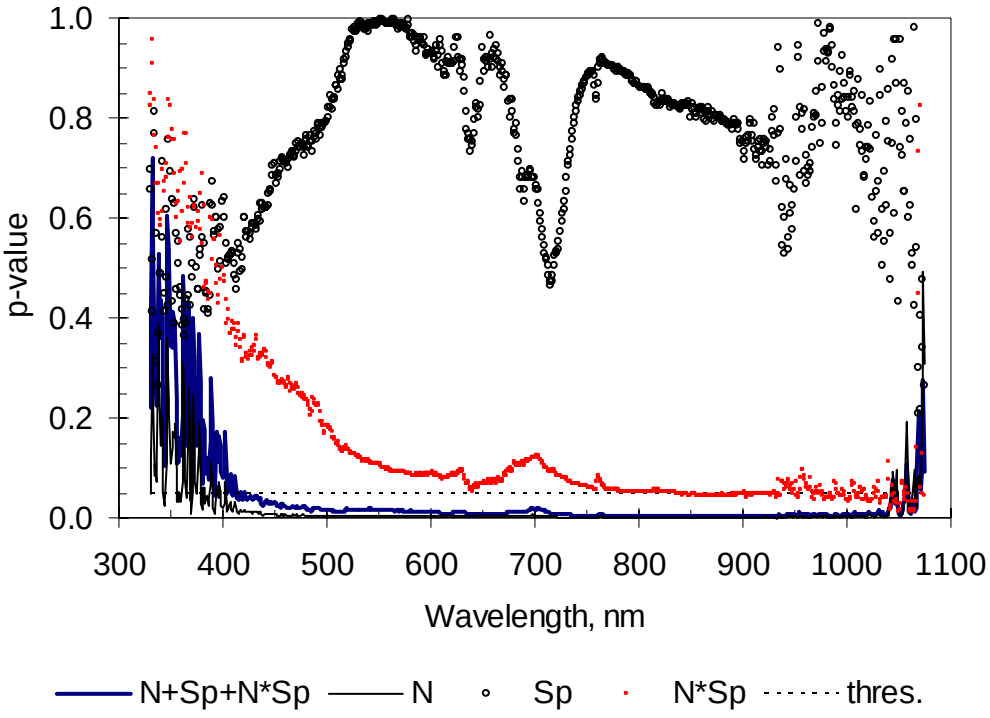

(c)

Figure 3.15. Significance of effects of nitrogen (N), species (Sp) and their interaction on reflectance 49 d after initiation of N fertilization for (a) all 4 species, (b) Acorus and Peltandra, and (c) Phragmites and Typha. (n=15 per species, except Typha n=14; thres = threshold of significance at p=0.05).

Fig. 3.16 shows the difference in spectrum reflectance between pair-wise nitrogen treatments for each 1 nm spectral band and the significance of the difference (Bonferroni's test). There were no significant differences across the spectrum for the 0N/1N comparison (Fig. 3.16a), but the mean NIR reflectance of the higher N treatment was 5 to 6% greater. Similarly, there was no significant difference between the 0N and 2N treatments (Fig. 3.16b), but there were faint indications of differences in the chlorophyll bands (400-460 and 610-680 nm) beginning to arise. The most significant difference was observed at 388 nm for the 0N/2N comparison. The contrast between 0N and 5N revealed a significant difference in the NIR at 756-760 waveband, but no difference in VIS wavebands (Fig. 3.16c). The UV bands at 341 and 348 nm were significantly different for the 0N/5N comparison, while the most likely different VIS bands were located around 671 nm, which is in the chl bands. All VIS bands, except for the green 533-556 nm waveband, reflected less for the 20N treatment compared to the 0N control, but there was no difference in NIR (Fig. 3.16d). The contrast between 1N and 2N treatments revealed significant differences only in a few NIR bands (951, 1020, 1038-40, 1046-47, 1061-62, 1066, 1074 nm) (Fig. 3.16e). The most likely VIS bands to be different were centered about 665 nm (p=0.17) and 487 nm (p=0.34), which are either in or adjacent to chl sensitive bands. There was no difference between the 1N and 5N treatment across the spectrum, except for 2 UV bands (332 and 348 nm, Fig. 3.16f), but the most likely different VIS band was centered about 663 nm (p=0.46). VIS bands for the 20N treatment reflected less than the 1N treatment (Fig. 3.16g). The majority of the UV bands (51 out of 70) also reflected less for the 20N treatment compared to the 1N, but the only NIR band to exhibit a difference was 1062-66 nm (Fig. 3.16g).

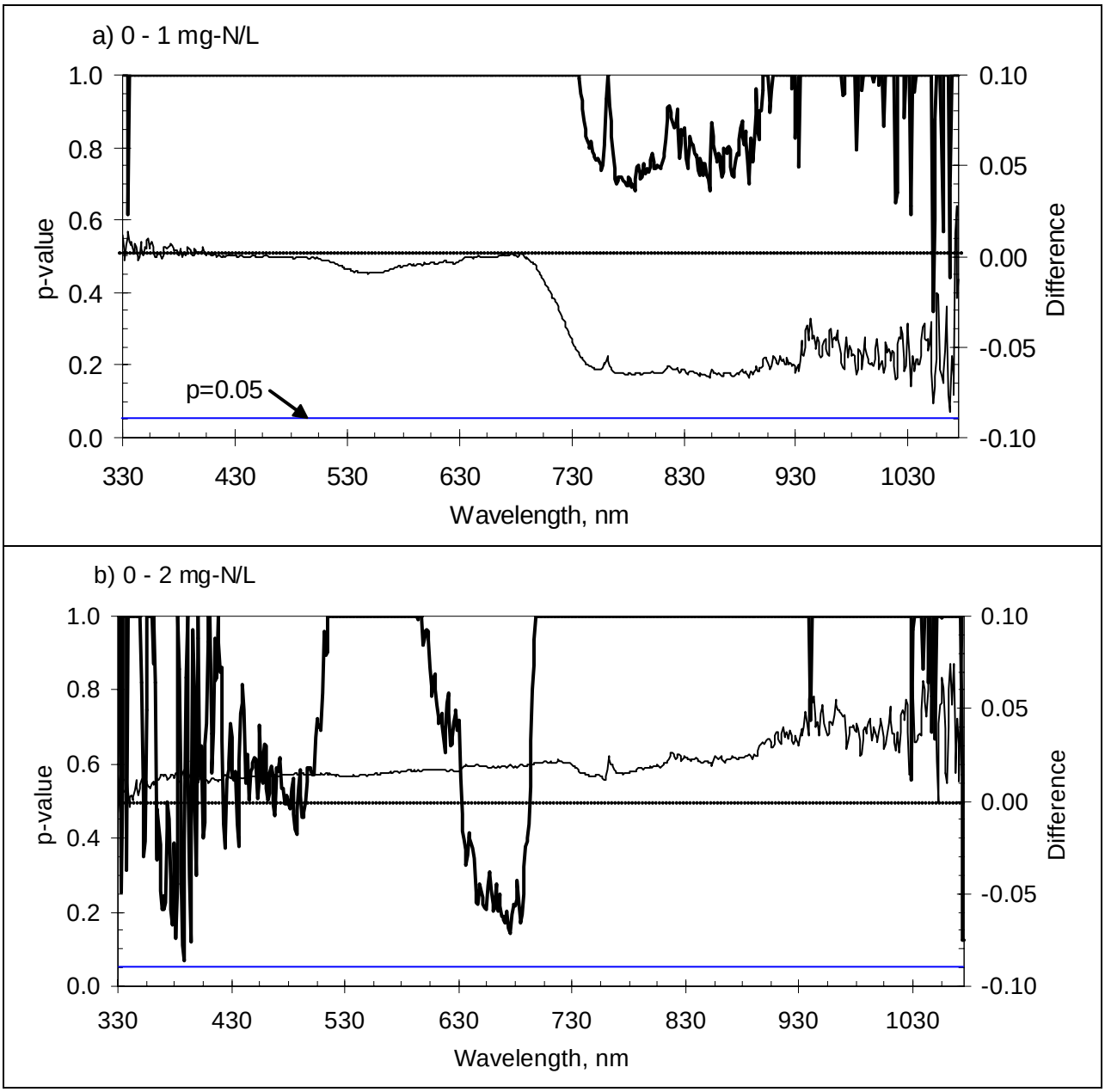
a) 0 - 1 mg-N/L
p-value
Difference
p=0.05
Wavelength, nm
1.0
0.8
0.6
0.4
0.2
0.0
0.10
0.05
0.00
-0.05
-0.10
330
430
530
630
730
830
930
1030
b) 0 - 2 mg-N/L
p-value
Difference
Wavelength, nm

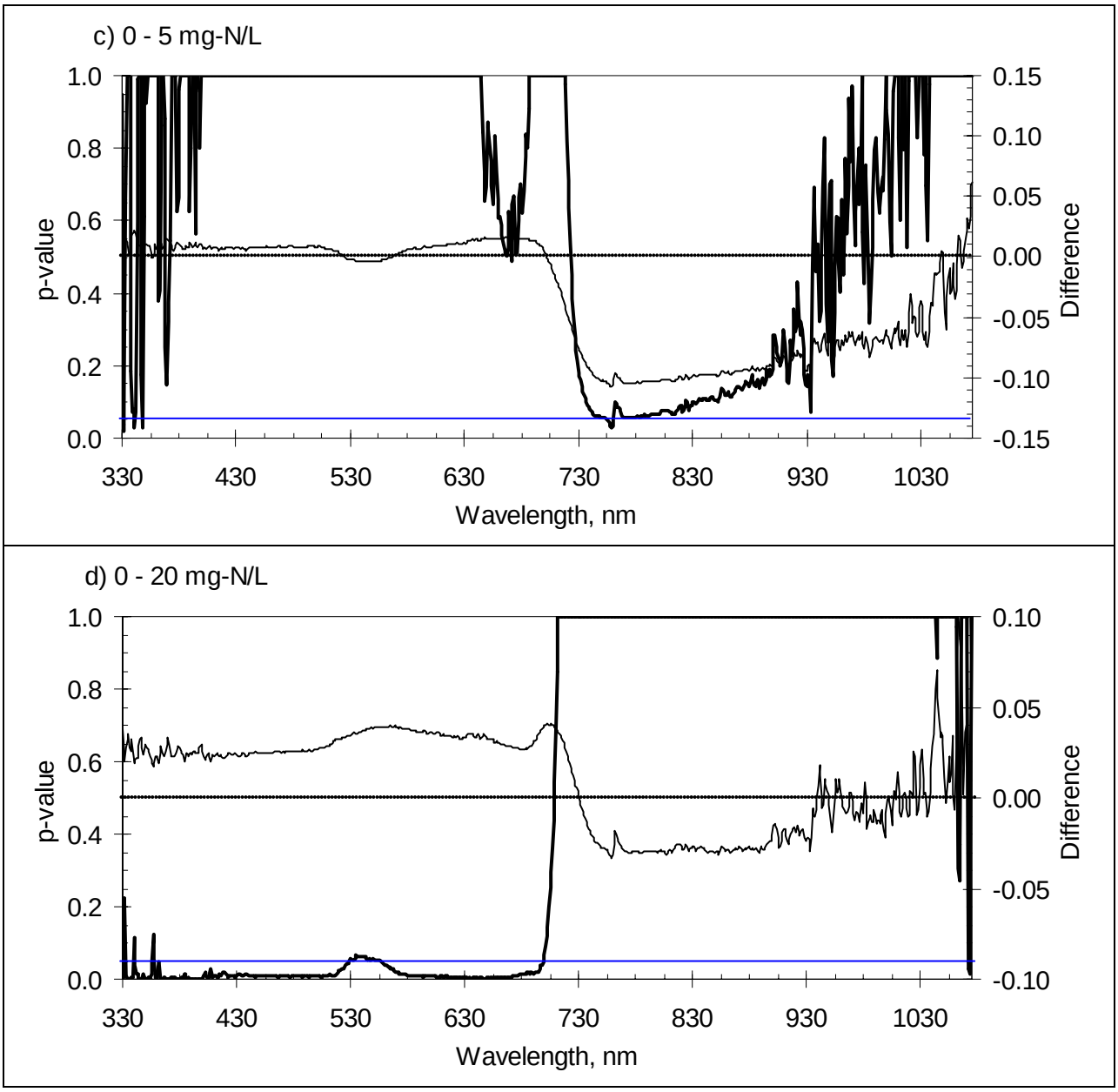
c) 0 - 5 mg-N/L
p-value
Difference
Wavelength, nm
1.0
0.8
0.6
0.4
0.2
0.0
0.15
0.10
0.05
0.00
-0.05
-0.10
-0.15
330
430
530
630
730
830
930
1030
d) 0 - 20 mg-N/L
p-value
Difference
Wavelength, nm
1.0
0.8
0.6
0.4
0.2
0.0
0.10
0.05
0.00
-0.05
-0.10
330
430
530
630
730
830
930
1030

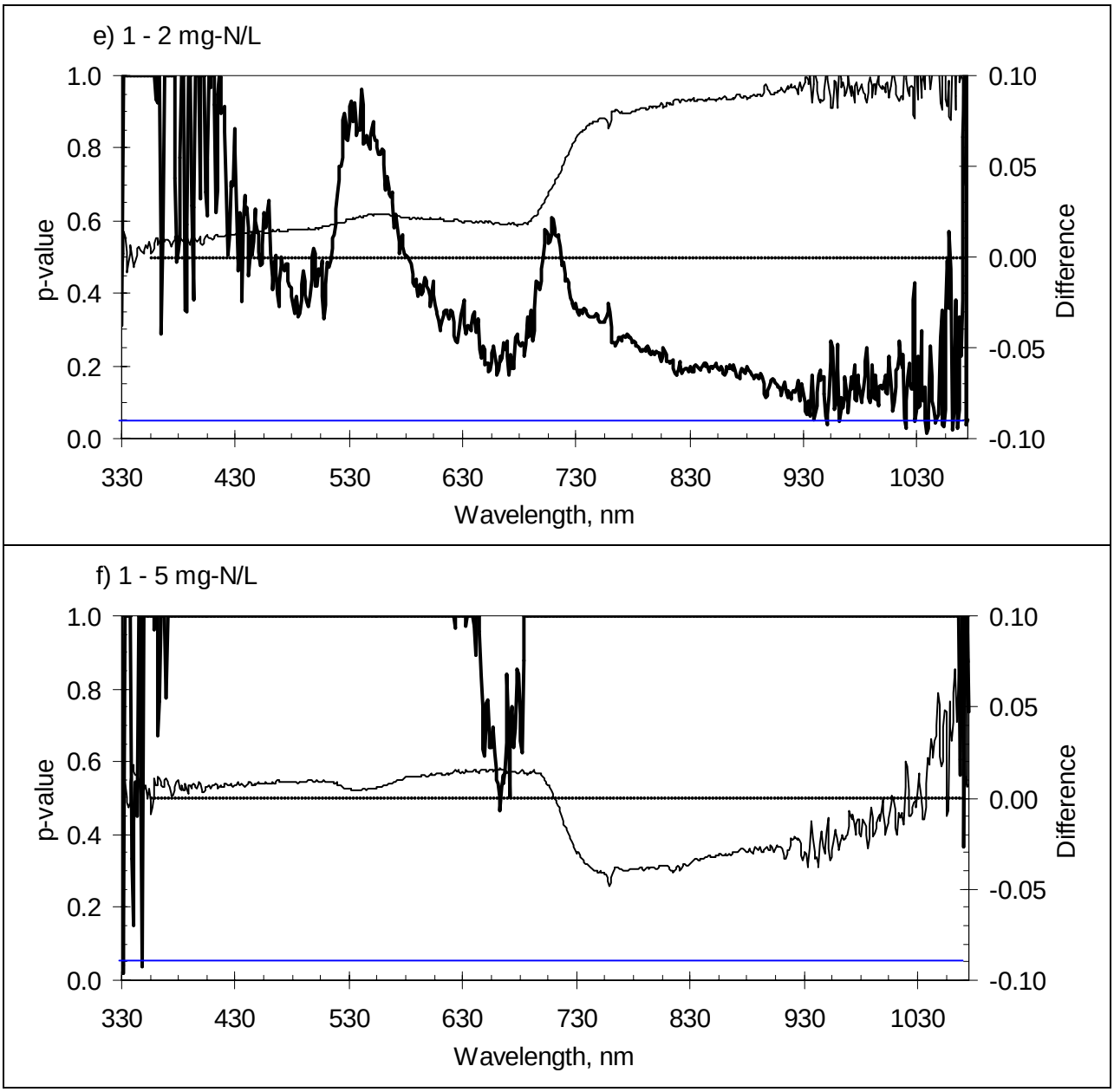
e) 1 - 2 mg-N/L
p-value
Difference
Wavelength, nm
1.0
0.8
0.6
0.4
0.2
0.0
0.10
0.05
0.00
-0.05
-0.10
330
430
530
630
730
830
930
1030
f) 1 - 5 mg-N/L
p-value
Difference
Wavelength, nm

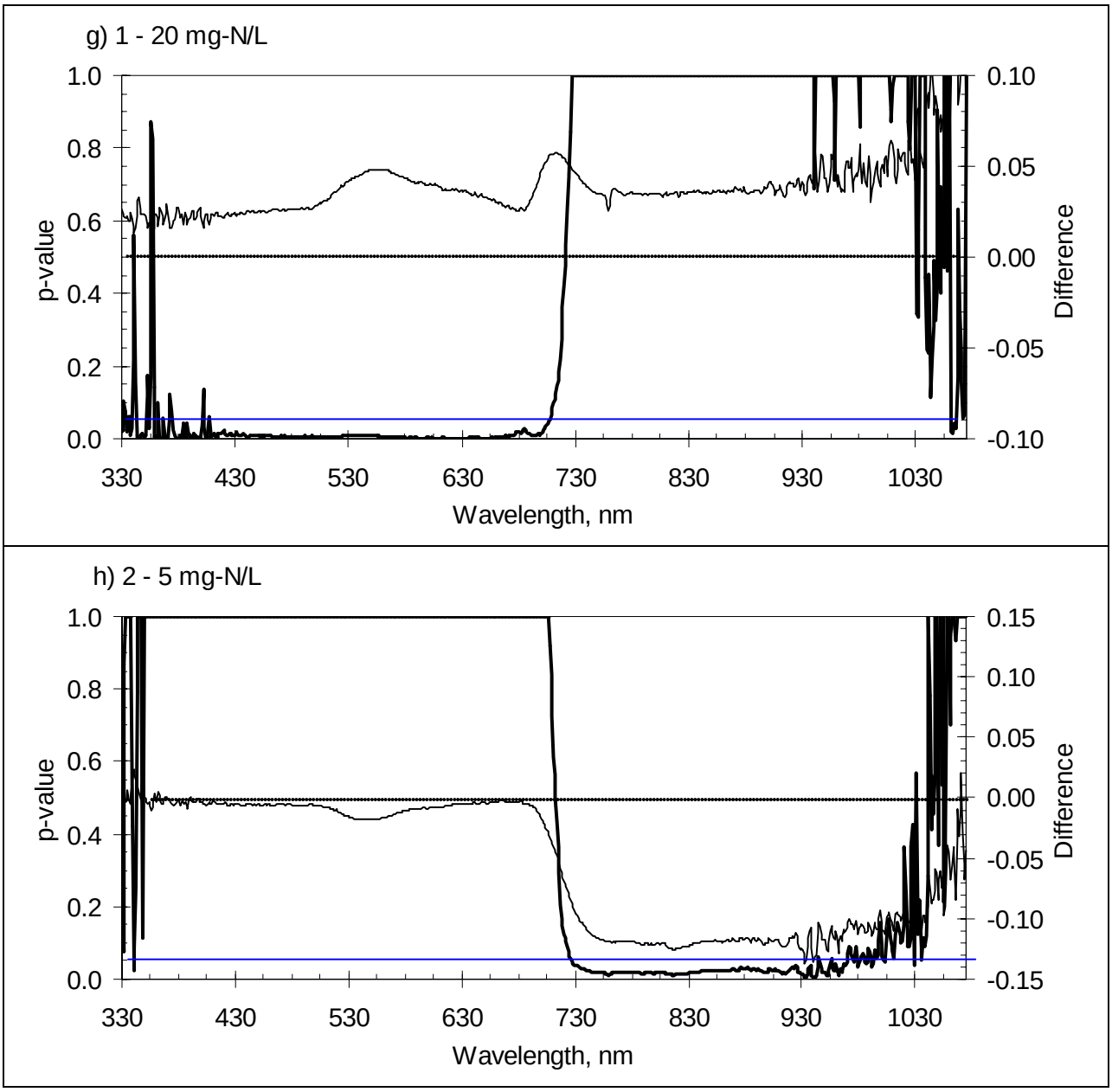
g) 1 - 20 mg-N/L
p-value
Difference
Wavelength, nm
1.0
0.8
0.6
0.4
0.2
0.0
0.10
0.05
0.00
-0.05
-0.10
330
430
530
630
730
830
930
1030
h) 2 - 5 mg-N/L
p-value
Difference
Wavelength, nm
1.0
0.8
0.6
0.4
0.2
0.0
0.15
0.10
0.05
0.00
-0.05
-0.10
-0.15
330
430
530
630
730
830
930
1030

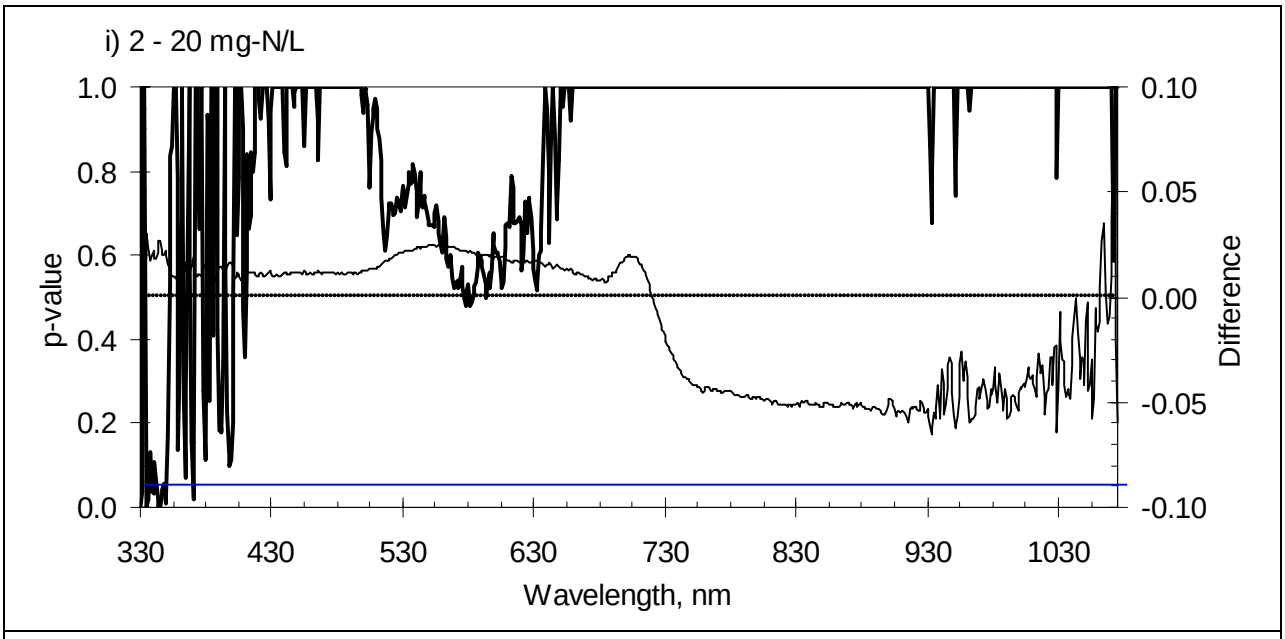

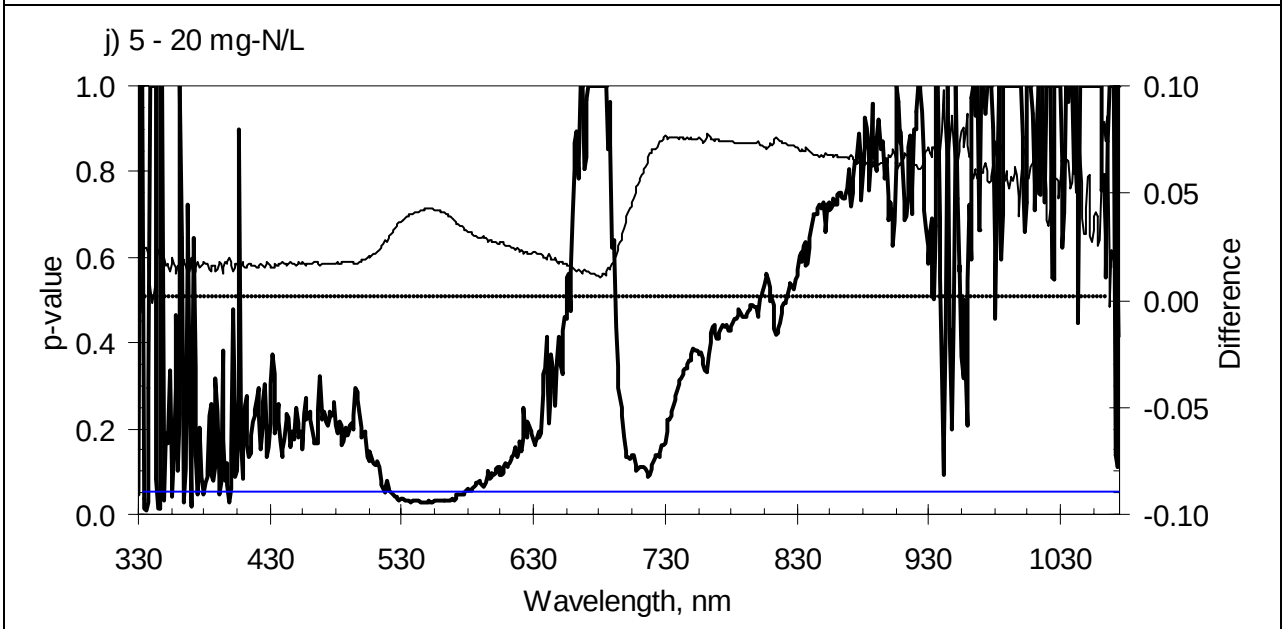

Figure 3.16. Detection of differences among pairwise contrasts of five N treatments using Bonferroni's multiple comparison test in a mixed effects two-factor ANOVA (main effects of species and N) for reflectance measured 35 d after starting fertilization. (a) 0N – 1N contrast, (b) 0N – 2N contrast, (c) 0N – 5 N, (d) 0N – 20N, (e) 1N – 2N, (f) 1N – 5N, (g) 1N –20N, (h) 2N – 5N, (i) 2N – 20N, and (j) 5N – 20N.

In general, plants supplied more N reflected less VIS, but left NIR unaffected (Fig. 3.16). A few NIR bands centered around 780 nm were different for the 0N/5N contrast (Fig. 3.16c) and a majority of NIR bands for the 2N/5N contrast were significantly affected by N (Fig. 3.16h). The VIS difference between the most extreme N treatments (0N and 20N, Fig. 3.16d) ranged from 2 to 4%. VIS differences between the lowest N level (0N) and the 1N, 2N and 5N treatment levels were not significant, but the spectral bands found most significantly different were centered around 670-680 nm (Fig. 3.16b,c).

The 1N level had no spectral bands different from either the 2N or 5N treatments (Fig. 3.16e,f), but reflected significantly more VIS than the highest N treatment (20N) (Fig. 3.16g).

Spectral bands that exhibited significant differences between the highest N treatment (20N) and the next highest (5N) were in the green waveband (530-580 nm) (Fig. 3.16j). A few spectral bands were moderately significantly different in the RE region (718 nm) (Fig. 3.16j).

Unexpectedly, the 10% difference in NIR reflectance (730-970 nm) between the 2N and 5N treatments was significant (Fig. 3.16h).

Fig. 3.17 shows that after N fertilization the reflectance response of the species formed two distinct groups (*Acorus+Peltandra* and *Phragmites+Typha*). That is, *Acorus* had no spectral bands different from *Peltandra* (Fig. 3.17a) and *Phragmites* had no bands different from *Typha* (Fig. 3.17f). However, nearly all of *Acorus*' spectrum exhibited more reflectance than *Phragmites* (Fig. 3.17b) and *Typha* (Fig. 3.17c). *Peltandra*'s reflectance spectrum was also less than that of *Phragmites* (Fig. 3.17d) and *Typha* (Fig. 3.17e), except for small wavebands centered about 530 nm and 700 nm. Notably the significant differences spanned the entire spectrum, including UV, VIS and NIR bands.

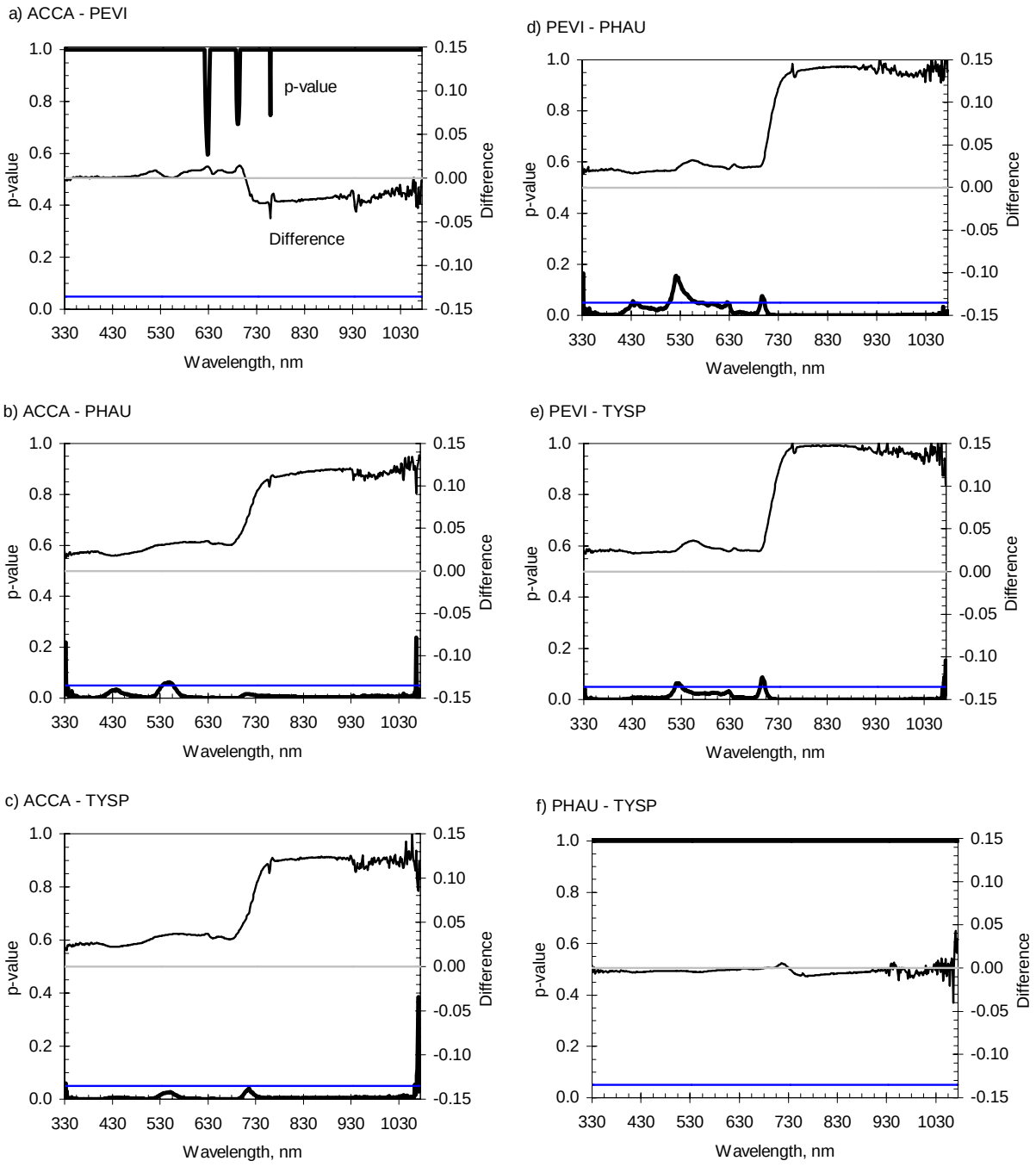

Figure 3.17. Significance of mean difference in spectral reflectance between species after nitrogen fertilization based on mixed effects two-factor ANOVA (main effects of species, nitrogen) and Bonferroni's test with n=15 for each species except Typha with n=14. (ACCA-Acorus, PEVI-Peltandra, TYSP-Typha, PHAU-Phragmites)

Phragmites and *Typha* are generally considered invasive wetland plants that tend to dominate vegetative composition in high nutrient or disturbed marshes. Their reflectance patterns, which were distinctly similar (Fig. 3.17f), showed that they reflected 2.5 to 4% less VIS irradiance and from 10 to 15% less in the NIR than the two non-invasive wetland species (*Acorus* and *Peltandra*). By reflecting less solar radiation after fertilization, *Phragmites* and

Typha are exhibiting a greater ability to capture and, presumably, transform energy, which likely contributes greatly to their superior ability to compete against other species under high N availability.

3.4 Partial Least Squares regression model of N Availability

Fig. 3.18a shows ability of PLS regression model to predict N treatment level. Correlation between prediction and observation was 0.848. Fig. 3.18b compares the RMSE of prediction (i.e., validation) and calibration as a function of the number of latent variables (i.e., PLS-components) included. RMSEC decreases towards 0.0, while RMSEP exhibited a local minimum at 12 PLS-components, which was the number of components included for the model shown in Fig. 3.18a.

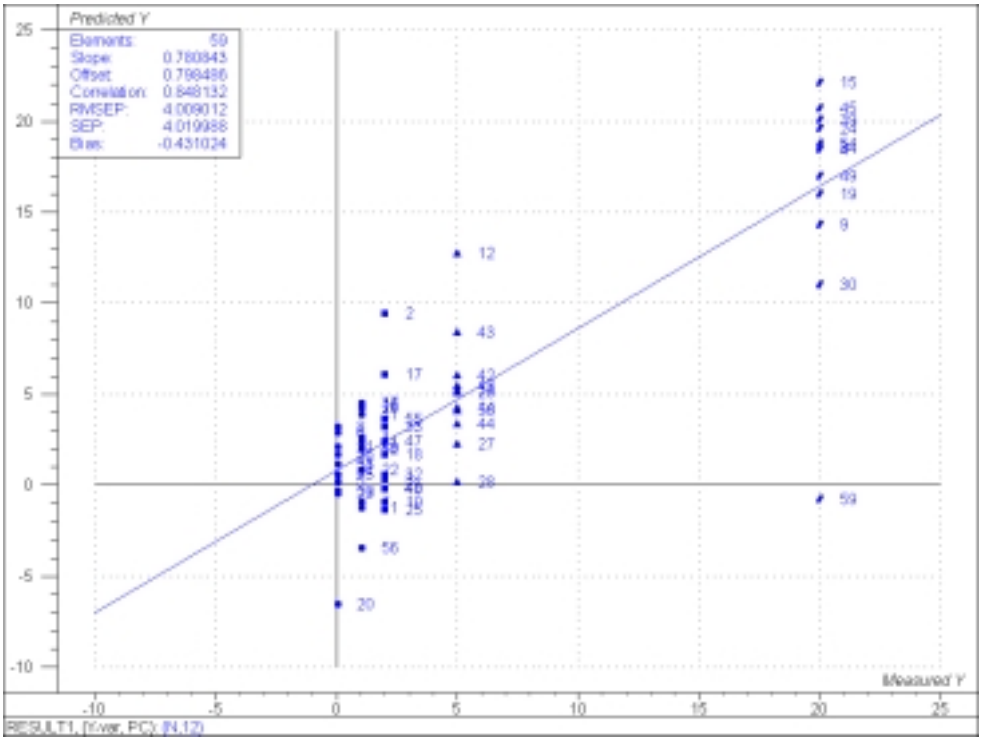

(a)

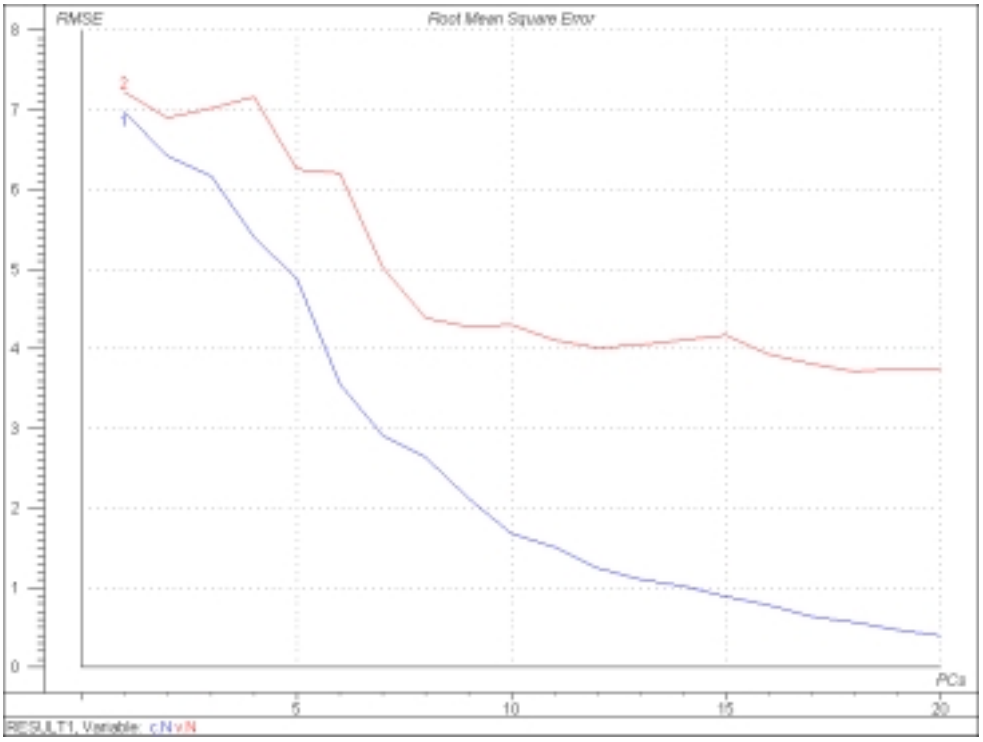

(b)

Figure 3.18. Predictive vs. observed N treatment level based on PLS of difference in reflectance between before and after fertilization for 59 samples (1 sample was lost) using full cross validation to select 12 PLS-components (a) and RMSE of prediction (line 2) and calibration (line 1) as a function of PLS components.

4 Ancillary Project Benefits

Our proposed research project supported the program objectives of the MWRRC by (1) exploring new ideas in wetland remote sensing and wetland water quality monitoring, (2) fostering the research of a new scientists (Tilley is an assistant professor), (3) training graduate and undergraduate students in the new technology and (4) exposing the public to wetland radiometry. Our research developed information helpful toward protecting and enhancing the water quality and habitat of natural marshes, especially marshes of the Chesapeake Bay watershed, Mid-Atlantic region and the nation.

A benefit of developing the reflectance models was to form a solid foundation for scaling the radiometric technique to canopy scale applications which can eventually lead to aerial or satellite remote sensing specifically focused on cost-effective monitoring and assessment of emergent marsh N availability. Use of a hypespectral wetland radiometry for assessing elevated N concentrations in emergent marshes may provide a valuable tool for detecting non-point source (NPS) pollution. Because the position of wetlands in the landscape is often between farms and rivers, wetlands frequently receive surface runoff and groundwater discharge containing excess nitrogen from agricultural operations. Remote sensing would allow rapid screening of large areas of wetlands, potentially identifying “hot-spots” where wetlands are in a eutrophic state due to agricultural runoff. Identifying these major sources of NPS, which has traditionally been very difficult, would allow for directed application of environmental management techniques to reduce nitrogen in runoff and groundwater. This capability will benefit society by improving science-based management of agricultural operations to reduce impacts on coastal resources. Locally, this is important since agriculture has been implicated as

the predominant cause of eutrophication in the Chesapeake Bay (Jaworski et al. 1992; Chesapeake Bay Program 1995).

By 2012 States will be required by the U.S. Environmental Protection Agency to report on the water quality conditions and ecological health of wetlands. Thus, development of the proposed sensor technology is timely and will have a significant impact on state monitoring strategies and capabilities.

MWRRC grant funds supported one Master's graduate research assistant (GRA) and partially-funded one undergraduate assistant. In addition, students enrolled in our Wetlands Ecology (ENBE 450) and Restoration Ecology (NRMT 489F) courses were given demonstrations of the technology. The public was introduced to the technology at the University's annual Maryland Day event in April 2005, which resulted in about 100 people seeing the technology. Thus, a total of about 25 college students were introduced to the technology. We are planning to demonstrate the radiometer system to state environmental managers this summer. We have received additional funding from the Washington, D.C. chapter of The Nature Conservancy and from the University of Maryland Agricultural Experiment Station.

5 Literature Cited

Ahmed, M., 2001. Spectral reflectance patterns of wetland vegetation along a water quality gradient in a self-organizing mesohaline constructed wetland in south Texas. M.S. thesis, Texas A&M University—Kingsville. 80 pp.

Anderson, J.E. and J.E. Perry, 1996. Characterization of wetland plant stress using leaf spectral reflectance: Implications for wetland remote sensing. Wetlands 16(4):477-487.

Boegh, E. H. Soegaard, N. Broge, C.B. Hasager, N.O. Jensen, K. Schelde, A. Thomsen, 2002. Airborne multispectral data for quantifying leaf area index, nitrogen concentration, and photosynthetic efficiency in agriculture. Remote Sensing of Environment 81:179-193.

Carter, G.A., R.L. Miller, 1994. Early detection of plant stress by digital imaging within narrow stress-sensitive wavebands. Remote Sensing of Environment 50(3):295-302

Chesapeake Bay Foundation. 1996. Nanticoke River watershed-natural and cultural resources atlas. Chesapeake Bay Foundation, Annapolis, MD.

Chesapeake Bay Program. The state of the Chesapeake Bay. CBP/TRS 260/02, EPA 903-R-02-002. 2002. Annapolis, Maryland, Environmental Protection Agency.

Clarke, E., and A.H. Baldwin, 2002. Responses of wetland plant species to ammonia and water level. Ecological Engineering 18: 257-264.

Crawley, M. J. 1997. Biodiversity. Pages 595-632 in M. J. Crawley editor. Plant Ecology. Blackwell Science, Oxford.

DiTommaso, A., and L. W. Aarssen. 1989. Resource manipulations in natural vegetation - a review. Vegetatio 84: 9-29.

Esbensen, K.H., 2002. Multivariate Data Analysis in Practice: An introduction to multivariate data analysis and experimental design (5th Ed.). CAMO Technologies, Woodbridge. 598 pp.

Fenn, M. E., M. A. Poth, J. D. Aber, J. S. Baron, B. T. Bormann, D. W. Johnson, A. D. Lemly, S. G. McNulty, D. E. Ryan, and R. Stottlemyer. 1998. Nitrogen excess in North American ecosystems: Predisposing factors, ecosystem responses, and management strategies. Ecological Applications 8: 706-733.

Froidefond, J., L. Gardel, D. Guiral, M. Parra, J. Ternon, 2002. Spectral remote sensing reflectances of coastal waters in French Guiana under the Amazon influence. Remote Sensing of Environment 80:225-232

Gamon, J.A., C.B. Field, W. Bilger, O. Bjorkman, A.L. Fredeen, J. Penuelas, 1990. Remote-sensing of the xanthophyll cycle and chlorophyll fluorescence in sunflower leaves and canopies. Oecologia 85(1): 1-7

Gamon, J.A., L. Serrano, J.S. Surfus, 1997. The photochemical reflectance index: an optical indicator of photosynthetic radiation use efficiency across species, functional types and nutrient levels. Oecologia 112:492-501

Grime J. P. 1979. Plant strategies and vegetation processes. Wiley, London.

Jago, R.A., M.E.J. Cutler and P.J. Curran, 1999. Estimating Canopy Chlorophyll Concentration from Field and Airborne Spectra. Remote Sensing of Environment, 68(3):217-224.

Jaworski, N. A., P. M. Groffman, A. A. Keller, and J. C. Prager. 1992. A watershed nitrogen and phosphorus balance: The Upper Potomac River Basin. Estuaries 15: 83-95.

Kahru, M., B.G. Mitchell, 1998. Spectral reflectance and absorption of a massive red tide off southern California. J. Geophysical Research-Oceans 103(C10):21601-21609

Koponen, S., J. Pulliainen, K. Kallio, M. Hallikainen, 2002. Lake water quality classification with airborne hyperspectral spectrometer and simulated MERIS data. Remote Sensing of Environment 79:51-59

Levine, J. M., J. S. Brewer, and M. D. Bertness. 1998. Nutrients, competition and plant zonation in a New England salt marsh. Journal of Ecology 86: 1-8.

MDNCWG, 2001. Maryland's Interim Nutrient Cap Strategy. Maryland Nutrient Cap Workgroup. http://www.dnr.state.md.us/bay/tribstrat/nutrient_cap.html visited: June 18, 2003.

McCormick J., and H. A. Somes, Jr. 1982. The Coastal Wetlands of Maryland. Maryland Department of Natural Resources, Coastal Zone Management, Jack McCormick and Associates, Inc., Chevy Chase, MD.

Mitsch W. J. and J. G. Gosselink. 2000. Wetlands, Third edition. Third edition. John Wiley and Sons, New York.

Morris, J. T. 1991. Effects of nitrogen loading on wetland ecosystems with particular reference to atmospheric deposition. Annual Review of Ecology and Systematics 22: 257-279.

Odum W.E., Smith III T.J., Hoover J.K. & McIvor C.C. The ecology of tidal freshwater marshes of the United States east coast: A community profile. FWS/OBS-83/17, 1-177. 1984. Washington, D.C., U.S. Fish and Wildlife Service.

Odum, W. E. 1988. Comparative ecology of tidal freshwater and salt marshes. Annual Review of Ecology and Systematics 19: 147-176.

Penuelas, J., I. Filella, S. Elvira, R. Inclan, 1995. Reflectance assessment of summer ozone fumigated Mediterranean white pine seedlings. Environmental and Experimental Botany 35(3):299-307

Penuelas, J., I. Filella, J.A. Gamon, C. Field, 1997. Assessing photosynthetic radiation-use efficiency of emergent aquatic vegetation from spectral reflectance. Aquatic Botany 58:307-315

Read, J.J., L. Tarpley, J.M. McKinion, K.R. Reddy, 2002. Narrow-waveband reflectance ratios for remote estimation of nitrogen status in cotton. J. Environ. Qual. 31:1442-1452.

Simpson, R. L., R. E. Good, M. A. Leck, and D. F. Whigham. 1983. The ecology of freshwater tidal wetlands. BioScience 33: 255-259.

Smith, M.L., M.E. Martin, L. Plourde, S.V. Ollinger, 2003. Analysis of hyperspectral data for estimation of temperate forest canopy nitrogen concentration: comparison between an airborne (AVIRIS) and a spaceborne (Hyperion) sensor. *IEEE Transactions on Geoscience and Remote Sensing* 41(6):1332-1337

Strachan, I.B., E. Pattey, J.B. Boisvert, 2002. Impact of nitrogen and environmental conditions on corn as detected by hyperspectral reflectance. Remote Sensing of Environment 80:213-224.

Stumpf, R.P., 2001. Applications of satellite ocean color sensors for monitoring and predicting harmful algal blooms. Human and Ecological Risk Assessment. 7(5):1363-1368

Szilagyi, J., 2000. Can a vegetation index derived from remote sensing be indicative of areal transpiration? Ecological Modelling 127:65-79

The Nature Conservancy. Nanticoke River Bioreserve Strategic Plan. 1998. Chevy Chase, MD, Maryland and District of Columbia Field Office and Delaware Field Office. Ref Type: Report

Thiemann, S., H. Kaufmann, 2000. Determination of chlorophyll content and trophic state of lakes using field spectrometer and IRS-1C satellite data in the Mecklenburg Lake District, Germany. Remote Sensing of Environment 73:227-235

Tilley, D.R., M. Ahmed, J. Son, H. Badrinarayanan, 2003. Hyperspectral reflectance of emergent macrophytes as an indicator of water column ammonia in an oligohaline, subtropical marsh. *Ecological Engineering* 21(2-3): 153-163.

Tilley, D.R., A.H. Baldwin, E. Poynter, 2004. Hyperspectral Reflectance of Freshwater Tidal Emergent Macrophytes as a Remote Sensing Tool for Assessing Wetland Nitrogen Status. Progress Report to Maryland Sea Grant College (R/CT-03)

Tilley, D.R., M. Ahmed, J. Son (in review). Detection of salinity stress in coastal freshwater marshes from narrow spectral reflectance bands.

Tiner R. W. 1993. Field guide to coastal wetland plants of the southeastern United States. The University of Massachusetts Press, Amherst, Massachusetts.

Tiner R.W. & Burke D.G. Wetlands of Maryland. 1-193. 1995. U.S. Fish and Wildlife Service, Ecological Services, Region 5, Hadley, Massachusetts and Maryland Department of Natural Resources, Annapolis, Maryland. Ref Type: Report

Townsend, P.A, J.R. Folster, R.A. Chastain, Jr., W.S. Currie, 2003. Application of imaging spectroscopy to mapping canopy nitrogen in the forests of the central Appalachian Mountains using Hyperion and AVIRIS. IEEE Transactions on Geoscience and Remote Sensing 41(6):1347-1354

Treitz, P.M., P.J. Howarth, 1999. Hyperspectral remote sensing for estimating biophysical parameters of forest ecosystems. Progress in Physical Geography 23(3):359-390

USEPA, 2002a. National Water Quality Inventory 2000 Report. U.S. Environmental Protection Agency, Office of Water, EPA-841-R-02-001. Washington, D.C.

USEPA, 2002b. National recommended water quality criteria: 2002. EPA 822-R-02-047. U.S. Environmental Protection Agency, Office of Water, Office of Science and Technology, Washington, DC.

Vitousek, P. M., J. D. Aber, R. W. Howarth, G. E. Likens, P. A. Matson, D. W. Schindler, W. H. Schlesinger, and D. G. Tilman. 1997. Human alteration of the global nitrogen cycle: sources and consequences. Ecological Applications 7: 737-750.

Wang, D., C. Wilson, M.C. Shannon, 2002. Interpretation of salinity and irrigation effects on soybean canopy reflectance in visible and near-infrared spectrum domain. Int. J. Remote Sens. 23(5):811-824

Wiegand, C.L., A.J. Richardson, 1990a. Use of spectral vegetation indices to infer leaf area, evapotranspiration and yield: I. Rationale. Agron. J. 82:623-629

Wiegand, C.L., A.J. Richardson, 1990b. Use of spectral vegetation indices to infer leaf area, evapotranspiration and yield: I. Results. Agron. J. 82:630-636

Williams, D.J., N.B. Rybick, A.V. Lombana, T.M. O'Brien, R.B. Gomez, 2003. Preliminary investigation of submerged aquatic vegetation mapping using hyperspectral remote sensing. Environmental Monitoring and Assessment 81:383-392

Beneficial reuse of Baltimore Harbor dredgings and coal fly ash in engineering applications and effects on the Chesapeake Bay

Basic Information

Title:	Beneficial reuse of Baltimore Harbor dredgings and coal fly ash in engineering applications and effects on the Chesapeake Bay
Project Number:	2004MD58B
Start Date:	3/1/2004
End Date:	3/1/2005
Funding Source:	104B
Congressional District:	5th District of Maryland
Research Category:	None
Focus Category:	Surface Water, Sediments, Treatment
Descriptors:	None
Principal Investigators:	Ahmet H Aydilek, MD MD

Publication

BENEFICIAL REUSE OF BALTIMORE HARBOR DREDGINGS AND COAL FLY ASH IN ENGINEERING APPLICATIONS AND EFFECTS ON THE CHESAPEAKE BAY

Final report submitted to the USGS/Maryland Water Resources Research Center

Project # 2004MD58B

by

Ahmet H. Aydilek

May 23, 2005

Geotechnical Engineering Program
Department of Civil and Environmental Engineering
University of Maryland
College Park, Maryland 20742

ABSTRACT

Dredged sediments are obtained from the process of dredging coastal areas and harbors in order to maintain navigable waterways. This study focuses on the potential of using dredged sediments as vertical cut-off wall backfill material. Materials used as vertical cut-off wall material are expected to have low hydraulic permeability and good workable characteristics. The Baltimore Harbor dredged sediments used for this study were plastic in nature and finer than the commonly encountered wall materials, and a research study was needed to evaluate their beneficial reuse in such an application.

The objective of this study was to find an appropriate mix of sediment and bentonite that will be able to function as a vertical cut-off wall backfill material. The preliminary tests on the bentonite were carried out for screening purposes and to find an appropriate water content that will satisfy the desired viscosity range. Bentonite was then added to the dredged sediment in ratios of 1%, 2% and 3% of the total dredged sediment weight. The preliminary tests were repeated for each of these mixes to determine applicable trends and at what percentages of bentonite, the viscosity of the mixture was still in the workable range. The 1% bentonite mix was additionally modified with the addition of 5% and 8% fly ash by weight. These mixtures were then subjected to API filter press tests to determine the effect these mixes would have on the hydraulic conductivity. Adsorption testing was also carried out on the dredged sediment and all the mixes to determine their adsorption capacities to see if they can potentially be employed in reactive cut-off wall applications.

The results show that a suitable moisture content and viscosity of the dredged sediments can be obtained that makes it usable in the mix design. Increased bentonite content, to the percent tested (3%), lead to a decrease in the hydraulic conductivity and increased fly ash content, to the percent tested (8%), lead to an increase in the hydraulic conductivity. For the metals tested, an increased bentonite content enhanced the adsorption capacity of the mix and an increased fly ash content diminished the adsorption capacity of the mix. With the appropriate mix design, dredged sediments can serve as an effective inhibitor to the flow of ground water and hence serve as an in-situ containment and remediation system.

TABLE OF CONTENTS

LIST OF FIGURES & TABLES

SECTION 1

INTRODUCTION

Nowadays, due to increasing environmental regulations, there is a focus on using suitable recycled materials for beneficial purposes. This brings us to exploring the potential of dredged sediments as a vertical cut-off wall material. Materials, mainly soil-bentonite mixtures, used in vertical cut-off wall construction are expected to have low hydraulic permeability and good workable characteristics. Vertical barriers are used to limit the flow of groundwater and contain and remove contaminants from sites where necessary. Vertical barriers are often implemented in construction operations where trenching is necessary. Dredged sediments are obtained from the process of dredging coastal areas and harbors in order to maintain navigable waterways. After the sediment has been excavated, it is transported from the dredging site to the placement site or disposal area. Dredged sediments are generally defined as elastic silt with moderate organic content (typically 8%) with a low % of fine sand and clay. The Baltimore Harbor dredged sediments were used for this study and are classified as CH (according to the unified soil classification system (USCS)).

In practice, approximately 400 million cubic yards of sediment must be dredged annually from waterways and ports to improve and maintain the United States (U.S.) navigation system (Palmero & Wilson, 1997). Of this amount, approximately 60 million cubic yards are placed at 108 U.S. Environmental Protection Agency (EPA) designated ocean disposal sites. The remaining 340 million cubic yards are placed in inland, coastal,

or estuarine open water sites, confined disposal sites, or beneficial reuse sites (Palmero & Wilson, 1997). Navigable waterways are needed for trade through U.S. ports as this contributes greatly to the economy. Therefore, alternatives for disposal of dredged material should be looked at from a technical, economic, and environmental point of view.

Until the 1970s, dredging state of the practice focused on efficiency of the dredging operation and production capacity, with an emphasis on economics (Palmero & Wilson, 1997). However, nowadays, with new environmental legislation (since the early 1970s), the state of the practice has evolved to include a wide range of environmental considerations, and so the emphasis has shifted to a balance of economics and the environment. Additionally, sites often need to be remediated before further construction can proceed in current construction practices. Research and development of technologies that involve in-situ containment and treatment are therefore being promoted by industry and the U.S. EPA. Through re-use of dredged material, the number of placement sites and disposal areas and associated environmental concerns should be reduced. In addition, because dredged sediment is a by-product of the dredging industry, the cost of the vertical barrier system can be reduced substantially than if natural resources were used.

The objective of this study is to find an appropriate mix of dredged sediments and bentonite that will be able to function as a vertical cut-off wall backfill material. The preliminary tests on the bentonite were carried out for screening purposes and to find an appropriate water content that will satisfy the desired viscosity range. Bentonite was then added to the dredged sediments in ratios of 1%, 2% and 3% of the total sediment weight. The preliminary tests were repeated for each of these mixes to determine applicable

trends and at what percentages of bentonite, the viscosity of the mixture was still in the workable range. The 1% bentonite mix was additionally modified with the addition of 5% and 8% fly ash by weight. These mixtures were then subjected to API filter press tests (used as a rigid wall permeameter) to determine the effect of these mixes on the hydraulic conductivity. Adsorption testing was also carried out on the dredged sediment and all the mixes to determine their adsorption capacities in the case that the cut-off wall is intended to act as a reactive barrier.

A literature review about the origin and properties of dredged sediments is given in Section 2. Section 3 includes the materials used in the testing program and the test methods. Practical application of the research work is discussed in Section 4. Results of physical property tests and hydraulic conductivity are presented in Section 5. The adsorption test results are discussed in Section 6. Section 7 is a summary and conclusion of all the results.

SECTION 2 – LITERATURE REVIEW

2.1 – DREDGING PRACTICE TODAY

Dredging means to dig or gather with a dredge (Palmero & Wilson, 1997) – to deepen (a waterway) with a dredging machine. After the sediment has been excavated, it is transported from the dredging site to the placement site or disposal area. Dredging is often carried out using trailing suction hopper dredges, which has three cycles: loading, sailing and unloading or using more modern machinery. The transport operation, most often, is accomplished by the dredge plant or by using additional equipment such as barges, scows, pipeline, and booster pumps. The actual depth to which a channel may be dredged is referenced to an appropriate low water elevation. It may be greater than the authorized depth to accommodate needed vessel clearances, dredging " over depth" also allows for the accuracy of excavation, and provides room for accumulation of material before the next dredging cycle (Palmero & Wilson, 1997). The tendency of the shipping industry is to design and construct larger vessels for increased efficiency. This in turn, requires harbor channels to be periodically deepened, which increases the dredging requirement.

There are three general alternatives that may be considered for placement or disposal of dredged material: open water disposal, confined (diked/ dredged fill containment areas located in an upland environment) disposal, and beneficial use applications. Beneficial reuses involve the placement or use of dredged material for some productive purpose. Generally, beneficial reuse involves either open water or confined placement in some form. Some beneficial reuses involve unconfined disposal, e.g.

wetland creation or beach nourishment. Other disposal methods, such as mine reclamation and aquaculture are occasionally used or considered, but there are usually limitations imposed (Palmero & Wilson, 1997). Dredged material has also been used for landfill capping and lining. Brick manufacture using dredged sediments is another innovation being explored (Hamer & Karius, 2001). Selection of a disposal alternative is made based on considering the technical, economic, and environmental issues. Of the approximately 400 million cubic yards dredged annually in the United States (U.S.), approximately 60 million cubic yards are placed at about 108 Environmental Protection Agency (EPA) designated ocean disposal sites. The remaining 340 million cubic yards are placed in inland, coastal, or estuarine open water sites, confined disposal sites, or beneficial reuse sites (Palmero & Wilson, 1997).

2.2 – TYPES, MINERALOGY AND DEPOSITION OF DREDGED FILL

Dredged fill can be comprised of five soil types: sand; mixed type of soil between sand and clay, sandy silty clay or clayey silty sand; clay; mixed type of soil between clay and rock and rock.

Dredged fill originates from coastal areas, where there is a need to maintain and improve navigable waterways and harbors and therefore dredging operations occur. A few such locations in the United States include the New York/New Jersey Harbor, the Baltimore Harbor in Maryland, the Mobile Harbor in Alabama, the Oakland Harbor in California; and internationally, The River Clyde in Scotland and coastal areas of Grand Cayman. The mineralogy varies somewhat depending on the coastal area from where the sediments are dredged. At the Fort point Channel in Boston, a typical subsurface profile

includes: Miscellaneous Fill (20 Feet), Harbor Bottom Sediments/Organic Deposits (15 feet), Marine Clay (Boston Blue Clay, 80 feet), and Glacial Till (10 feet), overlying argillite bedrock (Fig. 2.1) (Vaghar et al, 1997). In this case there are two separate aquifers, one above and one below the Boston Blue Clay. The water in Fort Point Channel is tidal. At the Houston-Galveston Ship Channel, east of Houston, the soil which forms the upper limit of the Pleistocene Age Formation, is a stiff to very stiff overconsolidated clay material locally referred to as the 'Beaumont Clay'. For the NY/NJ Harbor, the mineralogy of Newton Creek sediment was measured using x-ray diffraction (McLauglin & Ulerich, 1996), (Jones et al, 1997). These results are shown in Table 2.1. The amounts of the organic contaminants in the sediments at Newton creek are shown in Table 2.2.

Regarding deposition, the main aspects to be concerned with on a reclamation area are the bulking, the bearing capacity and the trafficability. In the case of sand, on hydraulic (dredged) fills above the water level, the relative density is 60-70%, (approximately 98% of the normal maximum Proctor density) (Verhoeven et al, 1998). This information is important in calculating the difference in volume between the pit (when there is a good indication of density) and the fill. The trafficability of the fill is dictated by the permeability. Therefore the bearing capacity of wet sands can be misleading (too low) if the amount of fines is increasing or a section of the fill can have a lower bearing capacity than the other because of local separation of fines (Verhoeven et al, 1998).

With clay fill, its behavior is mainly judged from the percentage of lumps in relation to the percentage of slurry. The main aspects, that is, bulking, bearing capacity

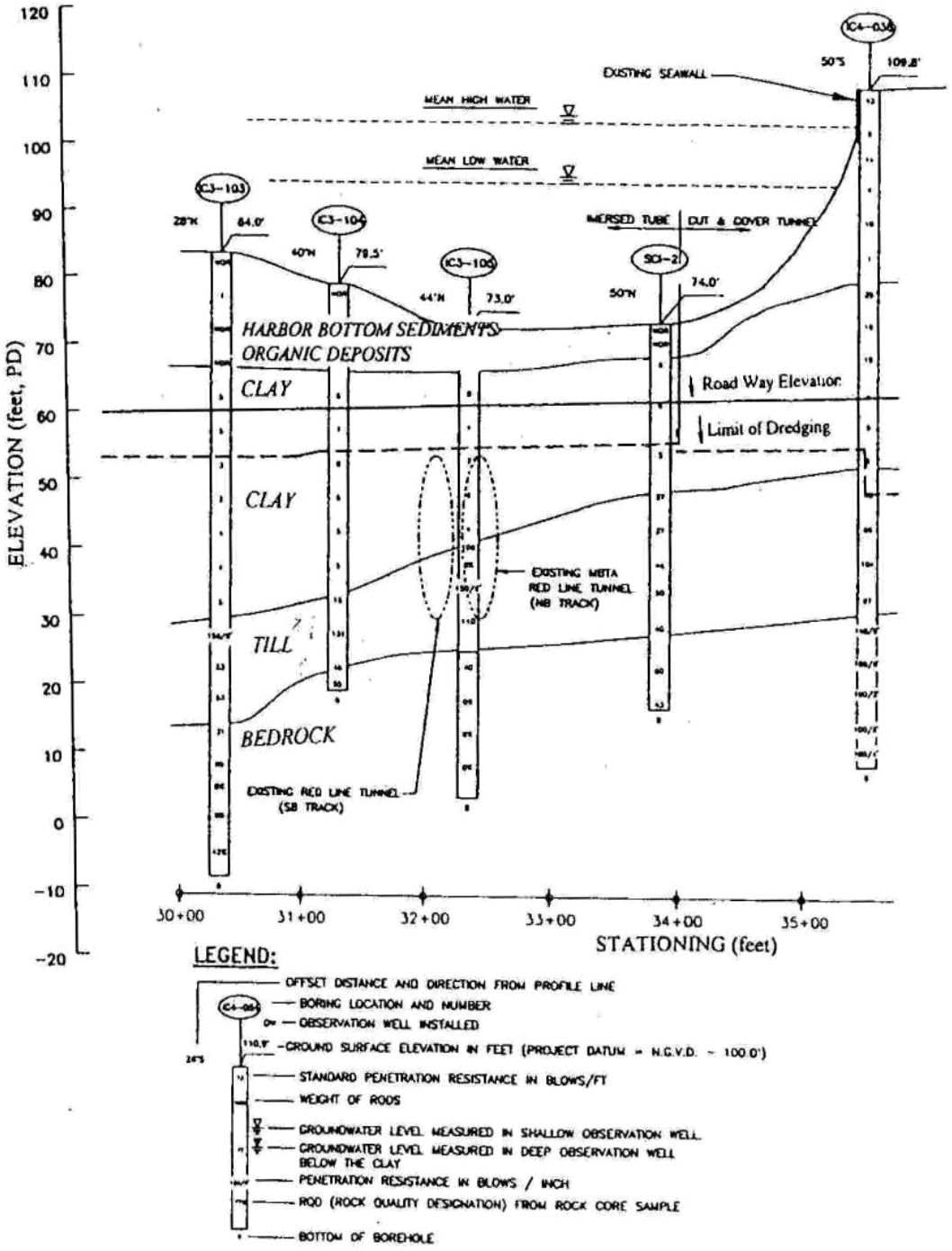

Fig. 2.1 – Fort Point Channel Subsurface Profile
(after Vaghar et al, 1997)

Table 2.1 – Sediment Mineralogy of Newton Creek

Mineral Species	**Chemical Formula**	**Weight Percent**
Quartz	SiO_2	66 to 75
Muscovite (Mica)	$K_2O.2MgO.Al_2O_3.8SiO_2.2H_2O$	11 to 15
Amorphous Phase	Organics	3 to 13
Kyanite	$Al_2O_3.SiO_2$	6 to 7
Hydrated Aluminum Silicate	$19Al_2O_3.173SiO_2.9H_20$	5 to 6
Cronstedtite	$4FeO.2Fe_2O_3.3SiO_2.2H_2O$	4 to 6

Table 2.2 – Summary of Organic Contaminants in Newton Creek Sediments

Contaminant	**Concentration (µg/g dry basis)**
Total Sulfides	7830
Total Organic Carbon (TOC)	73,200
Total Polychlorinated Biphenyls (PCB)	5.26
Total Chlorinated Pesticides	0.462
Total Polyaromatic Hydrocarbon (PAH)	117
Bis-2-ethylhexylphtalate	48.6
Fluoranthene	10.3
Phenanthrene	6.5
Others (24)	51.6
Total Dioxins	0.00645
Total Furans	0.0165

(after McLauglin & Ulerich, 1996)

and trafficability are influenced by this ratio. The bulking of the slurry can be determined from the consistency of the excavated soil and the Atterberg limits. It is assumed that a few days after the reclamation (at the start of consolidation under its own weight), the water content of the slurry is very high (2 to 3 times the liquid limit). The bulking can therefore be calculated from a clay with natural water content to the slurry. The bearing capacity and trafficability of clay fills are usually negligible when considering deposition.

In the case of the rock material, the main aspect concerned with its deposition is the amount of fines. If measures are not taken, a large amount of fines can be transported by the water outside the reclamation area leading to a pollution problem. The bulking can be estimated; the bearing capacity and the trafficability are generally good. Table 2.3, (Verhoeven et al 1998), shows a summary of soil parameters related to the dredging process.

For the mixed soil types, more information needs to be known. This information is needed to determine the soil parameters as similarly done for the clean soils.

Because of the deposition of dredged fill, that is, it is often hydraulically pumped along the banks of rivers or lakes or used to form small islands near dredging sites. In these areas the coarser solids settle from suspension and the excess water, with some suspended solids, then returns to the river/ lake through an overflow weir (Krizek et al, 1997). Problems with this method of disposal are high water content, low shear strength, and high compressibility of the dredged sediments. Therefore a landfill made using these materials would perform ineffectively for long periods of time. Also, the drainage condition at the bottom of the sediment layer has an effect on the consolidation rate during the period of deposition.

Table 2.3 – Summary of (In)direct Test Methods for Determination of Soil Parameters

Properties / Direct Tests	Mechanical/ Physical - A	In Situ Condition - B	Classification/ Identification - C
In situ	perm. probe, vane	dens. probe, pressiometer/dilatometer	field classification
Laboratory	(perm.) (triax.) (adhes.) (rheol.) tests	density/moisture c.	grain size, max/min density, spec. density, mineral comp., Atterberg limits
CORRELATIONS	(A)	(B)	(C)
	($D_{r)}$ –φ б (CPT/SPT)--dil. D_r/fines--k	CPT/SPT -- D_r	CPT/FR --comp.
	(SPT/CPT) (p. pen.) (LI -- C_u) (PI/σ_v) (CPT/FR)		
	(Brass. tens.) (point load) --σ_c		

(after Verhoeven et al 1998)

2.3 – CONVENTIONAL CONSOLIDATION AND STRENGTH PARAMETERS ASSOCIATED WITH DREDGED FILL

The soil properties can be sub-divided into three categories. Mechanical/physical properties, conditional properties and classification properties. The mechanical/ physical properties are associated with resistance (friction), strength and rigidity. Conditional properties include density and moisture content, which depend on stress history in the stages of loosening and deposition. They are important in mixing and transporting the individual particles or lumps (because of their resistance to disintegration and weight). The classification properties are those that are needed for the identification of the soil, that is from the grain-size distribution, the Atterberg limits and the density (maximum/minimum) of the soil.

The initial properties of sediments dredged from the bottom of a harbor are shown in Table 2.4 (Vaghar et al, 1997). The sediments mainly consist of a silt fraction and have an average bulk density of 76.2pcf. The initial water content exceeds 200%. These properties are usual for silty sediments in rivers and seas. (Need to show grain-size distribution chart). These soils are usually of very low strength. For sediments in this state, it is a common practice to add agents for solidification; some include quick lime, flyash, quicklime with ferric chloride and quicklime with calcium chloride. In order to decrease the water content of the mixtures, the pore water is extracted in a press chamber. The experimental results, for the different mixtures and the 'stand-alone' sample are shown in Table 2.5 (Vaghar et al, 1997).

Table 2.4 – Physical Properties of Dredged Harbor Bottom Sediment/Organic Deposits

Property	**Test Method**	**Result**
Bulk Wet Unit Weight	AASHTO T-19	74.2 – 78.1 pcf
Water Content	Modified AASHTO T255	260 – 270%
Specific Gravity of Solids	AASHTO T100	2.26
pH	ASTM D 4972	8 - 9
Organic Content	AASHTO T 267	< 1%
Classification	AASHTO M 145	Low Plasticity Inorganic to Organic SILT

(after Vaghar et al, 1997)

Table 2.5 – Summary of Tests on Dredged Harbor Bottom Sediments/Organic Deposits

T-180 (A) Compaction Conditions						
Additives (% by weight)	**MDD (pcf)**	**OMC (%)**	**Moisture Content (%)**	**Dry Density (pcf)**	**Percent Compaction**	**UU Shear Strength (psf)**
None	85.2	27.7	21.0	78.8	93	3500
7% CaO	80.3	32.2	43.0	70.9	88	5195
7% (CaO/FA 50/50 mix)	82.6	31.6	37.4	76.4	92	4112
5%CaO/ 2% $FeCl_3$	80.6	33.8	49.3	66.5	83	4535
5% CaO/ 2% $CaCl_2$	79.1	34.7	47.2	67.8	86	3688
7% (CaO/HCFA, 50/50 mix)	79.5	32.9	44.7	69.4	87	4663

(after Vaghar et al, 1997)

For the unconfined disposal site at Spilman's Island, located along the Houston-Galveston Ship Channel, east of Houston, the following soil parameters were found. Index properties, moisture content and undrained shear strength profiles are shown for clay fill and dredged sediments are given in Figure 2.2 and Figure 2.3 respectively (Kayyal & Hassen, 1998). The total/wet unit weight profile for clay fill and dredged sediment layers is shown in Figure 2.4 (Kayyal & Hassen, 1998). Figure 2.5 (Kayyal & Hassen, 1998) shows the plasticity chart for dredged sediments compared with clay. From the plasticity chart, the average PI = 75.

The dredged fill for the disposal site at South Blakeley Island (Figure 2.6) (Poindexter & Walker, 1998), was taken from the Mobile Harbor in Alabama. Laboratory tests were done on this material by the Waterways Experiment Station. The soil was classified according to the Unified Soil Classification System (USCS) as a CL-ML, with a liquid limit of 96, a plastic limit of 28, and a specific gravity of 2.7 (Poindexter & Walker, 1998). The self-weight consolidation test and the modified fixed ring consolidometer were used to determine the compressibility and permeability characteristics of the material, which are shown in Figure 2.7 and 2.8 (Poindexter & Walker, 1998) respectively. Predicted layer thickness over time for various drainage efficiency factors for this site is shown in Figure 2.9 (Poindexter & Walker, 1998). They realized though that additional comprehensive field data was needed for thorough model verification and to better correlate empirical model coefficients with field operations.

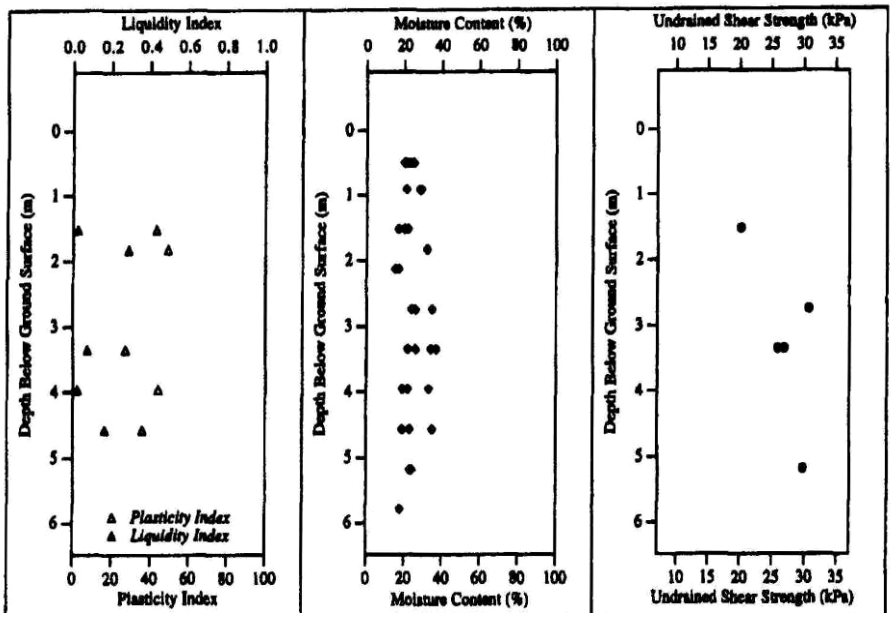

Fig. 2.2 – Index Properties, Moisture Content, and Undrained Shear Strength Profiles for Clay Fill Soil Material

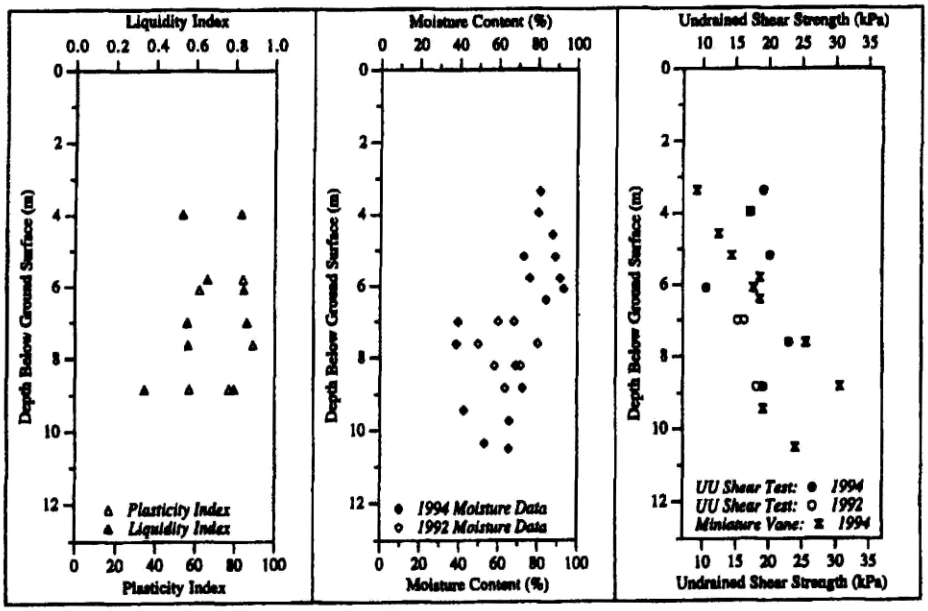

Fig 2.3 - Index Properties, Moisture Content, and Undrained Shear Strength Profiles for Dredged Sediment Soil Material

(after Kayyal & Hassen, 1998)

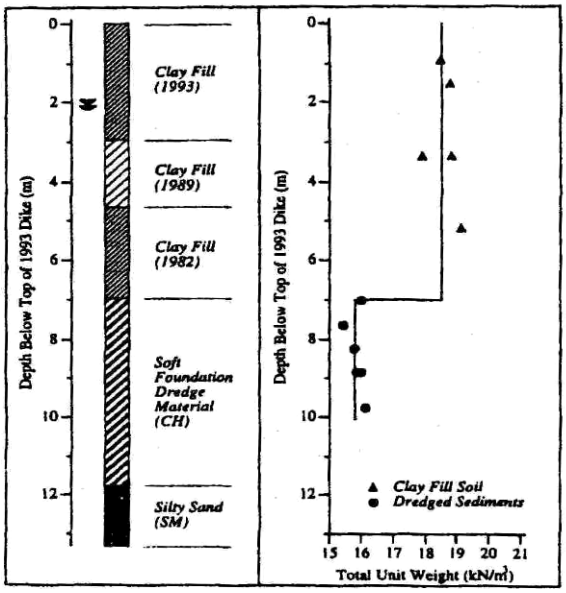

Fig. 2.4 – Total or Wet Unit Weight Profile for Clay Fill and Dredged Sediment Layers

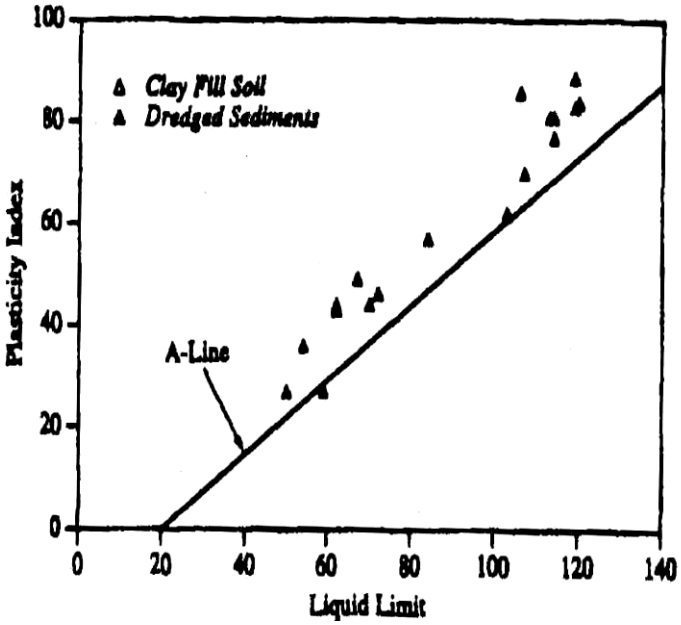

Fig 2.5 – Plasticity Chart for Dredged Sediments and Clay Soil Materials

(after Kayyal & Hassen, 1998)

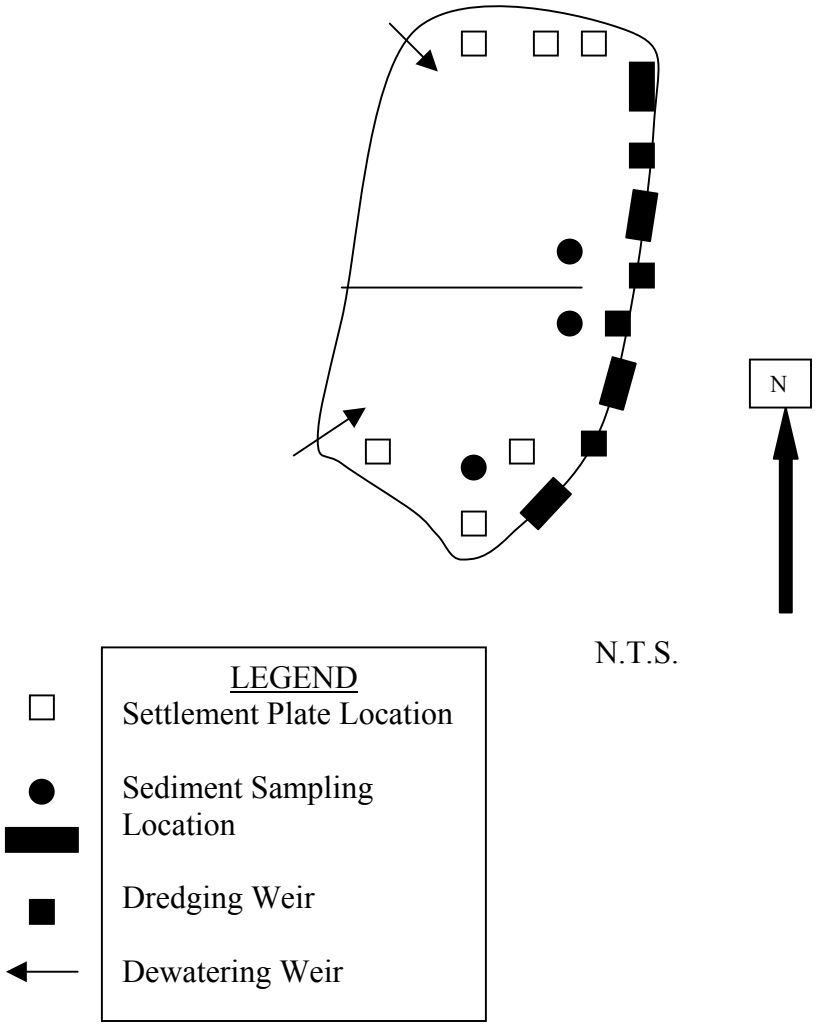

Fig. 2.6 – Configuration of South Blakeley Island Disposal Site
(after Poindexter & Walker, 1998)

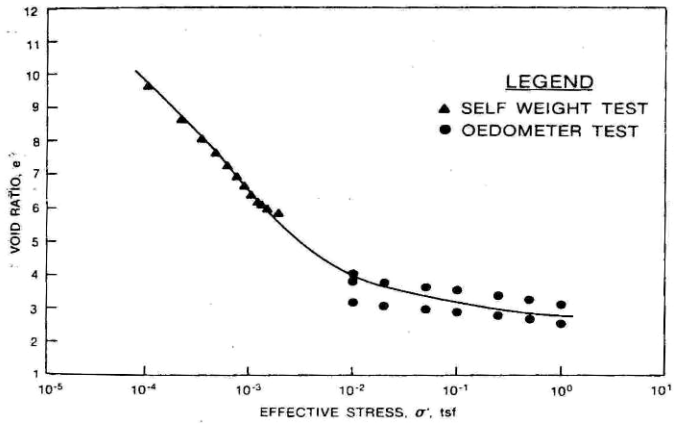

Fig. 2.7 – Compressibility data for Mobile Harbor Sediment

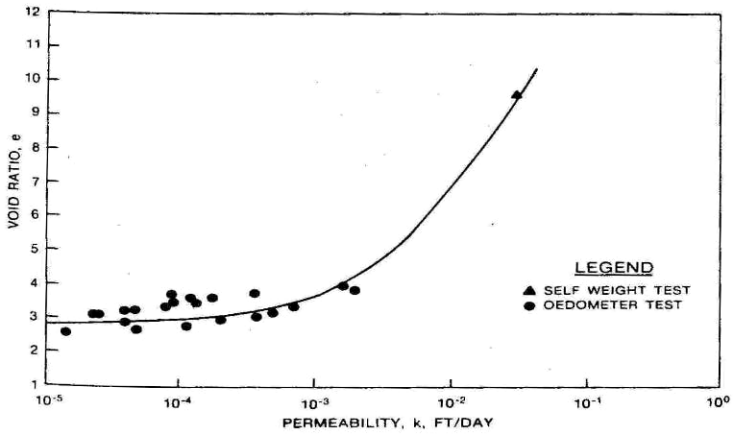

Fig. 2.8 – Permeability data for Mobile Harbor Sediment

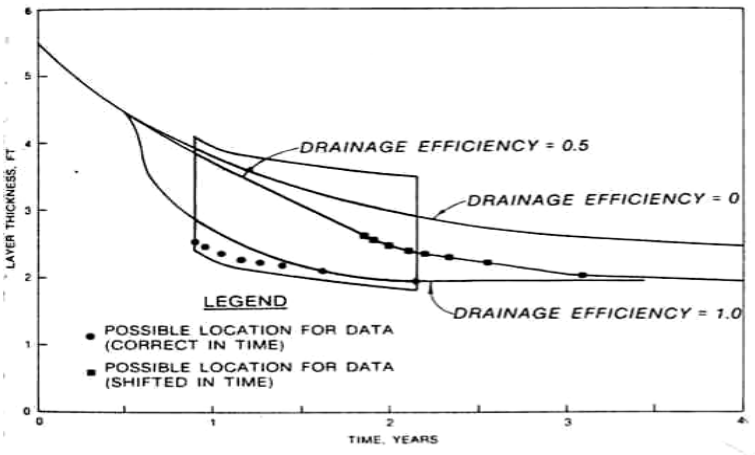

Fig. 2.9 – Predicted layer thickness over time for various drainage efficiency factors (Mobile Harbor Sediment @South Blakely Island)

(after Poindexter & Walker, 1998)

To more clearly understand the changes in water content that happen in sediments during and after the deposition process, a mathematical (empirical) model was developed to describe the flow of water through the consolidating media. The model gives the water content distribution in the fill at any time after the beginning of the deposition process; predicts the consolidation rate of the dredged sediments; and helps to evaluate the different techniques that can be used to accelerate the dewatering process (Krizek et al, 1997). Data was used from a laboratory and field test program done on dredged sediments from the harbor around Toledo, Ohio. These materials were found to have a liquid limit of 70%+_20%, a plastic limit of 35%+_10%, and a sand-silt-clay composition in the ratio of approximately 2:3:1 (Krizek et al 1997). Figure 2.10 (Krizek et al, 1997) shows the relationship for void ratio with coefficient of permeability for these materials. Figure 2.11 (Krizek et al, 1997) shows the characteristic water retention curves.

Concerning volume change characteristics, based on the results from a large number of conventional consolidation tests performed during this experimental program, the compression index Cc of dredged materials was confidently expressed as: $Cc = 0.01 (w - 7) = 0.01(37e - 7)$, where w = weight water content expressed as a percentage; and e = the void ratio (the specific gravity of the solids was assumed to be 2.70).

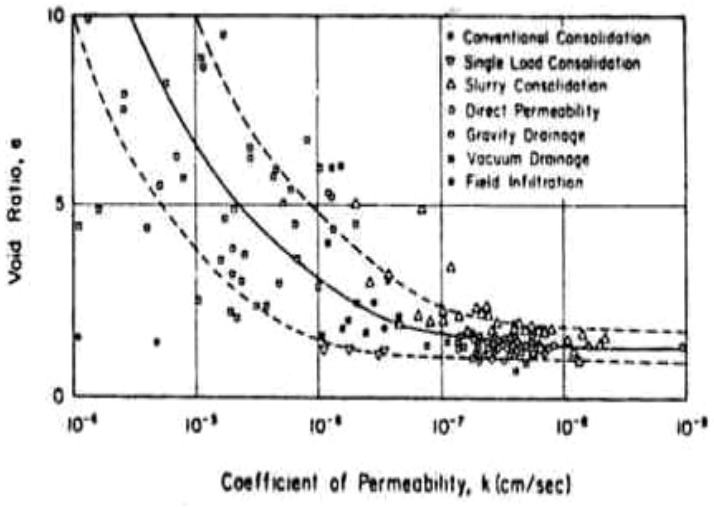

Fig. 2.10 – Summary of Values for Coefficient of Permeability (Toledo, Ohio Sediment)

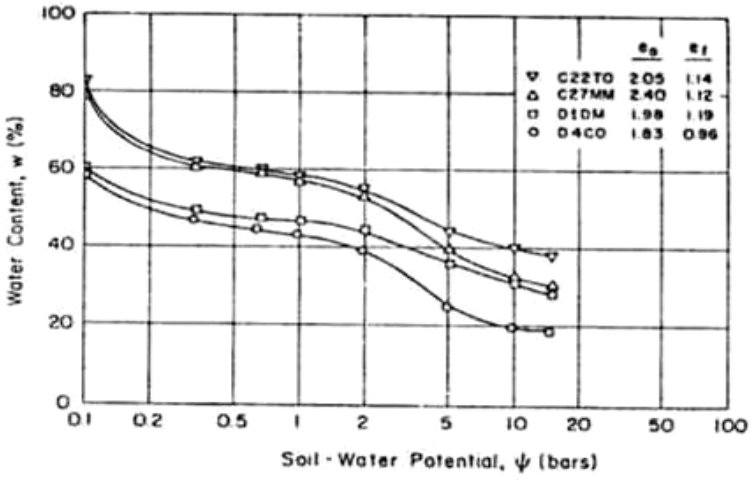

Fig. 2.11 – Characteristic Water Retention Curves (Toledo, Ohio Sediment)

(after Krizek et al, 1997)

2.4 - REVIEW OF RECENT 'BENEFICIAL REUSE' RESEARCH FOR DREDGED SEDIMENTS AND SIMILAR MATERIALS.

It has been established that there are several engineered beneficial reuses for dredged material. These include landfill/brownfield liners and covers, certain transportation applications, levee construction, use as structural and non-structural fill, and recently use as an ingredient in the brick manufacturing process.

The transportation applications that were investigated include reuse of the dredged sediments as roadway material and embankment material. The embankment study seems to be the most thorough, complete study on the reuse of dredged materials to date. This study involved use of the New Jersey dredged sediments. The New Jersey sediments were characterized as MH/OH, defined as an elastic silt with moderate organic content (8%) and they were found to have a low % of fine sand and clay. It was found that it performed satisfactorily as an embankment material. The dredged sediments were mixed with Portland Cement PC (4% and 8%) and fly ash - (in the case that already had the 8% PC). The dredge sediments were dewatered to near optimum moisture content before compaction - (specific % was not given). But in another beneficial reuse study, they mentioned generally dewatering to 85 to 45% water content.

The Baltimore dredged sediments compare with the NJ ones. There is a difference in that the Baltimore sediments are classified as a CH soil. The Baltimore sediments have more fines than the New Jersey ones. Therefore it seems appropriate that the Baltimore sediments would perform satisfactorily under similar circumstances.

In California, investigations are ongoing in terms of the beneficial reuse of dredged sediments for levee construction. Several demonstration projects have been initiated.

Flowable fills are self-leveling liquid-like materials that cure to the consistency of a stiff clay (Abichou et al 1998). Flowable fill is typically made up of sand or foundry sand (which contains bentonite), cement or flyash, and water. It is used for some applications similar to that which soil-bentonite is used for. These applications include use as backfill in utility trenches, building excavations and underground storage tanks. Design mixes are developed to satisfy local and state strength and flow requirements.

Foundry sands, a by product of casting and a mixture of fine sand and bentonite, (an ingredient in flowable fills), can potentially be used as a hydraulic barrier, e.g. in landfill liner and cover materials. A study done by Abichou et al (1998), indicated that foundry sands (green sands) offer a superior barrier than conventional clays and possibly at a lower cost. In order to determine the suitability of soil-bentonite mixes for vertical backfill material applications, it is hypothesized that similar testing can be conducted. The testing (as it relates to dredged sediments) includes determination of index properties and hydraulic conductivity testing.

Paper mill sludge is another material being investigated for its use as a vertical barrier material. A study by Moo-Young et al (2000) focused on the constructability, physical properties, and adsorption potential of paper mill sludge. A similar study was undertaken here with respect to dredged sediments.

This study will focus on the beneficial reuse of Baltimore dredged sediments as vertical cutoff wall backfill material.

2.5 – VERTICAL CUT-OFF WALLS

Vertical cutoff walls are installed in the subsurface to control horizontal movement of groundwater and contaminants (Daniel, 1993). The use of vertical cutoff walls in the subsurface initially began with groundwater control and structural applications in Europe before 1950 (Xanthakos, 1979). Slurry trench cutoff walls have been used in environmental applications since the 1970s and have come into widespread usage since the 1980s as a component in the overall remedial system to control flow of groundwater (Spooner et al., 1984), (Daniel, 1993).

In defining the vertical cutoff wall objectives, it is important to decide whether the barrier is to act as a ground water barrier with low hydraulic conductivity or as a contaminant transport barrier. Depending on the objective of the vertical cutoff wall, different criteria are considered in the design. For instance, if the objective is to minimize the rate of contaminant transport off-site, it is necessary to consider contaminant transport through the wall, potential degradation of the wall, and the consequences of inadequate cutoff wall performance. Also, the environmental control system could include a vertical cutoff wall along with a low permeability cover, groundwater withdrawal system and treatment systems for the pumpage. Vertical cutoff walls often key into a stratum of naturally low hydraulic conductivity. A key is not always necessary or cost effective when contaminated groundwater is being extracted or when the contaminants are concentrated near the ground surface or floating on the water table.

Here we will focus on vertical cutoff walls of low hydraulic conductivity. Typically, low permeability vertical cutoff walls are constructed by installing a vertical

barrier into the subsurface. The vertical wall has a lower hydraulic conductivity than the surrounding formation. The vertical cutoff walls can be divided into groups based on construction methods. Different types of vertical cutoff walls can be constructed using the slurry trench method of excavation and are therefore called 'slurry trench cutoff walls' (Daniel, 1993). In the slurry trench method of construction, a vertical trench is excavated into the subsurface using a slurry, typically of bentonite and water, for trench stability. The slurry is typically a bentonite-water mixture consisting of 5% bentonite and 95% water by weight. Bentonite, a montmorillonitic clay, swells in the presence of water, giving a viscous nature to the fluid and helps in the formation of a filter cake along the walls of the trench. For trench stability, the slurry level is kept at or near the top of the trench, typically within 1m. Trench widths vary between 0.6 and1.5m, with 0.9m trench widths being typical. The completed excavation is then used to form the geometry of the cutoff wall (Daniel, 1993). The completed cutoff wall can consist of soil-bentonite (Millet and Perez, 1981), cement-bentonite (Jefferis, 1981), plastic concrete (Evans et al., 1987), or structurally reinforced concrete (Boyes, 1975). Once the trench is excavated to the desired depth, the bentonite–water slurry is replaced with a (soil)-bentonite backfill with a low hydraulic conductivity. The backfilled trench forms the completed vertical cutoff wall. The backfill optimally consists of a mixture of sand, silt, and clay, and bentonite-water slurry. The soil-bentonite is placed in the trench at a consistency of high slump concrete (100-150mm) (Daniel, 1993). In order to attain this consistency, the material needs to be 'fluidized' by adding bentonite-water slurry to the soil. Figure 2.12 (Evans, 1993) shows a representation of the construction process.

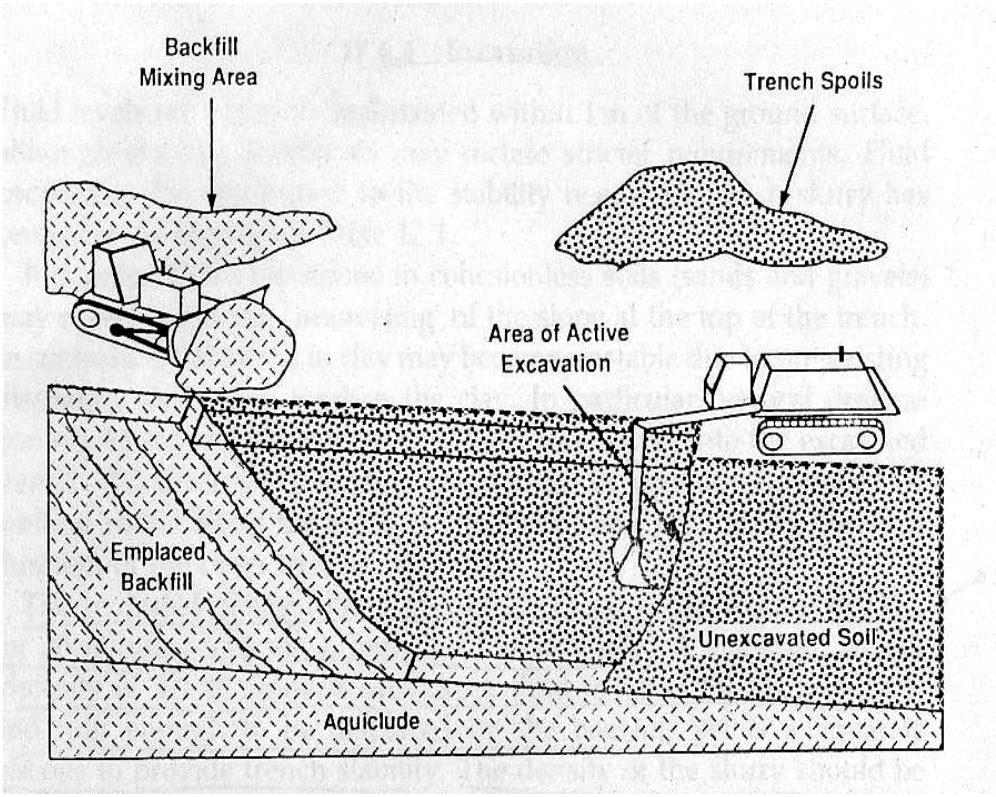

Fig. 2.12 – Excavation of trench and Placement of Soil-Bentonite Backfill
(after Evans, 1993)

Cutoff walls using the soil-bentonite backfill method of slurry trench construction were first used in the U.S. in the early 1940's (Daniel et al, 1994). In general terms, soil-bentonite slurry trench cutoff walls are among the least expensive techniques available in the U.S. for vertical barriers in the subsurface. Here we will be focusing on such soil-bentonite cutoff walls, with the possibility of substituting the soil with dredged sediments from the Baltimore Harbor. After evaluating the hydrogeologic and geotechnical aspects of the site, it is necessary to determine the appropriate properties for the soil-bentonite cutoff wall. During the feasibility studies, it is important to determine the short-term and long-term performance of the cutoff wall. That is, it is necessary to determine its properties in terms of hydraulic conductivity, strength, and compressibility. One needs to determine if these properties are satisfactory to meet the objectives of the project in the short-term as well as the long-term.

In this case, we will determine specific parameters of the Baltimore dredged sediment-bentonite slurry. These will be compared with typical parameter values of soil-bentonite slurry. The correct proportions of each ingredient in the sediment-bentonite slurry will be determined in order to achieve similar workability and purpose.

Sediment parameters that will be checked for include grain-size distribution, density, viscosity, and flowability/filtrate loss. The main mix parameters that will be tested for include: density and viscosity of the sediment-bentonite slurry (slump) and hydraulic conductivity of the sediment-bentonite slurry (using a rigid wall permeameter/ API filter press test). The adsorption potential of the mixes will also be tested.

2.6 – MOTIVATION FOR THE CURRENT RESEARCH

The prospect of substituting dredge sediments for soil in the bentonite slurry looks promising as the Baltimore sediments contain a high percentage of fines (classified as CH) and has a hydraulic conductivity of between $5x10^{-6}$ cm/s and $2x10^{-5}$ cm/s. Admixtures would be needed, which would further lower the mixture's hydraulic conductivity. This should not pose a problem though, as it has been proven that materials with lower hydraulic conductivities have performed effectively, namely soil-bentonite slurry trench cutoff walls ($1x10^{-7}$ to $1x10^{-8}$ cm/s).

Dredging projects are usually expensive and time consuming; they require large survey operations, sometimes making use of interactive Geographical Information Systems (GIS). In the beginning phase there is hardly enough time and opportunity to carry out a complete survey with the help of enough soil investigation methods. In practice, approximately 400 million cubic yards of sediment must be dredged annually from waterways and ports to improve and maintain the United States' navigation system (Palmero & Wilson, 1997). Therefore alternatives for the disposal of dredged material from these projects have to be carefully looked at and developed from an economic, technically feasible, and environmentally acceptable point of view. Until the 1970s, the dredging state of the practice focused on efficiency of the dredging operation and production capacity, with an emphasis on economics (Palmero & Wilson, 1997). However, nowadays, with new environmental legislation (since the early 1970s), the state of the practice has evolved to encompass a wide range of environmental considerations, and so the emphasis has shifted to being able to balance economics and the environment. The U.S. water transportation system has been operating since the early 1800s and has

played a major role in the growth of the U.S. economy. The importance of navigation is evidenced by the fact that approximately 95 percent of all U.S. international trade moves through its ports (Wilson 1996) (Palmero & Wilson, 1997). Baltimore Inner Harbor is rich in maritime history and has been an active new world port and center of trading since the early 1600's. Since then shipping has combined with heavy industrialization in the 1800s (Snyder et al, 1997).

Unfortunately, the U.S., like other countries, does not have naturally deep ports or channels. Therefore there is a great need for dredging, to maintain and improve these waterways. Dredging can be a difficult issue from the standpoint of environmental concerns, and so any national dredging program must be managed to balance economics and the environment.

Potential environmental impacts from dredged disposal may be caused by physical or chemical processes. Physical impacts could come about from direct burial of organisms, loss of habitat, or generation of turbidity. Many of the waterways are located in industrial and urban areas therefore sediments are often contaminated from these sources. Table 2.6 (DeSilva et al, 1991) shows a comparison of elements in local topsoil material with dredged material and ameliorant mixes. The contaminated sediment, in turn, has led to concerns about water quality and aquatic organisms. Therefore good planning, design and management, (with appropriate environmental controls), of dredging operations are necessary for dredged material disposal to be done efficiently.

In addition, in current construction practices, sites often need to be remediated before further construction can proceed. Present remediation methods include pump and

Table 2.6 – Comparison of Local Topsoil Material with Dredged Material and Ameliorant Mixes

		Dredged Material Treatments										
		Night Soil	Sewage Sludge	Saw Dust	R. Cart	R. Cart/ Peat Night Soil	PFA	Bark	MC	DM	Peat only	Peat
TOPSOIL higher in	Soil Pb	***	***	***	***	***	***	***	***	***	***	***
	Soil Zn	***	***	***	***	***	***	***	***	***	***	***
	Soil Fe	***		***			***	***	***			
	Soil Cd		***	***		***	***	***			***	***
	Soil Cu		***	***	***	***	***	***	***		***	***
	Soil Ni		***	***	***		***	***	***	***	***	
	Soil Hg		***						***			
	Soil Cr								***			
	Soil Cu					**			**			
	% germ biomass	***	***	***	***	***	***	***	***	**	***	
TOPSOIL lower in	Soil Cu									***		
	Soil Cd	***			***				***	***		
	Soil Cr	***	***					***			***	***
	Soil Hg	***								***	***	***
	Soil Fe				***							***
	Soil Zn	**	***	***	***	***	***	***		***	***	***
	Soil Mn	**	***	***	***	***	**	***	***	***	***	***
	Soil Pb	**				***	**					
	Soil Cd	**						***				
	Soil Ni											***

Left hand column indicates status of the topsoil control in relation to each of the other treatments

MC – Mushroom Compost

DM – Dredged Material

* - Significant at $p < 0.05$

** - Significant at $p < 0.01$

*** - Significant at $p < 0.001$

(after DeSilva et al, 1991)

treat and electrokinetics. They generally require a large amount of energy and maintenance and have been found to produce limited long-term success (Suthersan 1997). Factors that affect the long term cost and success of a remediation project include composition of the contaminant, permeability and composition of the soil matrix, geologic setting and hydraulic characteristics of the area (Gallager 1998, Moo-Young et al 2000). Therefore research and development of technologies that involve in-situ containment and treatment are being promoted by industry as well as the EPA. Soil-bentonite barriers are commonly used for these purposes. These barriers basically form large containment systems and need another component to remove the contaminant from the ground. The dredged sediment barrier is one that is anticipated to contain and remove contaminants with relatively little energy input compared to pump and treat technologies. If this material proves to be suitable for limiting water flow and reacting with the representative contaminant, then the vertical cut-off wall can contain and attenuate the representative contaminant as the ground water passes slowly through the barrier system. In addition, because dredged sediment is a by-product of the dredging industry, the cost of the barrier system should be reduced substantially.

The slurry wall technique of stabilization is considered an outstanding innovation in underground construction. So, in developing another useful engineering application, specifically this one using dredged sediments, it is anticipated that this will offset some costs of having to use natural resources for such applications. It is also hoped that this will minimize the number of necessary disposal sites and associated environmental problems. It is also hoped that this investigation will give knowledge on the proposed

technology, thereby encouraging further research leading to possible widespread use of the technology.

SECTION 3

MATERIALS AND METHODS

3.1 MATERIALS

3.1.1 Dredged Sediments

The dredged material used for this study was obtained from Tolchester Channel located in Baltimore Harbor, Maryland. The dredged material was dredged from six different points in the channel. The extraction points are shown in the Figure 3.1. The material was black in color and had some odor. As it was received, the natural water content of the material was 400-600%.

Sieve analysis indicated that 95% of the material passed through the No. 200 sieve size (0.075 mm). The grain size distribution curve, obtained from hydrometer testing, is given in Figure 3.2. The Atterberg limits were measured in accordance with ASTM D 4318. The liquid limit and plastic limit of the material were found to be 85 and 35, respectively. The material was classified as a high plasticity clay (CH) according to the Unified Soil Classification System (USCS). Table 3.1 summarizes the index parameters of the dredged material.

3.1.2 Bentonite

Bentonite is a common clay mineral found in sedimentary and residual soils. Bentonite is commonly mixed with soils to form material for use in vertical cut-off walls.

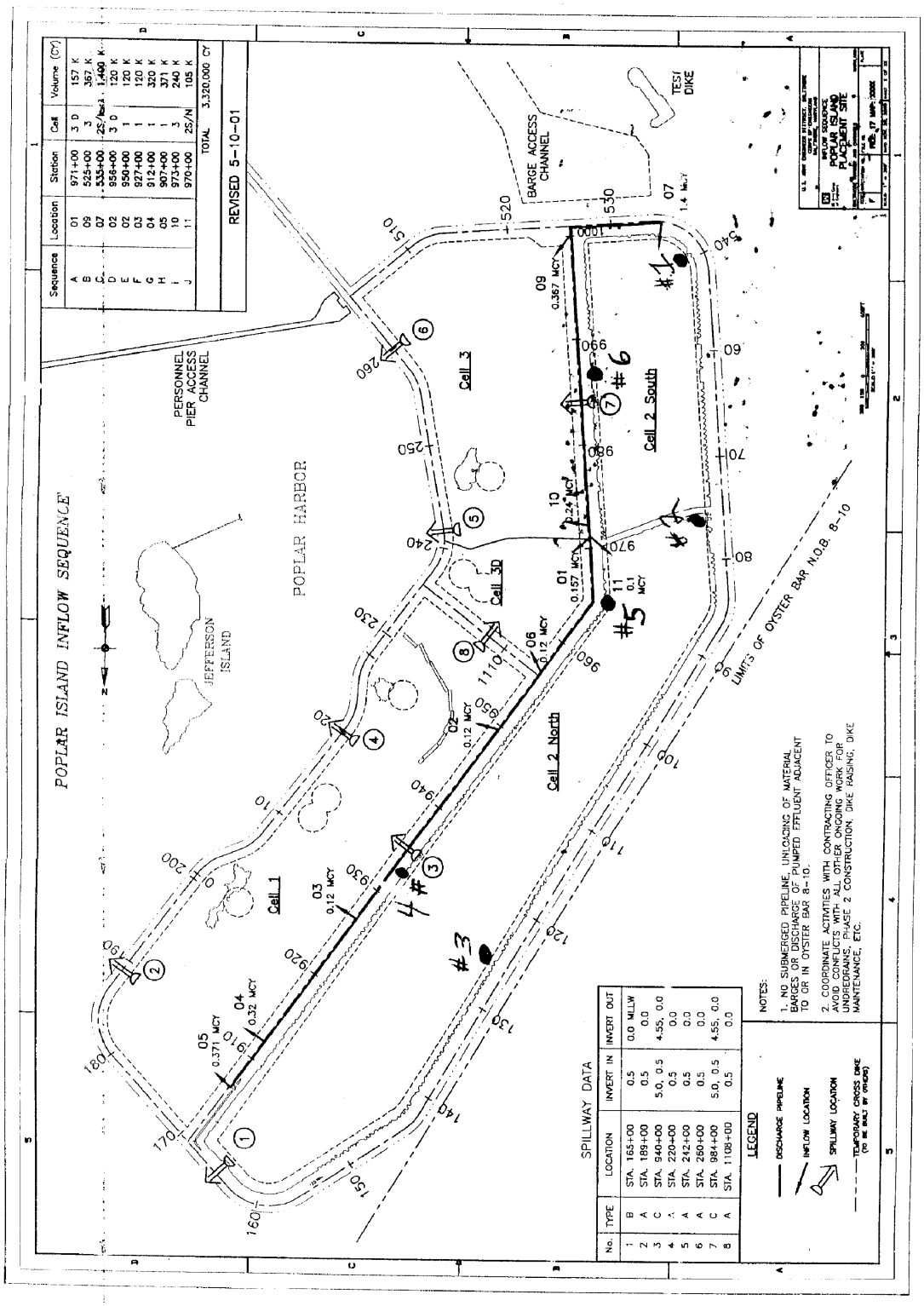

Figure 3.1 – Extraction points for dredged material

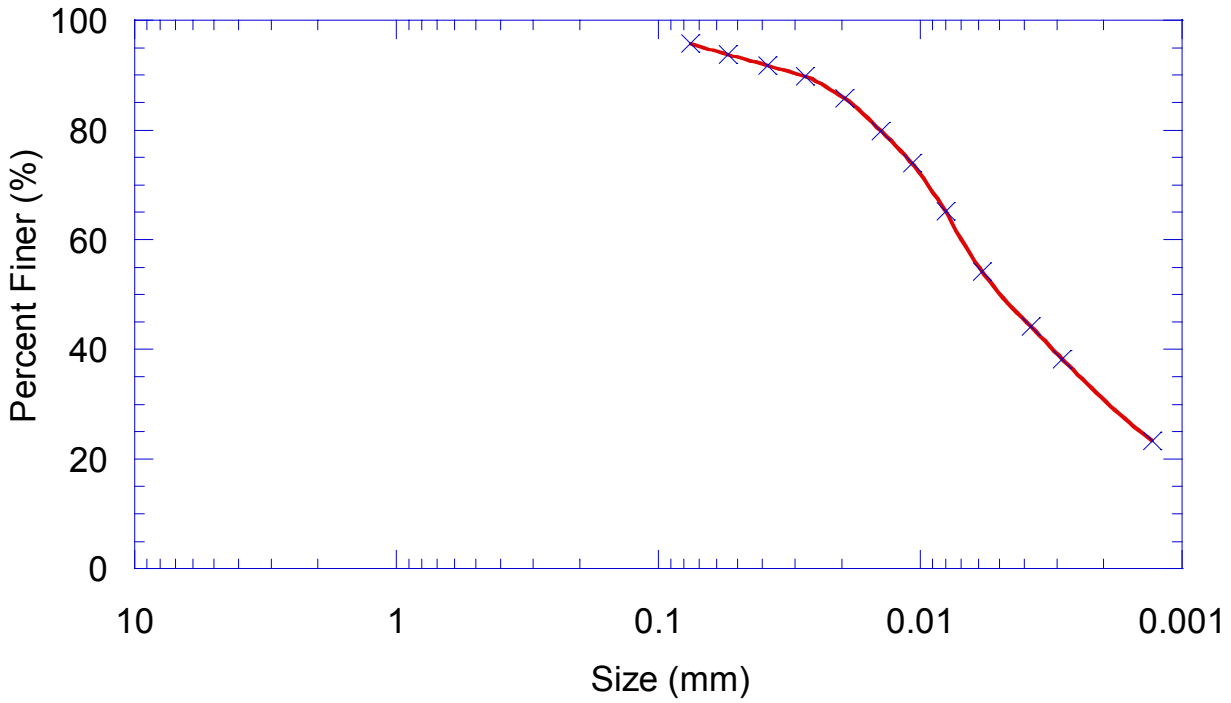

Figure 3.2 – Grain size distribution of the dredged material used in the current study

Table 3.1 - Engineering parameters of the dredged material used in the study.

D_{15}, (mm)	D_{50}, (mm)	D_{85}, (mm)	D_{90}, (mm)	C_u, (D_{60}/D_{10})	Specific Gravity G_s	Liquid Limit (LL)	Plastic Limit (PL)	Plasticity Index (PI)	USCS Class.
0.0009	0.005	0.019	0.038	11.7	2.6	85	35	50	CH

In this study, different mixes of sediment and bentonite were experimented with to find an optimum combination that could be used for vertical cut-off wall backfill material. The bentonite used in this study, BARA-KADE 90 was provided from Bentonite Performance Minerals, Inc. from the Colony, Wyoming Plant. The material obtained was a high quality, powdered sodium bentonite used in slurry wall construction, soil sealing and other hydraulic barriers. The product conforms to API specification 13A. Because of its fine particle size, it is mainly used with pugmill mixing operations in soil/bentonite liner construction. The typical physical properties are given in Table 3.2, and the typical chemical properties are given in Table 3.3. Wet sieve results according to ASTM WK217 resulted in 98% fines.

3.1.3 Fly ash

The fly ash used in the study was obtained from Brandon Shores Facility of Baltimore Gas and Electric Company, located in Baltimore, MD. The fly ash was produced from burning bituminous coal and had pozzolanic properties. The natural water content of the fly ash was 30 % when it was received. The appearance of the material was like fine-grained gray powder, and it had no odor. Specific gravity of the material was measured in accordance with the ASTM D 854 and found to be 2.22. Optimum moisture content and maximum dry density of the material were determined by using the test method ASTM D 1557 (modified proctor effort) and found to be 25 % and 12.8 kN/m^3, respectively.

Particle size analysis indicated that 85 % of the material passed the No. 200 U.S. standard sieve size. Figure 3.3 provides the complete particle size distribution curve of

Table 3.2 Typical Physical Properties of Bentonite

a) Slurry Properties (6% Suspension)

Property	**Value**	**Specification**
Viscosity, FANN 600 rpm	37	30 min
Marsh Funnel, s/quart	36	NA
Apparent Viscosity, cps	18.5	NA
Plastic Viscosity	12	
Yield Point, (N/m^2)	0.479	3x max plastic viscosity
Filtrate loss at 30 min under $\sigma' = 696.5$ KPa	14	15 cm^3 max
Filter cake thickness, mm	2.38	NA

b) Industrial Properties

Moisture Content (%)	9	NA
Swell Index	28	NA
Specific Gravity	2.7	NA
pH, 6% suspension	9.5	NA
Bulk Density (kN/m^3) (uncompacted)	7.7	NA
Bulk Density (kN/m^3) (compacted)	11.32	NA

Table 3.3 – Chemical Properties

a) X-ray Analysis

Mineral	Percentage (%)
Montmorillonite	88-90
Quartz	0-6
Feldspar	5-7
Cristobalite	0-1
Biotite & Mica	0-2

b) Chemical Analysis

Compound	Percentage (%)
SiO_2	63.59
Al_2O_3	21.43
Fe_2O_3	3.78
CaO	0.66
MgO	2.03
Na_2O	2.07
K_2O	0.31
Bound Water	5.50

* Metals listed in the chemical analysis are complexed in the mineral. They do not necessarily exist as free oxides.

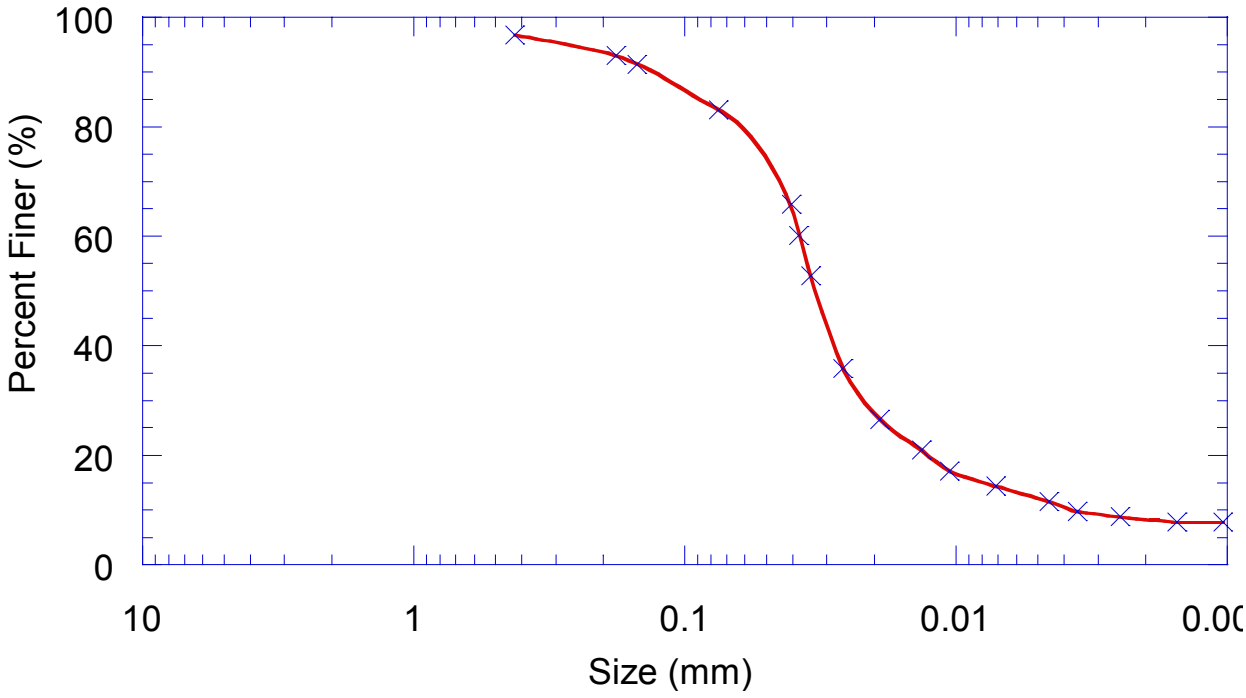

Figure 3.3 – Particle size distribution of the fly ash used in the current study

the fly ash, determined by sieve and hydrometer analyses. Characteristic particle sizes (D_{15}, D_{50}, D_{85} and D_{90}), coefficient of uniformity (C_u) and water and solids contents of the fly ash are given in Table 3.4.

Chemical analysis of the fly ash indicated that silicon dioxide, aluminum oxide and ferric oxide make up approximately 94% of the material. Details of the chemical analysis and the corrosion test results are shown in Table 3.5 and 3.6, respectively.

3.2 TEST PROCEDURES ON THE SEDIMENT

3.2.1 Density Testing and Determination of Water Content

The density of the sediment was first determined by measuring the physical dimensions of the material. That is the weight, and actual volume which the mass occupied was determined. The mass of a given volume (500 mL) of the sample of sediments was found on a grams scale. Density was found as the mass per unit volume the sediments occupied. Unit conversions were necessary to convert the measured value of grams per milliliter to kilonewtons per cubic meter. Samples were taken from each of the two buckets of sediments collected from the shore, Craighill Angle Project. One set of samples were called Sample A, and the other was called Sample B. Two series of tests were done on each sample. Figure 3.4 shows a picture of the beaker of sediment on the scale.

The water content was determined using the ASTM D2216 procedure. Figure 3.5 shows a picture of the laboratory oven at 110 degrees with the soil samples.

Table 3.4 Grain parameters and water and solids content of fly ash used in the tests.

D_{15}, (mm)	D_{50}, (mm)	D_{85}, (mm)	D_{90}, (mm)	C_u, (D_{60}/D_{10})	Specific Gravity G_s	Water Content (%)	Solids Content (%)
0.008	0.033	0.092	0.137	9.87	2.22	30	77

Table 3.5 Chemical composition of the fly ash.

Elements		%
SiO_2		50
Al_2O_3		30
Fe_2O_3		14
CaO		1.8
MgO		0.3
K_2O		1.5
TiO_2		1.1
Arsenic		0.03
Other		1.27

Table 3.6 Corrosion test results of the fly ash.

Test	Results
pH	7.7
Resistivity (ohm-cm)	1700
Sulfides (mg/kg)	<1
Soluble sulfates (mg/kg)	1550
Chlorides (mg/kg)	145
Redox potential (mV)	350

Fig 3.4 - Picture of Beaker of Sediment on Scale

Fig. 3.5 - Laboratory Oven at 110 degrees with soil samples

3.2.2 Marsh Funnel Viscosity Test

Viscosity is the measure a fluid's resistance to flow in an unenclosed apparatus. Therefore the test used to determine the viscosity of the dredged sediments was the Marsh Funnel viscosity test. The test measures the total-time it takes for a given volume of dredged sediments to pass through a calibrated orifice. Figure 3.6 shows a picture of the Marsh Funnel.

The orifice at the bottom of the Marsh Funnel was stopped by a finger. The funnel was then filled with the dredged sediments by pouring it through the screen on the top of the funnel until it reaches the screen level. A 1-quart test cup was placed under the funnel. The stop-watch was started simultaneously while removing the finger from the funnel orifice to allow the fluid to flow into the test cup. The stop-watch was stopped when the fluid level reached the 1-quart line in the test cup. The fluid viscosity is described in terms of the amount of time, in seconds, that was necessary for 1 quart of the fluid to flow through the calibrated orifice.

3.2.3 The Filter Press Test

The American Petroleum Industry (API) filter press test is commonly used to measure the hydraulic conductivity of soil - bentonite mixtures (Filz et al. 2001), slurries, oil well cements and cement additives (Aydilek 1996). The filter press test was used in this case to determine the filtrate loss and flow rate of the dredged sediments. The sediments were placed into the filtration device.

Fig. 3.6a – Side View of Marsh Funnel

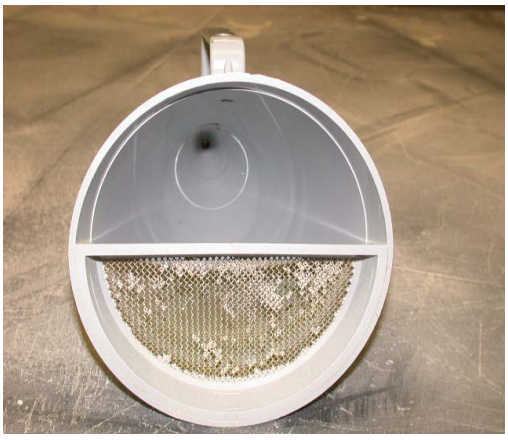

Fig. 3.6b – Top view of Marsh Funnel

The filter press test equipment consisted of (1) a pressure cell made of a steel pipe which had a diameter of 79 mm and a height of 90 mm, (2) a cap having a pressure hole and (3) a bottom part which had a flow hole (refer to Figure 3.7). There were two O-ring rubber gaskets at the connections between the cap and cell and bottom part to prevent leakage. A T-screw was used to tighten the cap, the pressure cell and the bottom part. The test method determined the flow rate of the dredged sediments.

The time for a given volume of filtrate was recorded in order to determine the flow rate. When it was observed that the rate at which the water came out of the bottom decreased, the main part of the experiment had been completed. The volume of water collected under the filtration device was recorded in given increments, along with the corresponding time it took to reach that volume. Finally, the characteristics of the filter-cake were recorded to observe the compacted dredged material.

The clean, dry parts of the filter cell were assembled in the following order (refer to figure 3.4); base cap, rubber gasket, screen, a sheet of geotextile, rubber gasket, filter cell. The cell was secured to the base cap by rotating it clockwise. The cell was filled with the test sample to within approximately ¼" (6mm) of the top. The filter press cell assembly was set in place within the frame. The top cap was checked to make sure that the rubber gasket was in place. The top cap (already connected to the pressure source) was placed onto the filter cell and secured in place with the T-Screw. A dry graduated cylinder was placed under the filtrate tube. Varying pressures were applied to the cell. At the end of the test, the pressure source valve was closed, the regulator was backed off

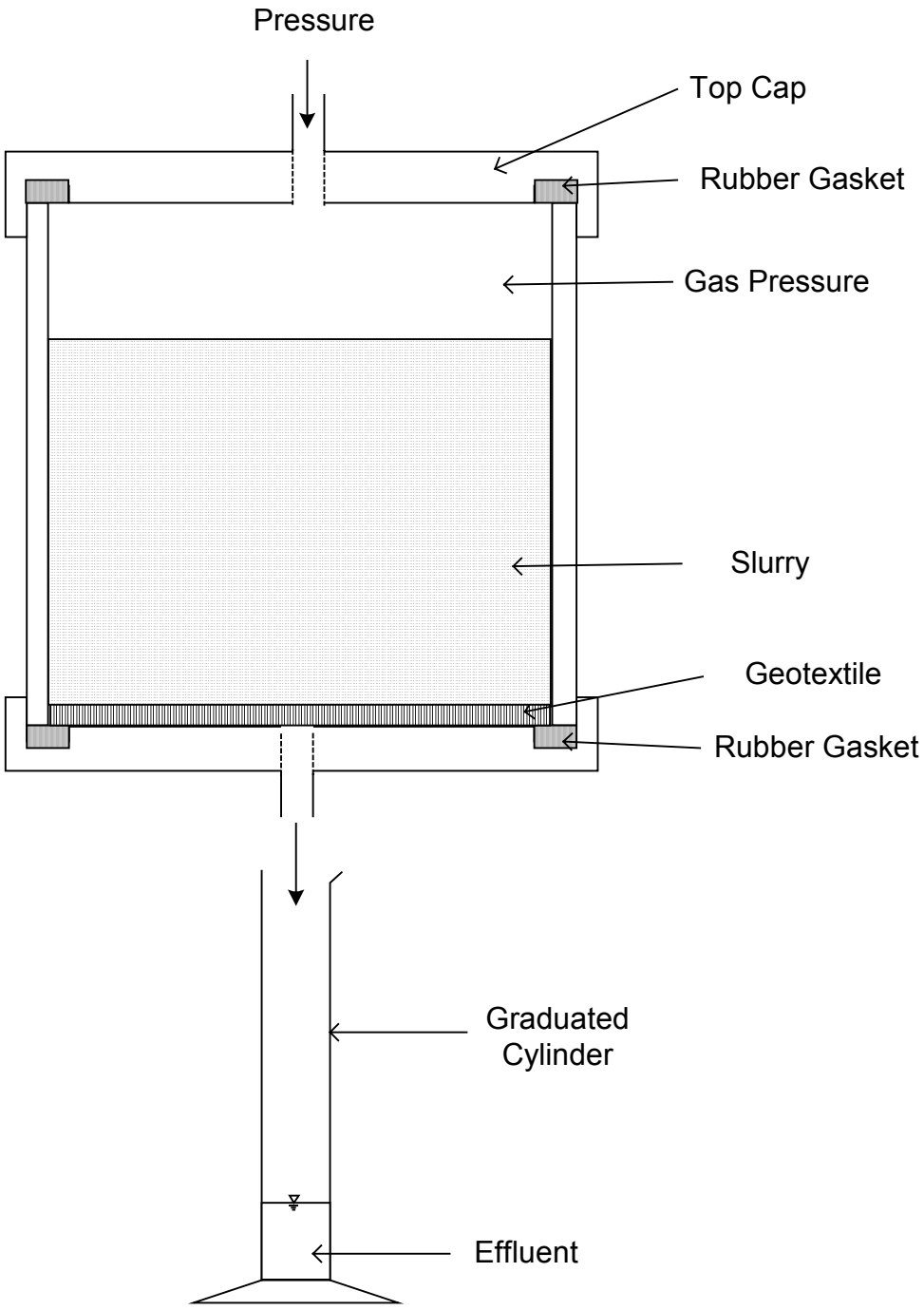

Figure 3.7 - Filter Press Test Apparatus Setup

and the safety-bleeder valve was opened. This releases the pressure on the entire system. The volume of filtrate collected was then measured in mL in the graduated cylinder. The T-screw was loosened, the top cell removed, and the cell removed from the frame. The filter cell was disassembled and the filter cake, geotextile and filter paper were carefully removed from the base cap. The thickness of the filter cake was measured and recorded to the nearest 1/32" (0.8mm). The properties of the filter cake such as texture, hardness and flexibility were recorded.

3.3 TEST PROCEDURES ON THE SEDIMENT-BENTONITE MIX

The sediments were mixed with bentonite in proportions including 1%, 2% and 3% of bentonite by weight. Similarly, density testing was performed on these different mixes of the sediment-bentonite. The moisture content of the mixes was also determined in a similar fashion to that of the sediments. The viscosity of the mixes was determined using the Marsh Funnel test. Some of the mixtures prepared with 1% bentonite were modified with the addition of fly ash. Flyash was added in the proportions of 5% and 8% by weight. Hydraulic conductivity testing was performed on the bentonite mixes as well as the fly ash mixes. Adsorption testing was also performed on the dredged sediment and mixes.

3.3.1 Hydraulic Conductivity Testing

The hydraulic conductivity of the mixes was determined using the rigid wall permeameter test as specified in ASTM D 5856. The API filter press test apparatus was used for the testing. The American Petroleum Institute (API) filter press is a rigid wall

cell used to determine the filtrate loss of bentonite slurries (American Petroleum Institute 1985). It is also commonly used to measure the hydraulic conductivity of soil-bentonite, both during mix design and as part of construction quality assurance and quality control (Filz et al, 2001). This study also compared hydraulic conductivity testing using a rigid-wall consolidometer permeameter test, flexible-wall permeameter test as well as the API filter press test. The analysis showed that the results compared well. This test is also a little less labor intensive than the other tests. A study by Zamojski et al ( ) showed similar results obtained for hydraulic conductivity through using both flexible-wall and fixed-wall permeameter tests. A study by Evans, (1994) reveals that a fixed wall API Filter Press has been used to conduct rapid evaluations of hydraulic conductivity in the field as the construction progresses. D'Appolonia, (1980) also mentions use of the API Filter Press Test for testing purposes representative of field conditions during slurry trench construction. This provided justification for the test method used in the present study.

3.3.2 Adsorption Testing

Equilibrium batch testing, according to ASTM D4646 specification was performed on the dredged sediments and mixes with aqueous solutions containing heavy metals to determine the adsorption capacities of the dredged material and mixes. The metal sorbates used were cadmium, chromium, lead and zinc.

3.4 TEST PLAN

The intention of this testing plan is to find an appropriate mix of sediment and bentonite that will be able to function as a vertical cut-off wall backfill material. The preliminary tests on the bentonite were carried out for screening purposes and to find an appropriate water content that will satisfy the desired viscosity range.

Bentonite was then added to the dredged sediment in ratios of 1%, 2% and 3% of the total dredged sediment weight. The preliminary tests were repeated for each of these mixes to determine applicable trends and at what percentages of bentonite, the viscosity of the mixture was still in the workable range. The 1% bentonite mix was additionally modified with the addition of 5% and 8% fly ash by weight. These mixtures were then subjected to API filter press tests (used as a rigid wall permeameter) to determine the effect these mixes would have on the hydraulic conductivity. Adsorption testing was also carried out on all the mixes to determine their adsorption capacities. Table 3.7 shows a legend for the composition of the mix designs and Table 3.8 shows a summary of the tests performed.

Table 3.7 - Legend and the composition for the mix designs

Sample ID	Description
1B	Sediment +1% Bentonite
1B-5FA	Sediment, 1% Bentonite, 5% Flyash
1B-8FA	Sediment, 1% Bentonite, 8% Flyash
2B	Sediment, 2% Bentonite
3B	Sediment, 3% Bentonite

Table 3.8 - Summary of Tests Performed

Sample	Density Testing	Moisture Content	Viscosity	Filter Press Test	Adsorption Testing
Dredged Sediment	X	X	X	X_1	X
1B	X	X	X	X_2	X
2B	X	X	X	X_2	X
3B	X	X	X	X_2	X
1B-5FA				X_2	X
1B-8FA				X_2	X

X_1 – Test carried out to determine filtrate loss results

X_2 – Test carried out to determine hydraulic conductivity of mix

SECTION 4

TRENCH STABILITY

4.1 TRENCHING

Trenching is used for many construction operations today including controlling groundwater flow, contaminant migration, construction shafts, foundation pits, bridge foundations, basement walls, tunneling for subways, slope stabilization and sewage projects. Trenches can be stabilized using primarily braced stabilization or slurry stabilization. A few projects, involving the use of slurry walls, are shown in Fig. 4-1a, and a detail in Fig. 4-1b.

4.1.1 Stabilization Methods

In practice, two types of stabilization methods are commonly used; braced stabilization (involving the use of timber or steel supports with struts) and slurry stabilization which has become more popular in recent years. Table 4.1 shows a comparison of the effect of rigid lateral support and slurry support stabilization methods for plane strain, where the upper part is rigidly supported, as well as, unsupported axisymmetric excavations – the investigation was carried out under undrained conditions. Both wall failure and base failure are considered. In summary, it shows that the slurry support method is more effective than the rigid lateral support method for all failure conditions examined except for plane strain wall failure, refer to Table 4.1 (Brito and Kusakabe, 1984). The slurry support method reduces the amount of surface settlement and also stabilizes the trench against base failure. The slurry support method is, therefore,

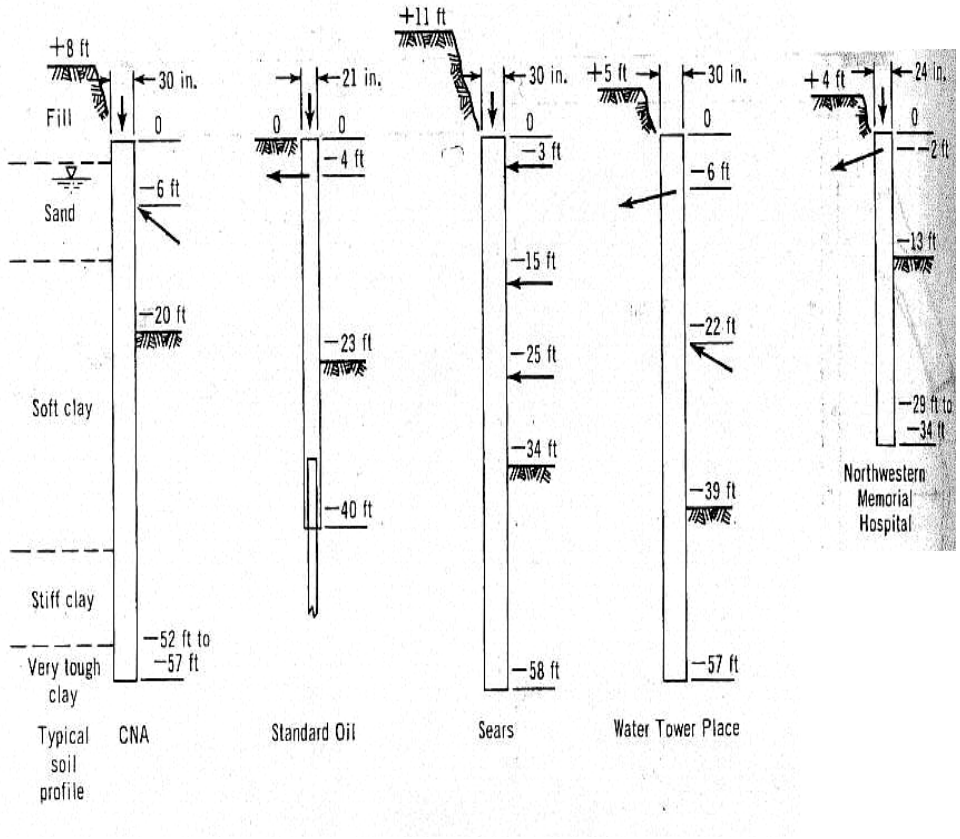

Fig. 4.1a - Slurry walls for projects in Chicago
(after Gill, 1980)

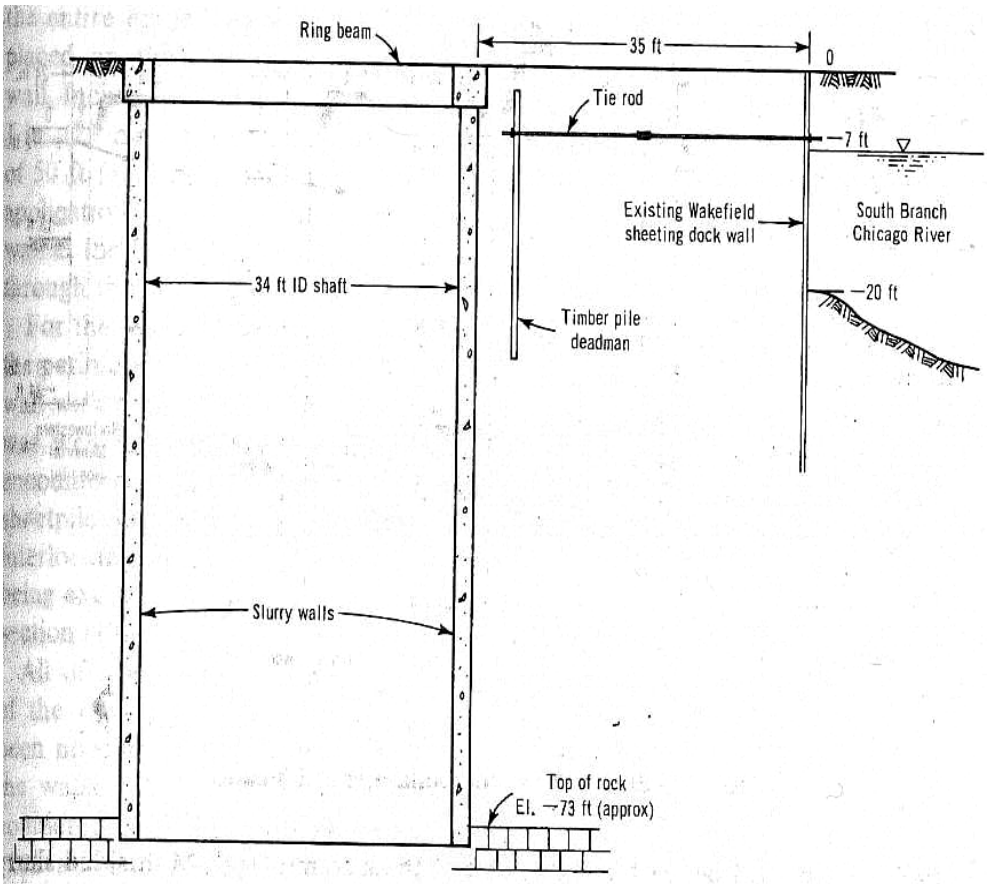

Fig 4.1b – Slurry Walls for Projects in Chicago
(after Gill, 1980)

Table 4.1 – Comparison of rigid wall support and slurry support for plane strain and axisymmetric excavations

Type		**Rigid Lateral Support**	**Slurry Support**
Plane Strain	Wall failure	More effective against wall failure	Less effective than lateral support*
	Base failure	No effect	Effective
Axisymmetry	Wall failure	Less effective than slurry	Effective
	Base failure	No effect	Effective

*****Dependent on the density of slurry.

(after Brito and Kusakabe, 1984)

a preferred method of trench stabilization. The use of slurry wall projects has increased during the past two decades. Soil-bentonite slurry trench cutoff walls are most commonly used, because of their relatively low hydraulic conductivity and cost. In this study, the efficiency of a dredged sediment/ bentonite vertical backfill material (used to displace the slurry) are considered, therefore it is helpful to understand the design principles behind slurry stabilization.

4.2 SLURRY STABILIZATION

4.2.1 Design Principles

The main factors involved in slurry stabilization are change in strength of slurry with time and the theoretical build-up of filter cake with time on the walls of the trench. Slurry trench stabilization depends on the bentonite cake to prevent ground water flow and erosion of soil grains. A study by Nash (1974) revealed that the build-up depends on the square root of time (from original placement) and leads to a thickness of about ½ cm after 24 hr. for typical slurry and filter cake at a depth of 20m. Refer to Figure 4.2 and 4.3.

There is limited information on the effective stresses that exist within the soil-bentonite slurry trench cutoff wall in its as constructed condition. It is thought that a portion of the stability is given by incalculable forces such as gel strength, resistance of the filter cake, electric potential between the slurry and the soil, dynamic gradient of slurry flowing into the soil, rigidity imparted to the slurry by the bentonite as well as by the suspended cuttings and the effect of permeating slurry on the soil strength (Gill,

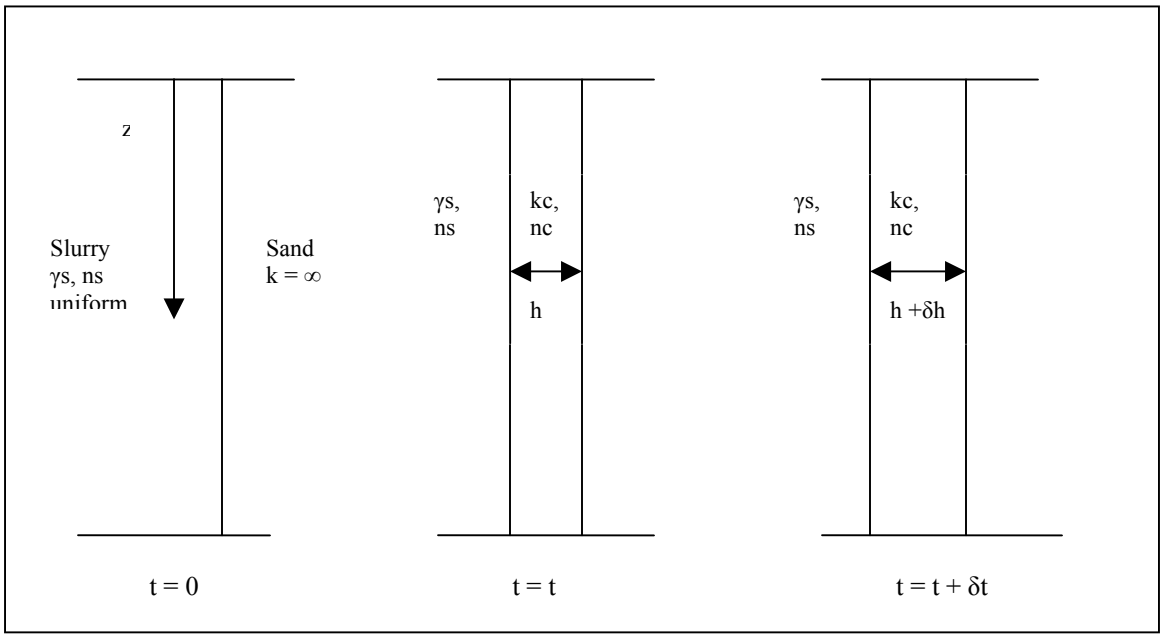

Fig 4.2 – Theoretical build-up with time of filter cake on walls of trench (after Nash, 1974)

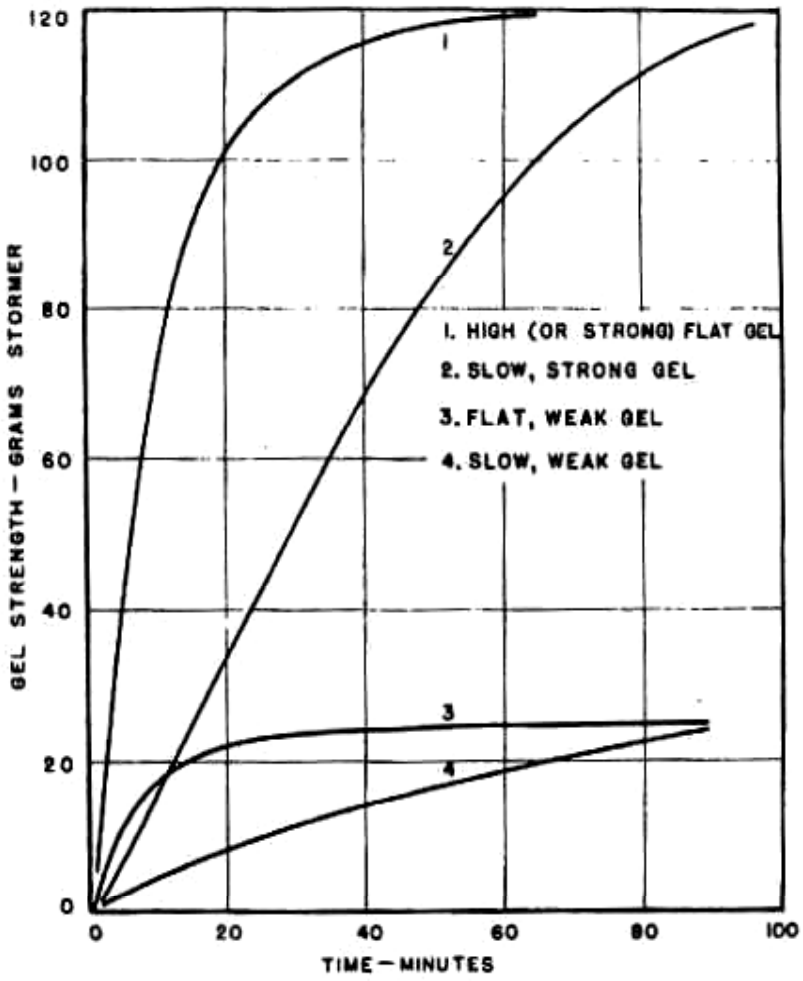

Fig 4.3 – Change in strength of slurry with time
(after Nash, 1974)

1980). However Evans et al (2000) has suggested that the state of effective stress does not increase geostatically. Sidewall friction forces "support" the backfill and the resulting

stress is usually less than the geostatic stresses. Data also show that after an initial non-linear increase, within a relatively short distance, the stresses at a given depth become essentially constant and predictable. By using these data and assuming a constant Cu/Po' ratio results in an estimate of the effective stress profile similar to that developed from consolidation testing. Using the predicted effective stress, the hydraulic conductivity (which is strongly stress dependent) can be more reliably determined.

The study by Nash (1974) shows the effect of slurry density. With reductions in slurry density (as well as excavation) there is horizontal movement of the sides of the trench as shown in Figure 4.4, Nash (1974) used the distribution of forces involved for the stability analysis, based on the Coulomb wedge theory with hydrostatic thrust against the vertical face and these diagrams are shown in Figure 4.5. The factor of safety, F, can be defined by the equations below:

$$\text{For clays: } F = 4C_u / H(\gamma - \gamma_f) \qquad (4.1)$$

$$\text{For sands and gravels: } F = 2(\gamma - \gamma_f)^{\wedge}½ \ \tan\phi_d / \gamma - \gamma_f \qquad (4.2)$$

where, C_u is the undrained cohesion, H is the depth of trench, γ is the total unit weight of the soil, γ_f is the total unit weight of the fluid mud and ϕ_d is the drained friction angle of soil.

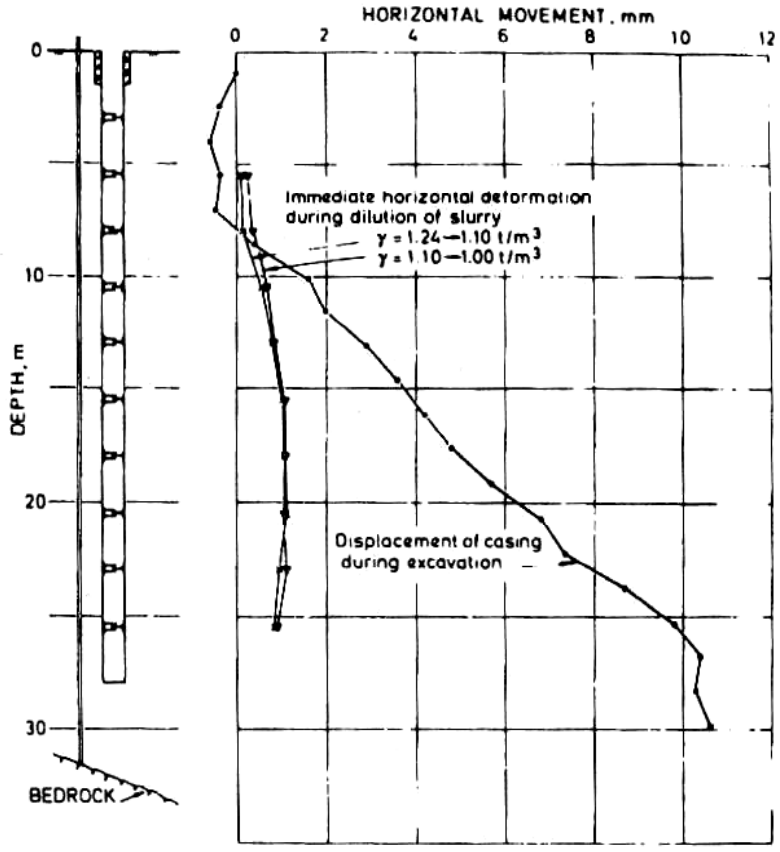

Fig 4.4 – Horizontal movement of sides of trench caused by excavation and reduction in density of slurry.

(after Nash, 1974)

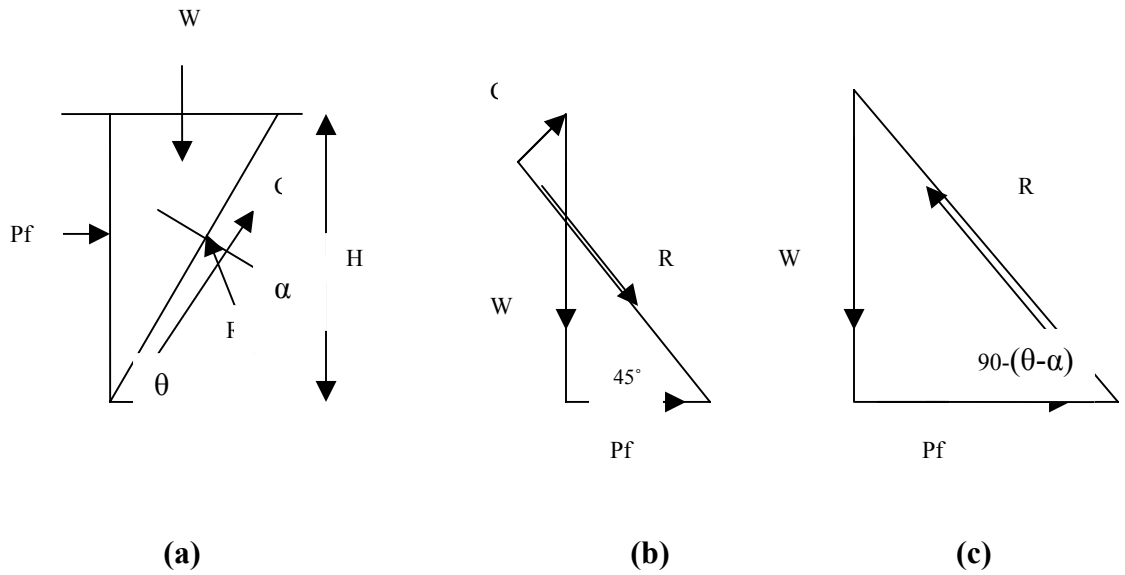

Fig 4.5 – (a) Stability analysis of slurry trench for c-ø soil (b) Polygon for forces when øu=0 (c) Triangle of forces when Cd=0

(after Nash, 1974)

Reliance is still mostly placed on experience in similar soil and ground water conditions. When there are unstable conditions, adjustments are made in the construction

procedures, level and density of the slurry, length of the panels, and in the shape and type of cutting tools (Gill, 1980). The presence of artesian water pressure, large gravel and boulders, very loose soils, soft clays, recently placed hydraulic fill with undissipated pore pressures, and sudden changes in the soil strata are potential conditions of instability and require careful consideration prior to deciding on the construction procedures.

Surcharge loads are more important when the slurry is located near to existing footings, the settlement of the structure that is supported should be considered.

4.2.2 Advantages of using slurry stabilization

There are several advantages that can be realized through using the slurry method of stabilization. These include minimal disruption of the surface, minimal construction noise and vibrations and positive cutoff for ground water. This method also eliminates underpinning of adjacent structures and these slurry walls can be constructed through soil and rock. Apart from having the slurry displaced by a soil-bentonite backfill material, the slurry method of stabilization can be used in combination with cast-in-place (C.I.P.) or precast concrete walls. This provides a rigid, smooth, watertight wall that can be used for earth retention purposes and serve as the permanent structure. The precast prestressed method also allows for large unsupported spans between bracing levels. It is ideal for use under dams, excavations in water bearing soils and containment of wastewater ponds and leachate from landfills. Specialist contractors are working on advances in the joint system for the future to eliminate the weak link and seepage path between panels. The use of slurry walls is projected to happen at an accelerated rate in the future.

4.2.3 Case histories for slurry stabilization – analyzed by the arching method

Trench stability is affected by factors such as electric potentials in the ground and adjacent building/foundation surcharges. Three case histories of slurry trench excavation including two failures were back-analyzed using the arching theory (Wong, 1984). The case histories analyzed were Gerstheim along the River Rhine, Charter Garden Test Panel in Hong Kong and Swire House in Hong Kong. The soil type was fill, marine deposit, and colluvium. From Prandtl's limiting plasticity theory, the distribution of the vertical pressure being exerted on soft clay, which mobilizes the driving lateral pressure, is calculated considering the arching effect induced by the finite length of the slurry trench.

In this process of designing a slurry trench for stability, a minimum value of the factor of safety (excess bentonite pressure/earth pressure) needs to be decided on, a value of 1.2 is commonly used. The geological parameters of cohesion (c) and friction angle (ø) and design ground water level need to be determined. Adjacent building foundations, foundation loads, and building superstructure should be studied for the magnitude and position of surcharge loads so that an allowable distortion and settlement can be decided on. A preliminary design of trench panel length, slurry density and slurry head then needs to be done. The reduction in surcharge load (if applicable) should then be determined. The (reduced) surcharge load should be applied to evaluate the earth pressure. The calculated earth pressure should then be compared with the effective slurry pressure to obtain the factor of safety. If the factor of safety is inadequate, the trench stability should be redesigned by using a higher slurry density, higher slurry head, shorter panel length, lowering the ground water table or strengthening adjacent buildings to increase stiffness.

The findings of the case histories revealed that failure usually occurred when the slurry head in the trench fell to approximately 1m below ground water level. The point at which the earth pressure became greater than the excess (over ground water pressure) slurry pressure was termed the critical depth. The local failure propogated, and a general failure occurred with the slip surface starting from the critical depth. Therefore the failure zone extended only to a depth of 5-12m, although at the time of failure, the trenches were excavated over 20m. The failure occurred progressively. It is thought that failure progresses upward from the critical depth to form a sliding soil mass. The analysis showed that for typical cases where the critical depth is 5-12m; because of the arching effect, the failure zone extended laterally on the ground surface to a distance of half the panel length behind the trench face. It was also found that slurry trenches subjected to surcharge load will develop very large earth pressures near the point of application. When the point of application is within half-panel length of the trench, the surcharge will act totally on the trench wall. Surcharge located more than half-panel length away from the trench will be distributed to soil adjacent to the panel.

4.2.4 Failure analysis based on lateral extrusion of weak soil

The failure based on the lateral extrusion of sandwiched weak soil in a slurry-supported trench was evaluated through use of a field case study in Southwest Taiwan, refer to Figure 4.6, (Tsai et al, 1998). The problem was theoretically modeled as the compression of weightless soft clay between rough plates. It was evaluated using a factor of stability. The factor of stability is defined as the ratio of the slurry pressure to the (horizontal) lateral extrusion pressure at the level of the weak soil.

The total stress concept was used. Important factors for the stability of the weak sublayer include the undrained shear strength of weak soil, the slurry pressure being exerted on the trench face and the ground water level. A theory on the bearing capacity of a thin clay layer of soil along with the theory of soil arching was used (using the modified Schneebeli's formula, (Schneebeli 1964, Wong 1984)) to calculate the vertical driving pressure on the top boundary of the weak soil. The analysis was performed by assuming a limiting equilibrium state where both the strength and the arching of soil are fully mobilized. Limiting equilibrium was considered for the lateral pressure being exerted on the open end of a weak sublayer. It was realized that an approximate, simplified, but realistic solution could therefore be arrived at. Figure 4.7 shows the forces acting on a representative soil element for lateral extrusion analysis. And Figure 4.8 shows the arching effect on a sandwiched weak sublayer in a slurry trench.

From the study, if the vertical driving pressure is greater than the threshold pressure ($1.57S_u$), the factor of stability is given by:

$$FS = P_{sl}\text{-}0.43S_u/\sigma_v\text{-}1.57S_u \qquad (4.3)$$

If the vertical driving pressure is equal to or less than the threshold pressure ($1.57S_u$), the factor of stability is given by:

$$FS = Psl/0.43S_u \qquad (4.4)$$

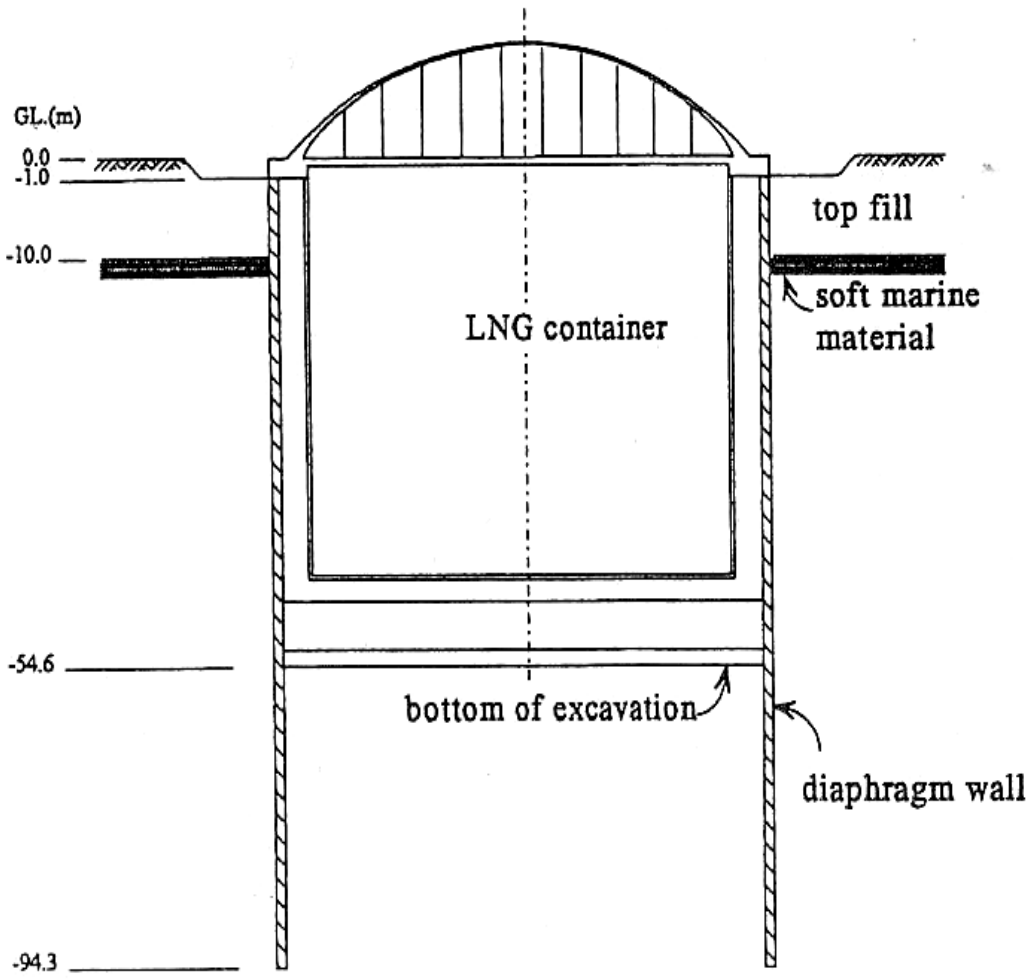

Fig 4.6 – Layout of container and slurry trenches

(after Tsai et al, 1998)

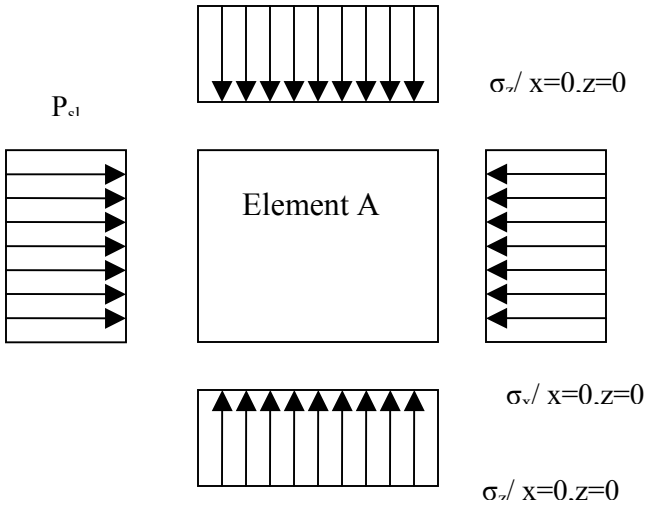

Fig 4.7 – Representative soil element for lateral extrusion analysis

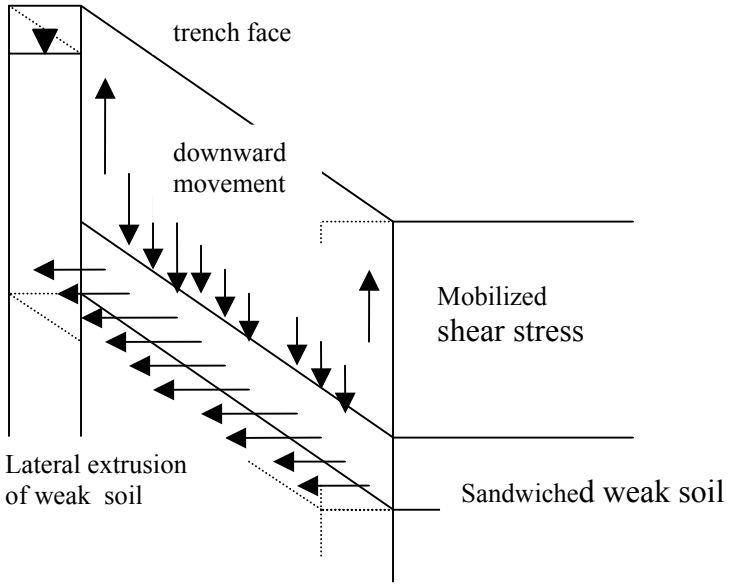

Fig 4.8 – Arching effect upon sandwiched weak sublayer in slurry trench

(after Tsai et al, 1998)

where, P_{sl} is the slurry pressure, S_u is the undrained shear strength and σ_v is the vertical driving pressure. The application of the above method for a given site gives favorable agreement with field observations. Figure 4.9 a-d shows a failure scenario involving the lateral extrusion of a weak layer of soil. Table 4.2 shows the simplified soil profile of the site and Table 4.3 shows the factors of stability of a weak sublayer.

4.2.5 Comparison of Analysis Methods and Limitations

In the current practice of slurry trench design, the earth pressure exerted on the trench wall at various depths is calculated by the Huder or Schneebeli formula. The estimated earth pressures are compared with the excess bentonite pressure at the corresponding depth. If the factor of safety (excess bentonite pressure/earth pressure) at each depth is more than 1.2, it is stable overall. From back-analysis of several case histories (Wong, 1984), the Schneebeli's method of analysis adequately predicts trench stability. It is thought that the Schneebeli's method can be better applied to practical problems than the Huder method. The Schneebeli's method, however, usually results in earth pressure lower than the Huder's method (using Huder's recommended earth pressure coefficient). The Huder's method is therefore conservative for the case histories analyzed. The wedge method of analysis is thought to be less conservative than the arching methods because it considers global equilibrium of the failure mass. The finite element method can be used to solve the problem as well.

Practically, a complete analysis of a soil mass loaded to failure is a very complicated problem. It deals with an elastic-plastic-rupture transition, which involves an initial linear elastic state, a post yielding state, a near-failure state, and the post-failure

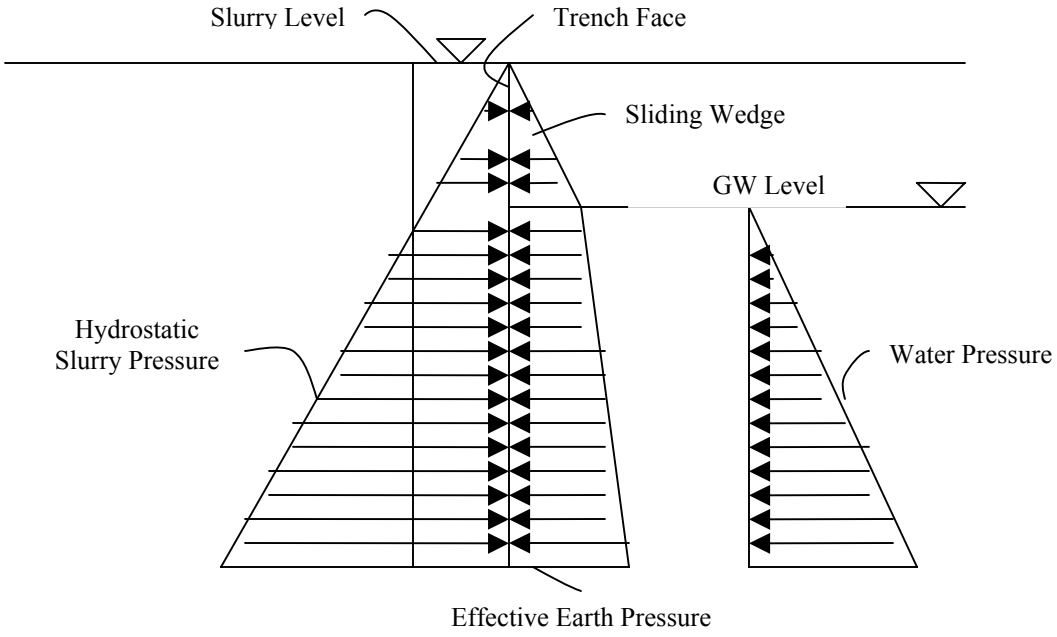

Fig 4.9a - Equilibrium of Pressure along Trench Face for Stability of Slurry Trench

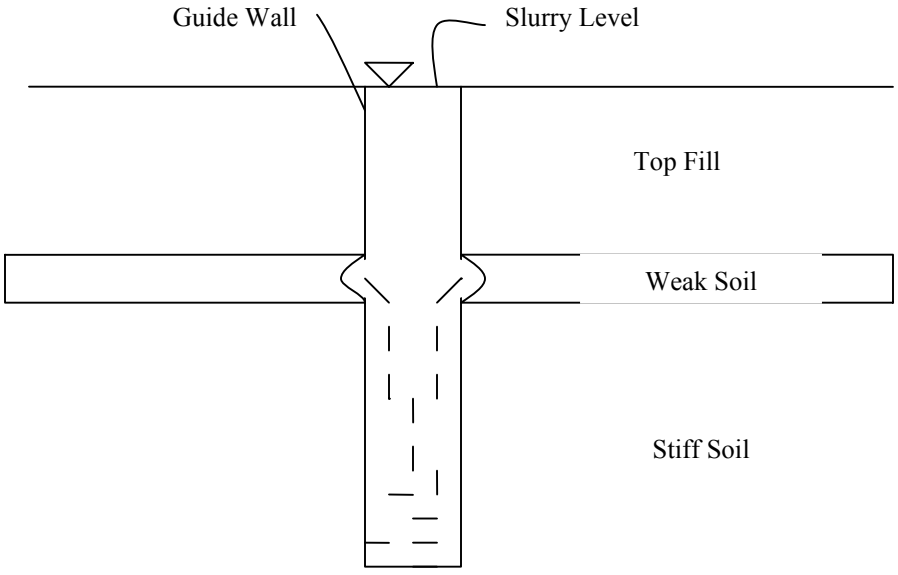

Fig 4.9b – Falloff of Sandwiched Weak Soil

(after Tsai et al, 1998)

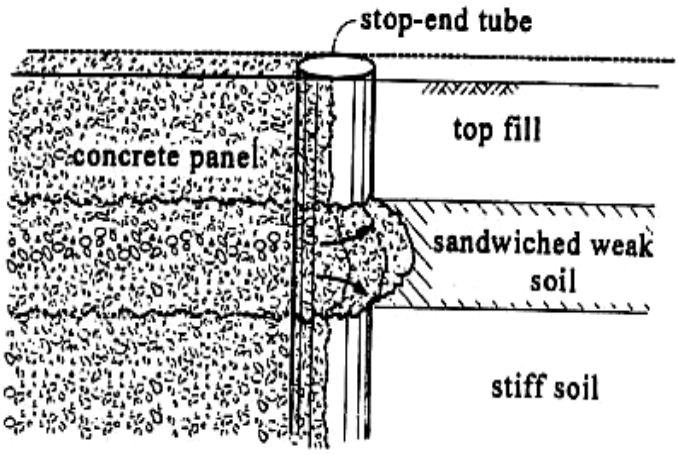

Fig 4.9c – Penetration of Concrete beyond Stop-End Tube due to Falloff at Sandwiched Weak Soil

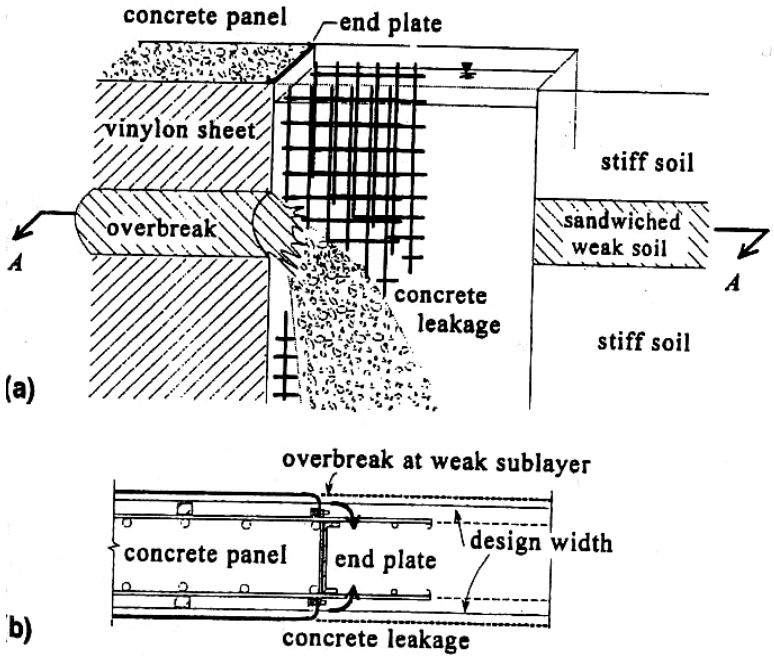

Fig 4.9d – Vinylon Sheet and Steel-Plate Joint: (a) Concrete Leaking into Overlapping Section through Broken Vinylon Sheet, (b) Plan View of Overlapping Joint

(after Tsai et al, 1998)

Table 4.2 – Simplified soil profile of site

Layer	Depth (m)	USCS	γ_t (kN/m³)	γ_{sat} (kN/m³)	C_{u*}	$Ø_{u*}$	PI	S_u (kPa)
1	0-10.0	SM/fill	17.0	19.6	-	33	-	-
2	10.0-11.5	CL	-	19.0	-	-	10	20.0
3	11.5-15.0	SM	-	19.2	-	38	-	-
4	15.0-22.0	CL	-	20.0	28.0	14	25	-
5	22.0-28.0	SM	-	20.0	-	35	-	-
6	28.0-30.0	CL	-	19.8	86.0	18	16	-
7	>30.0	SM	-	20.1	-	37	-	-

USCS is the Unified Soil Classification System
C_u and $ø_u$ are the strength parameters and results of consolidated undrained triaxial tests

Table 4.3 – Factors of stability of weak sublayer

Trench length (m)	Analytical method	K_z	P_{sl} (kPa)	P_a (kPa)	P_w (kPa)	S_u (kPa)	σ_v (kPa)	FS	Remark
L=10.2	Proposed	-	94.5	-	-	20.0	141.3 (142.0)	0.78	Falloff
	Rankine's	0.27	94.5	31.4	70.0	-	186.2 (193.0)	0.92	Falloff
	Hajnal's	0.27	94.5	21.2	70.0	-	148.6 (149.3)	1.04	Falloff
L=4.0	Proposed	-	94.5	-	-	20.0	110.6 (111.3)	1.08	Stable
	Rankine's	0.27	94.5	31.4	70.0	-	186.2 (193.0)	0.93	Stable
	Hajnal's	0.27	94.5	13.3	70.0	-	119.1 (119.8)	1.13	Stable

K_d value used in Rankine's and Hajnal's methods is estimated by effective shear strength parameters ø' = 35°, which is correlated with PI of weak sandwiched soil according to data of some normally consolidated natural and remolded clays (Kenney 1959).
Values in parenthesis are vertical driving pressures including self-weight of weak soil. They show that influence of self-weight of weak soil is negligible in the proposed method.

(after Tsai et al, 1998)

state. Therefore for the latter case study, the proposed limit analysis is a great simplification of the true behavior of the soil.

4.2.6 Summary

In summary, the slurry stabilization of trenches is a widely used method, relatively cost effective, performs well and provides for versatile uses. Furthermore, the prospect of using dredged sediments as the soil in soil-bentonite backfill material should not pose any problems, provided that the adequate design and construction procedures are adhered to.

SECTION 5

HYDRAULIC CONDUCTIVITY TEST RESULTS

5.1 TESTING ON DREDGED SEDIMENT AND SEDIMENT MI X

Preliminary testing on the dredged sediments was done to determine suitable moisture content and corresponding viscosity of the sediment, that could then be used in the mix design. The sediment was tested for density, moisture content, viscosity and filtrate loss.

Similar tests were performed on the sediment mixes, made with 1%, 2% and 3% of bentonite by weight. These tests were carried out to determine the effect of bentonite on mud weight densities, moisture content, viscosity, filtrate loss and hydraulic conductivity. Some of the mixtures prepared with 1% bentonite were modified with the addition of fly ash, to determine the effect of fly ash on hydraulic conductivity.

5.1.1 Results of preliminary testing on dredged material.

Density testing of the dredged sediments revealed an average density of 10.8kN/m³ (68.49 pcf), which compares to results from a study conducted on dredged harbor bottom sediments by Vaghar et al (1997), which gave unit weight values in the range of 11.70-12.32 kN/m^3 (74.2-78.1 pcf). The mud weight density of the Baltimore Harbor dredged sediments also falls within the range of the density of bentonite slurries (64-80pcf).

The moisture content of the sediment ranged between 400-600 %. For the dredged material to be in the upper allowable viscosity range of 32-40 s, the moisture content was

on the lower end of its range, and when the viscosity was in the lower end of the allowable range, the moisture content was on the upper end of its range.

The filtrate loss test resulted in a volume filtrate of 23.8mL collected after 30 min, 50 ml after 1½ hours, and a total volume of filtrate of 375mL collected after an estimated time of 11hrs. 13min. The gradient of the filtrate loss curve was 8.6×10^{-3} mL/s. The filter cake thickness was 10 mm, it was smooth and black in color.

5.2 EFFECT OF BENTONITE ON SEDIMENT MIX

5.2.1 Effect of Bentonite on Mud Weight Densities & Moisture Content

The results of the mud weight densities revealed that with increasing bentonite content, the mud weight density increased. This is an expected trend. Refer to Table 5.1.

With increasing bentonite content there was decreasing moisture content. Bentonite , a montmorillonite clay, usually swells in the presence of water, therefore it is expected that the bentonite introduced would absorb some of the water in making the homogeneous mixture. Table 5.2 and Figure 5.2 show the resulting trend.

5.2.2 Effect of Bentonite on Viscosity

The results showed that the viscosity increased as the bentonite content increased. An initial water content which gave a viscosity measure on the lower end of the suitable range (32-40 s) was used. It was not difficult to adjust the water content, so that with the initial addition of bentonite a higher or lower viscosity could be attained. Also, the sediment-bentonite mix was workable, even though there was some difficulty in attaining a homogeneous mixture in the laboratory due to the nature of the materials. As bentonite is a type of clay and denser than the dredged sediments, it is expected that the mixture,

Table 5.1 – Mud Weight Densities

Mud Weight Density (kN/m³)	
	Sample A
Bentonite	Test Series
Content (%)	#1
1	10.66
2	10.82
3	10.87

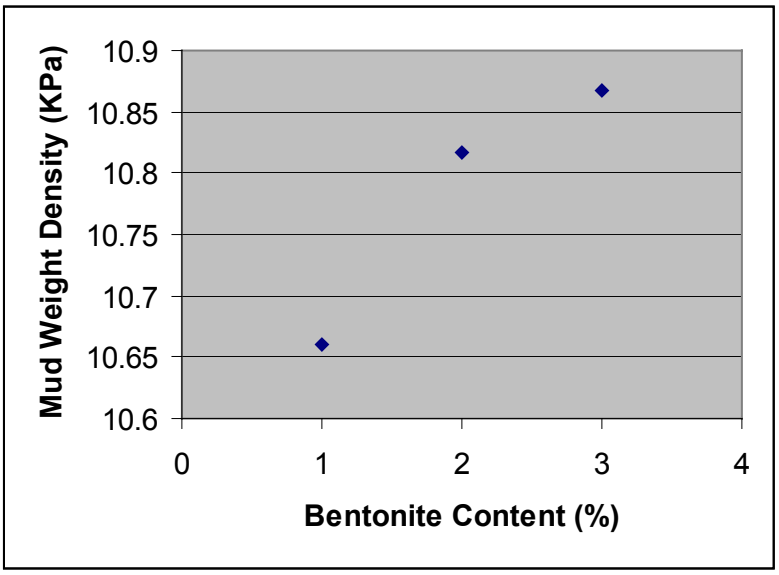

Fig 5.1 – Effect of Bentonite on Mud Weight Density

Table 5.2 – Moisture Content Results

	Moisture Content (%)	
	Sample A	**Sample B**
Bentonite	Test Series	Test Series
Content (%)	#1	#2
1	583.4	531.5
2	552.9	494.0
3	517.0	462.4

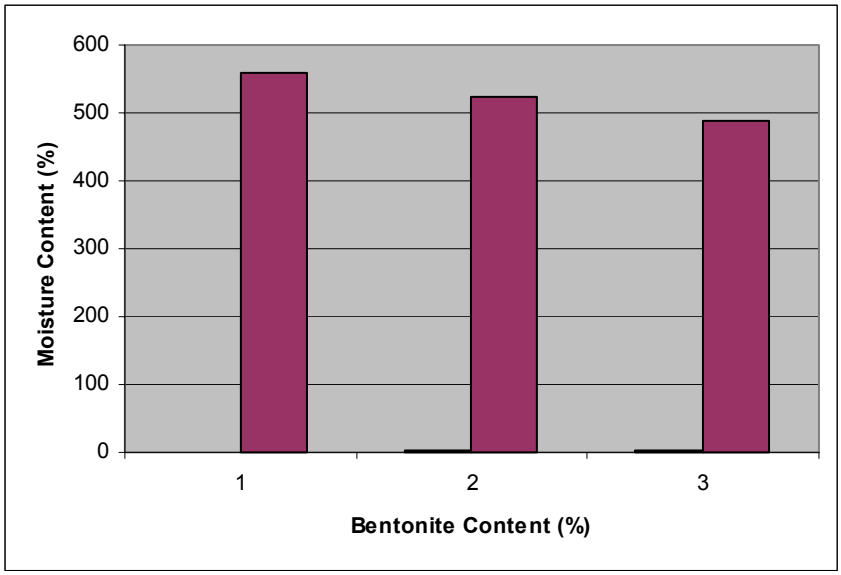

Fig 5.2 – Effect of Bentonite Content on Moisture Content

will become more viscous with increasing bentonite content. Table 5.3 and Figure 5.3 show the values measured with increasing bentonite content.

5.2.4 Effect of Bentonite Content on Hydraulic Conductivity

The principal factor in the performance of vertical barrier systems is the hydraulic conductivity (Evans, 1994). Increasing bentonite content resulted in decreasing hydraulic conductivity. Comparable results have been found in studies by Evans, (1994). It was found that increasing the bentonite content in a vertical barrier will decrease the hydraulic conductivity in soil-bentonite and in-situ mixed walls; there may, however, be an optimum. For a particular mix used, the minimum hydraulic conductivity was found at a bentonite content of about 3%. A similar trend of decreasing hydraulic conductivity with increasing bentonite content was found in a study done by D'Appolonia (1980). The hydraulic conductivity of soil-bentonite used in vertical barrier construction is typically between $1x10^{-7}$ cm/s and $1x10^{-8}$ cm/s (Evans, 1994).

The hydraulic conductivity, k in cm/s, was calculated by use of the following equation:

$$k = (q/h) \times t \qquad (5.1)$$

where q is the ratio of the flow in mL/s and the area of the apparatus (cm^2), h is the pressure head converted to cm, and t is the thickness of the filter cake formed. The permeability was then normalized through dividing by the relevant filter cake thickness.

Tables 5.4 through 5.6 and the corresponding Figures 5.4 through 5.6 show the effect of bentonite content on hydraulic conductivity at given applied pressures. The

Table 5.3- Marsh Funnel Test Results

Marsh Funnel Viscosity (s)	
Bentonite	Test
Content (%)	Series #1
1	36.53
2	39.39
3	42.05

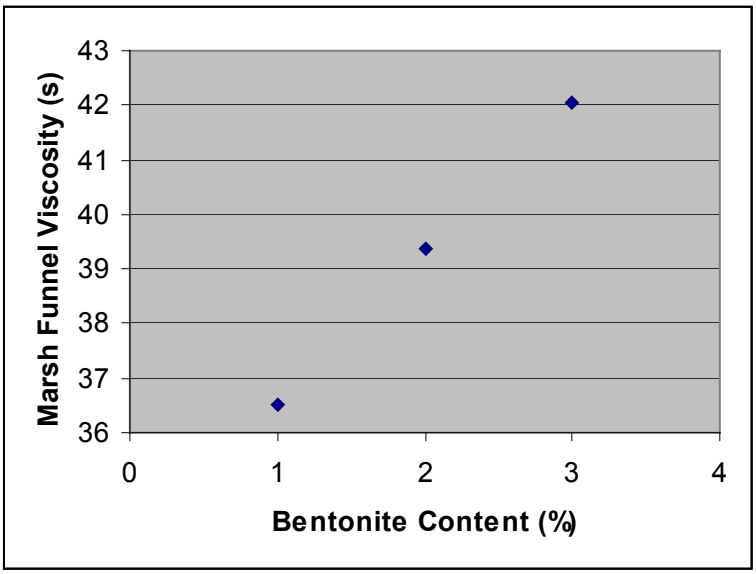

Fig. 5.3 – Marsh Funnel Viscosity versus Bentonite Content for Different Bentonite Slurries.

Table 5.4 – Effect of Bentonite Content on Hydraulic Conductivity, σ'= 48.3kPa

Specimen ID	Mix Type	Q (ml)	Flow rate (ml/s)	Kc	Kc/tc
N	B1	200	0.101	3.78E-07	4.20E-06
M	B1	195	0.100	4.16E-07	4.16E-06
E	B2	91	0.040	1.98E-07	1.65E-06
A	B3	324	0.011	4.48E-08	4.48E-07

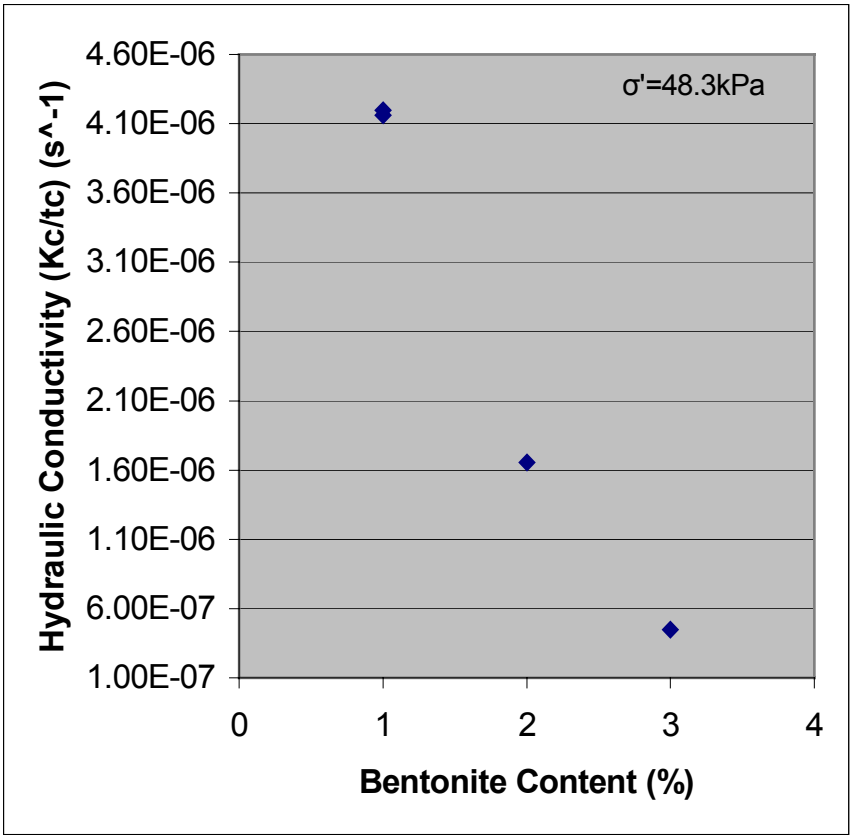

Figure 5.4 – Effect of Bentonite Content on Hydraulic Conductivity, σ'=48.3kPa

Table 5.5 - Effect of Bentonite Content on Hydraulic Conductivity, σ' = 13.79kPa

Specimen ID	Mix Type	Q (ml)	Flow rate (ml/s)	Kc	Kc/tc
P	B1	200	0.069	1.00E-06	1.00E-05
O	B1	37	0.100	1.01E-06	1.45E-05
F	B2	299.7	0.076	5.51E-07	1.10E-05
T	B3	44	0.032	4.61E-07	4.61E-06

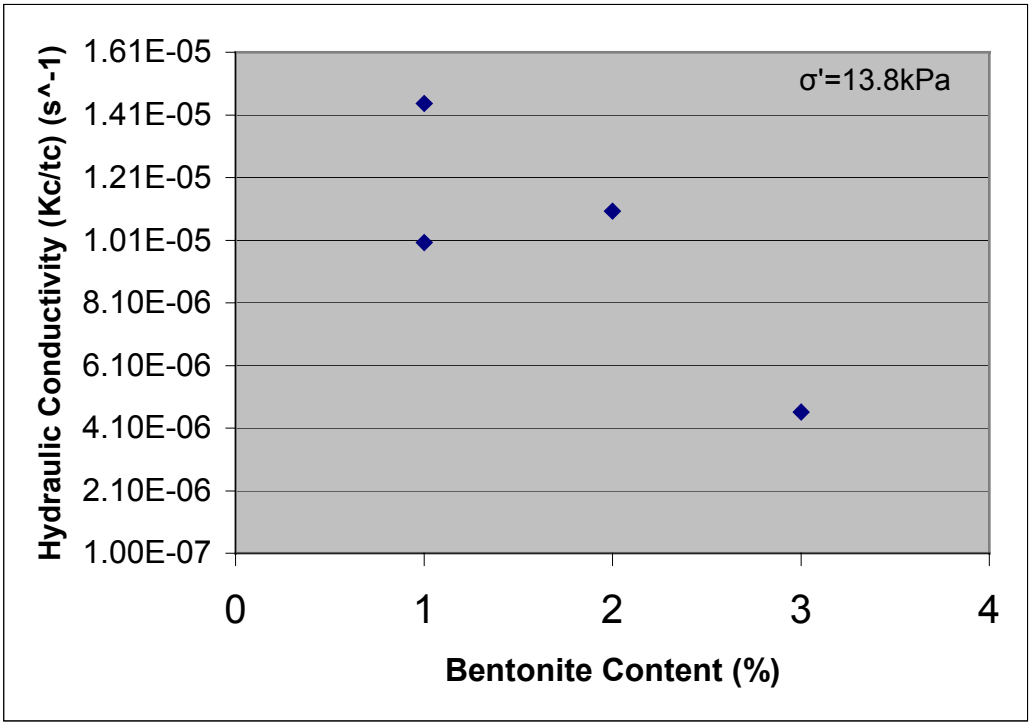

Figure 5.5 – Effect of Bentonite Content on Hydraulic Conductivity, σ'= 13.8kPa

Table 5.6 – Effect of Bentonite Content on Hydraulic Conductivity, σ'= 6.9kPa

Sample ID	Mix Type	Q (ml)	Flow rate (ml/s)	Kc	Kc/tc
H	1B	50	0.072	2.31E-06	2.1E-05
K	1B	195	0.071	2.87E-06	2.05E-05
Y	1B	45	0.099	3.17E-06	2.88E-05
R	1B	200	0.127	2.21E-06	3.69E-05
L	2B	200	0.069	9.98E-07	2.00E-05
S	2B	200	0.052	1.50E-06	1.50E-05
X	3B	287	0.010	3.11E-07	2.82E-06

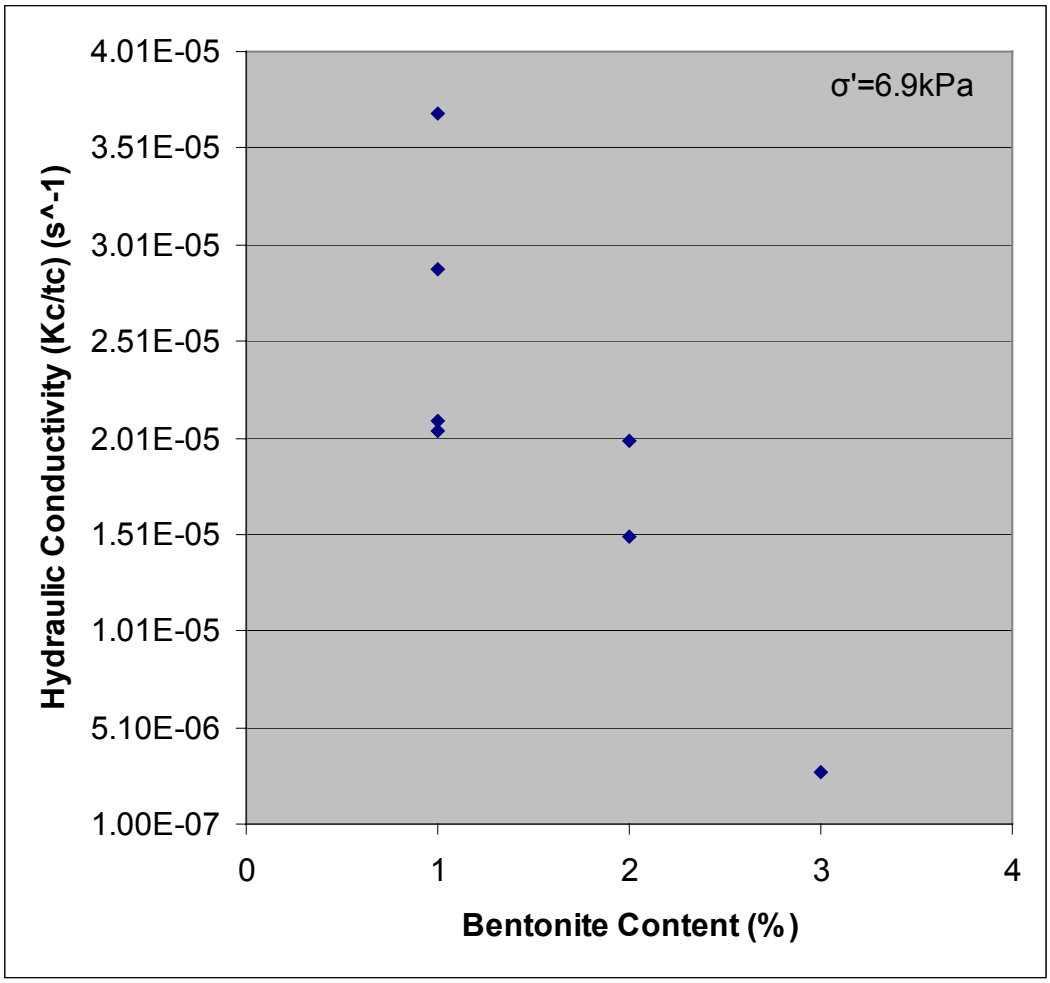

Figure 5.6 – Effect of Bentonite Content on Hydraulic Conductivity, σ'= 6.9kPa

hydraulic conductivity achieved was also generally lower for the same mixes, when greater pressure was exerted. This is expected as with increasing effective stress, the void ratio decreases and so would the hydraulic conductivity. A study by Evans (1994) showed similar results. For any given sample of vertical barrier material, the hydraulic conductivity decreases as the effective consolidation pressure increases.

5.3 – EFFECT OF FLY ASH ON SEDIMENT MIX

5.3.1 – Effect of Fly Ash on Hydraulic Conductivity

With increasing fly ash content, and the same base mixture, the hydraulic conductivity of the mix was increased. This can be theoretically explained in that as the fly ash attaches itself to the fines present, the mixtures resemble a more granular structure, hence increasing the void ratio and hydraulic conductivity. Tables 5.7 through 5.9 and the corresponding Figures 5.7 through 5.9 show the effect of fly ash on hydraulic conductivity at given pressures.

5.4 – FILTRATE LOSS RESULTS FROM SEDIMENT MIX

There does not seem to be a particular trend with the filtrate loss curves, apart from the fact that those developed at 1% bentonite and different pressures have a more irregular shape than those developed at 2% and 3% bentonite. The filtrate loss results for the bentonite specimens tested ranged from 2.27 mL/s to 0.04 mL/s. The filtrate loss results for the fly ash specimens tested ranged from 14.29 mL/s to 1.54 mL/s. Figure 5.10 is given as an example to show the filtrate loss with time. The tests shown were

Table 5.7 – Effect of Fly Ash on Hydraulic Conductivity, σ'= 48.3kPa

Sample ID	Mix	Q (ml)	Flow rate (ml/s)	Kc	Kc/tc
B	1B-5FA	336	0.383	7.93E-07	1.59E-05
W	1B-8FA	20	1.333	7.18E-06	5.52E-05

Note: Pressure is 48.3kPa and base mixture is 1% bentonite

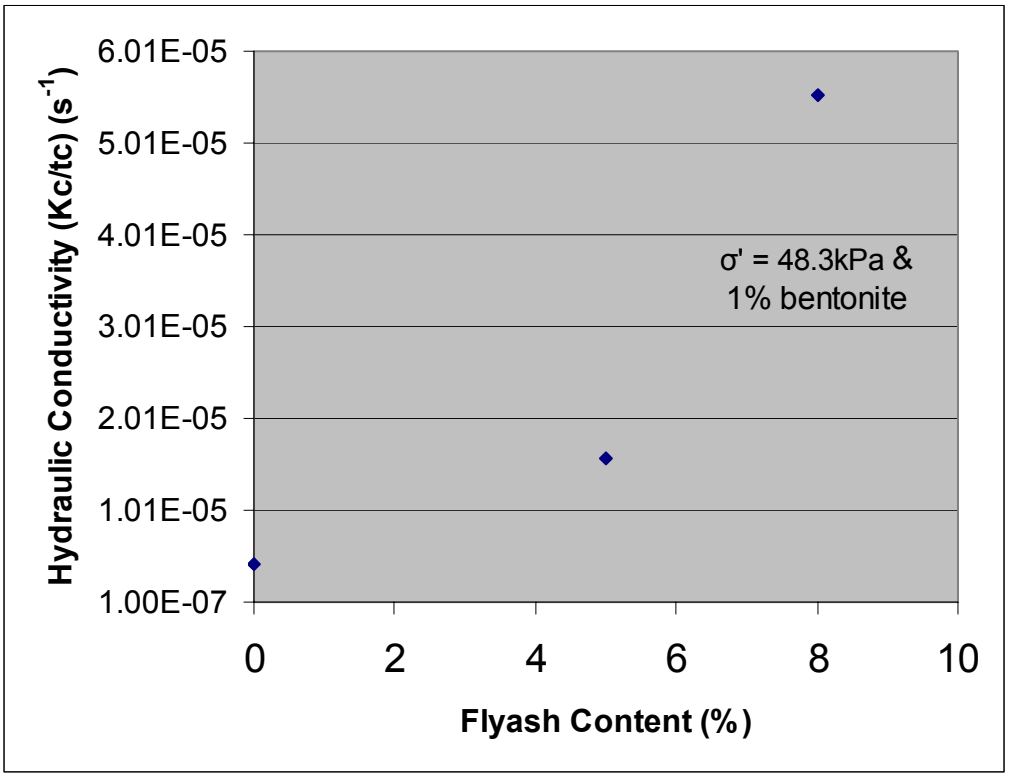

Figure 5.7 – Effect of Fly Ash on Hydraulic Conductivity, σ'= 48.3kPa

Table 5.8 – Effect of Fly Ash on Hydraulic Conductivity, σ'= 13.8kPa

Sample ID	Mix Type	Q (ml)	Flow rate (ml/s)	Kc	Kc/tc
I	1B-5FA	263.5	0.151	2.20E-06	2.2E-05
C	1B-8FA	259	0.778	1.13E-05	1.13E-04

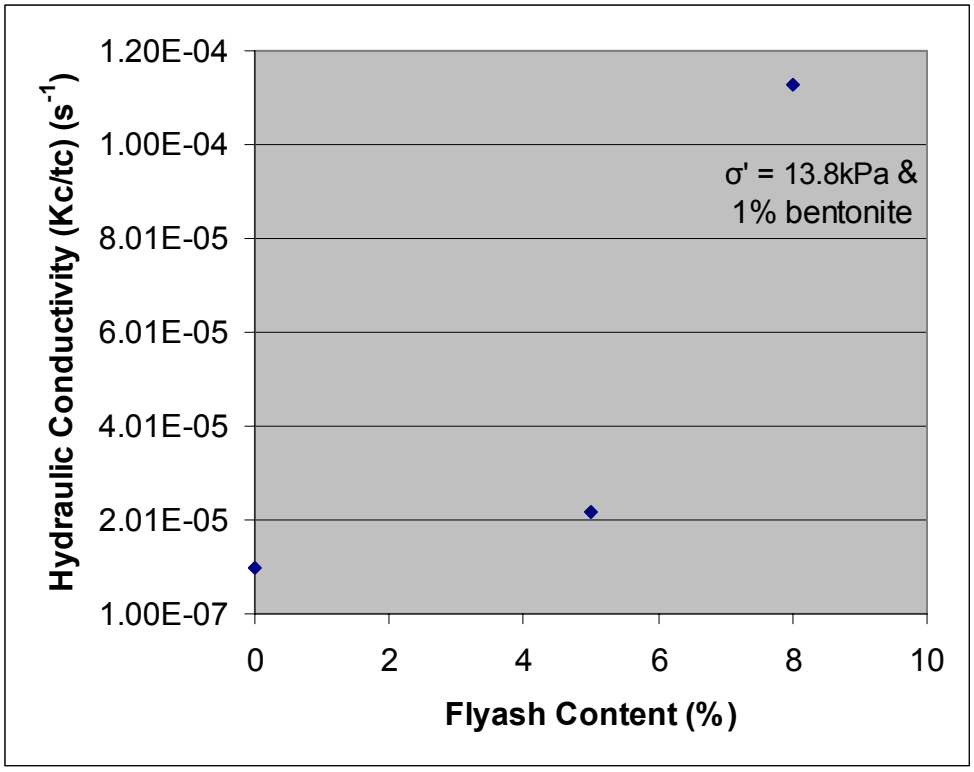

Figure 5.8 – Effect of Fly Ash on Hydraulic Conductivity, σ'= 13.8kPa

Table 5.9 – Effect of Fly Ash on Hydraulic Conductivity, σ'= 6.9kPa

Sample ID	Mix Type	Q (ml)	Flow rate (ml/s)	Kc	Kc/tc
D	1B-5FA*	318	0.530	1.08E-05	1.54E-04
J	1B-8FA	340	0.567	1.64E-05	1.64E-04
G	1B-8FA*	259	0.778	5.64E-06	1.13E-04

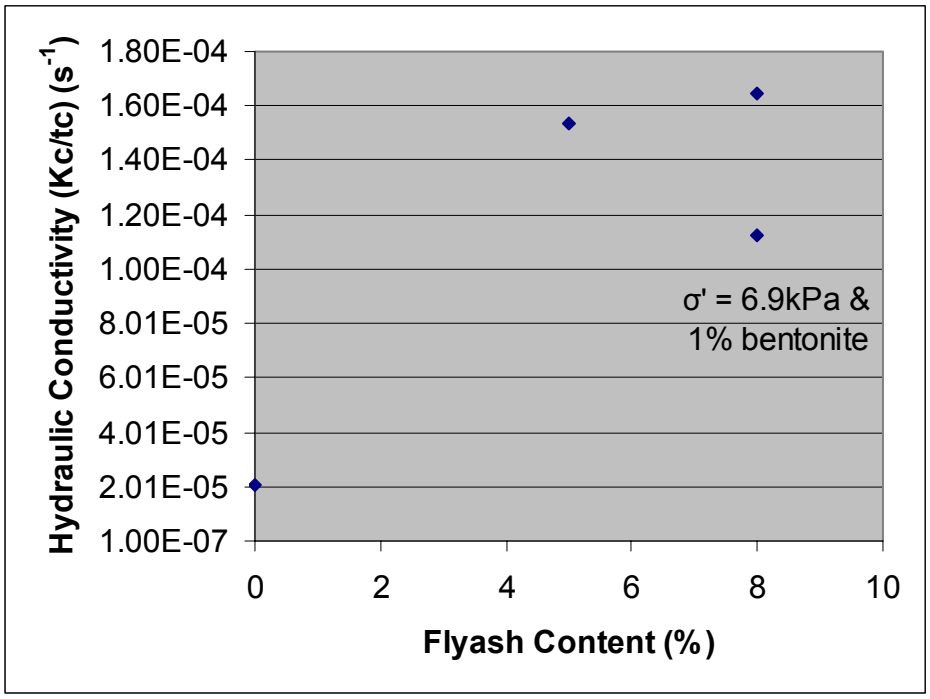

Figure 5.9 – Effect of Fly Ash on Hydraulic Conductivity, σ'= 6.9kPa

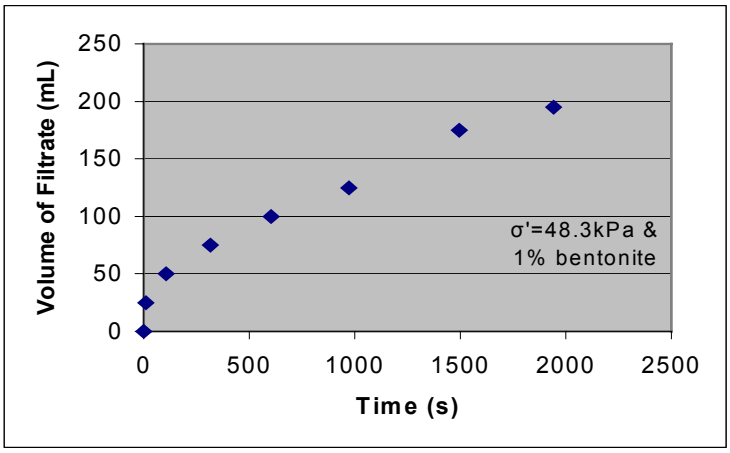

Figure 5.10a – Filtrate loss for specimen at σ'= 48.3kPa and 1% bentonite

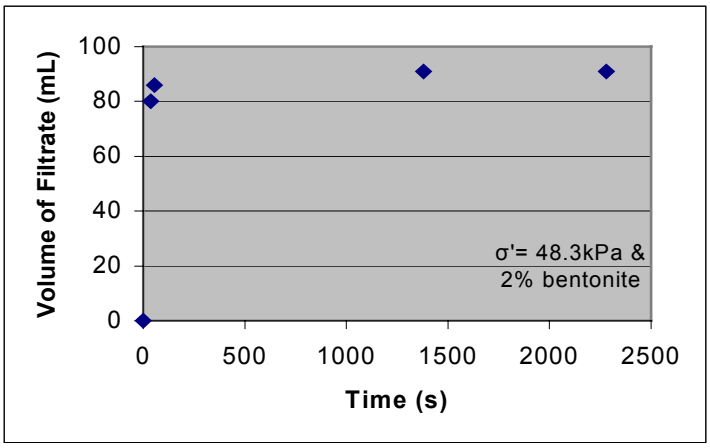

Figure 5.10b – Filtrate loss for specimen at σ'= 48.3kPa and 2% bentonite

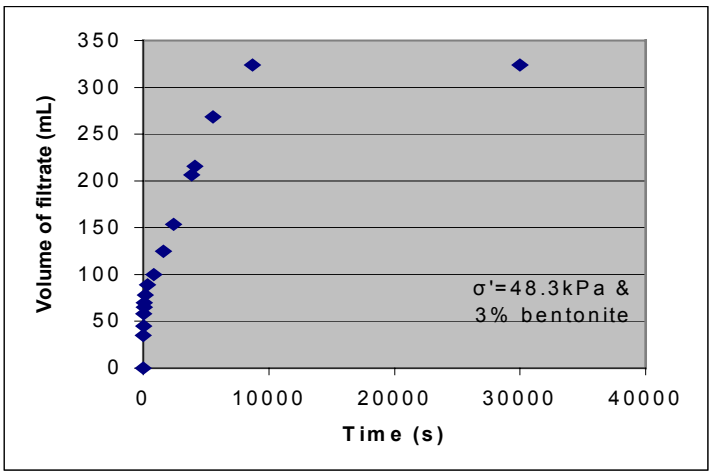

Figure 5.10c – Filtrate loss at σ'= 48.3kPa and 3% bentonite

conducted under a pressure of 48.3kPa. Figure 5.10a shows the filtrate loss (gradient) of 0.21 mL/s at 1% bentonite. Figure 5.10b gives a gradient of 1.54 ml/s at 2% bentonite and Figure 5.10c gives a gradient of 0.04 mL/s at 3% bentonite. In a study by D'Appolonia (1980), it was said that filtrate loss properties of the slurry have a minor influence on (Kc/tc). It was also said that slurries having a high filtrate loss develop a thicker but more pervious filter cake than slurries having a low filtrate loss. As a result, the ratio (Kc/tc) is relatively unchanged.

5.5 – SYNTHESIS

The dredged sediments were put through preliminary testing of mud weight density, moisture content, marsh funnel viscosity and filtrate loss to determine properties and a suitable moisture content and viscosity that could be used in the mix design.

Upon the addition of 1%, 2% and 3% bentonite by weight, several tests were performed on the mix to determine the effects of the bentonite added. The effects on density, moisture content, Marsh funnel viscosity were examined. Upon the addition of 5% and 8% fly ash by weight to the 1% bentonite mix, hydraulic conductivity and filtrate loss were examined for all the mixes.

The conclusions that can be drawn are as follows:

- The mud weight density of the dredged sediments 10.77KN/m³ (68.49 pcf) falls within the range of bentonite slurries (64-80pcf).
- A suitable moisture content and viscosity of the dredged sediments can be attained that will make it usable in the mix design.

- Increasing bentonite content leads to an increase in mud weight density. This is helpful as the backfill material must be denser than the slurry in order to displace it in the construction process.
- An increase in bentonite content allows for decreased moisture content and correspondingly increased viscosity.
- Increasing bentonite content, to the percent tested (3%), resulted in a decrease in hydraulic conductivity. The optimum range to serve the purpose of use as a vertical cutoff wall ($1x10^{-7}$ to $1x10^{-8}$) was near realized ($4.48x10^{-7}$) at 3% bentonite and an applied pressure of 48.3kPa.
- Increasing the fly ash content to the percent tested (8%), (with the base as dredged sediments and 1% bentonite by weight), increased the hydraulic conductivity.
- The filtrate loss results did not show any distinct trends. The filtrate loss on the bentonite specimens tested ranged from 2.27mL/s to 0.04mL/s. The filtrate loss on the fly ash specimens tested ranged from 14.29mL/s to 1.54mL/s.
- Dredged sediments can therefore serve the purpose of inhibiting the flow of ground water which is the most important function of a vertical cut-off wall.

SECTION 6

ADSORPTION RESULTS

6.1 ADSORPTION TESTING

Equilibrium batch testing, according to ASTM D4646 specification was performed on the sediment mixes and aqueous solutions containing heavy metals to determine the adsorption characteristics of the sediment mix. The mixes were made with 1%, 2% and 3% of bentonite by weight. These tests were carried out to determine the effect of bentonite on the adsorption capacity of the mix. Some of the mixtures prepared with 1% bentonite were modified with the addition of fly ash, to determine the effect of fly ash on its adsorption capacity. Fly ash was added in the proportions of 5% and 8% by weight. Typical field values of thickness of barrier (L), hydraulic gradient (i) and effective porosity (n_e) were used in the analysis. The metal sorbates used were cadmium, chromium, lead and zinc.

K_d was determined from the equilibrium batch testing. K_d (L/mg) is the linear partitioning coefficient (slope of the linear portion of mass sorbed per mass sorbent versus equilibrium contaminant concentration in solution at the end of test (mg/ L)). The results obtained from the batch reaction testing were used to model the transport of certain metals through the dredged sediment 'barrier'. This follows analysis done in determining the adsorption characteristics of paper clay, Moo-Young et al (2000), and clay liners. The advection-dispersion-adsorption equation was used for modeling contaminant flow. The effluent concentration passing through a barrier is predicted with the advection-dispersion-adsorption equation which is defined as follows:

$$C/C_o = 0.5\{erfc\,[(1-T_r)/(2(Tr/P_l)^{0.5})] + \exp(P_l)\,erfc[(1+T_r)/(2(Tr/P_l)^{0.5})]\} \quad (6.1)$$

where C/C_o = dimensionless relative concentration, C = effluent concentration (mg/L), C_o = influent concentration (mg/L), T_r = dimensionless time factor (Eqn. 6.2), v = seepage velocity, t = time, L = length of barrier (thickness) (m), P_l = peclet number (Eqn. 6.4), D_x = hydrodynamic dispersion (m^2/s) (Eqn. 6.5), D_m = diffusion coefficient, R_d = retardation factor (Eqn 6.6), erfc = complementary error function.

In defining equation 6.1, other equations should be defined:

$$T_r = vt/LR_d \quad (6.2)$$

$$v = ki/n_e, \quad (6.3)$$

$$P_l = v\,L/D_x \quad (6.4)$$

$$D_x = (0.1Lv + D_m) \quad (6.5)$$

$$R_d = 1 + (\gamma K_d/n_e) \quad (6.6)$$

where k is the experimentally determined hydraulic conductivity. In using Equation (6.1), certain values were assumed, and certain typical field values were varied. D_m was assumed to be $2x10^{-10}$ m^2/s, the hydraulic gradient was varied between (0.02 and 0.08), the wall thickness was varied between (0.8 and 1.1m) and the porosity was varied between (0.27 and 0.37).

Equation (6.1) was used to calculate the dimensionless effluent concentration (C/C_o) for a range of times. By plotting (C/C_o) versus the dimensionless time factor T_r, a breakthrough curve was obtained to estimate the time required to reach a point where the

effluent concentration exceeded established limits. After this point, the dredged material would have to be replaced, or an alternate remediation method would have to be used.

6.1.1 Effect of Bentonite Content on Adsorption

The adsorption capacity of the mix for the given metals was increased (i.e. the breakthrough time was extended) with increasing bentonite content. A range of values of typical field conditions related to hydraulic gradient in the field, effective porosity and the thickness of the barrier were varied in the analysis. The following reported values, however, are the results obtained using the average of these typical field values.

With respect to the sorption of cadmium, 1% , 2% and 3% bentonite mixes gave corresponding breakthrough times of approximately 1, 2.25 and 4.5 years respectively. Table 6.1 and Figure 6.1 illustrate this trend. Figure 6.1(a) shows C/C_o versus the dimensionless time factor, T_r. To more clearly show the time effects, Figure 6.1 (b) shows C/C_o versus time in years. With respect to the sorption of chromium, using 1% , 2% and 3% bentonite gave corresponding breakthrough times of approximately 0.75, 1.75 and 20 years respectively. Table 6.2 and Figure 6.2 illustrate this trend.

For the lead sorption, 1%, 2% and 3% bentonite mixes gave corresponding breakthrough times of approximately 2.75, 10 and 72 years respectively. Table 6.3 and Figure 6.3 show this trend. For the zinc sorption, 1%, 2% and 3% bentonite mixes gave corresponding breakthrough times of approximately 1.25, 5 and 13.5 years respectively. Table 6.4 and Figure 6.4 show this trend.

Table 6.1 (a) – Adsorption of Cadmium

1% BENTONITE

Time (yrs.)	Time Factor	C/Co
0.100	0.343	9.49E-03
0.250	0.859	4.47E-01
0.500	1.717	9.28E-01
0.750	2.576	9.93E-01
1.000	3.435	9.99E-01
1.250	4.293	1.00E+00
1.500	5.152	1.00E+00
1.750	6.011	1.00E+00
2.000	6.869	1.00E+00
2.250	7.728	1.00E+00
2.500	8.587	1.00E+00
2.750	9.445	1.00E+00
3.000	10.304	1.00E+00

(b)

2% BENTONITE

Time (yrs.)	Time Factor	C/Co
0.100	0.153	1.22E-06
0.250	0.382	1.95E-02
0.500	0.764	3.45E-01
0.750	1.146	7.01E-01
1.000	1.528	8.83E-01
1.250	1.910	9.57E-01
1.500	2.292	9.84E-01
1.750	2.674	9.94E-01
2.000	3.057	9.98E-01
2.250	3.439	9.99E-01
2.500	3.821	1.00E+00
2.750	4.203	1.00E+00
3.000	4.585	1.00E+00

(c)

3% BENTONITE		
Time (yrs.)	**Time Factor**	**C/Co**
0.100	0.078	1.96E-13
0.500	0.391	2.39E-02
1.000	0.783	3.68E-01
1.500	1.174	7.19E-01
2.000	1.565	8.92E-01
2.500	1.957	9.60E-01
3.000	2.348	9.86E-01
3.500	2.739	9.95E-01
4.000	3.131	9.98E-01
4.500	3.522	9.99E-01
5.000	3.914	1.00E+00
5.500	4.305	1.00E+00
6.000	4.696	1.00E+00

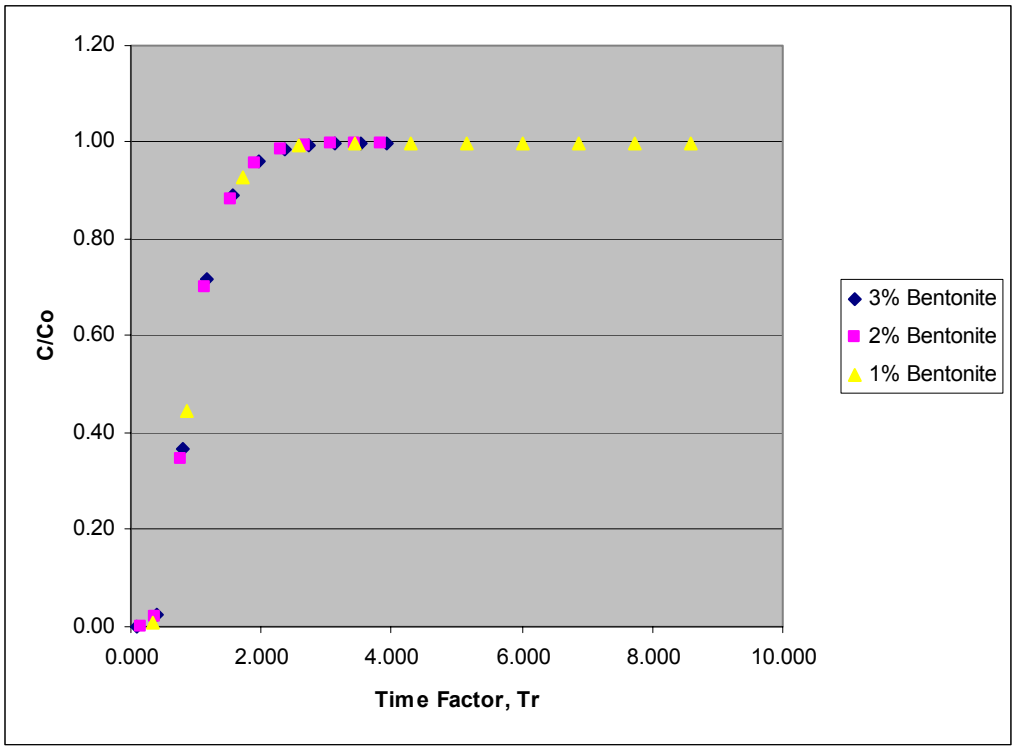

Fig 6.1(a) – Effect of Bentonite on Cadmium Adsorption

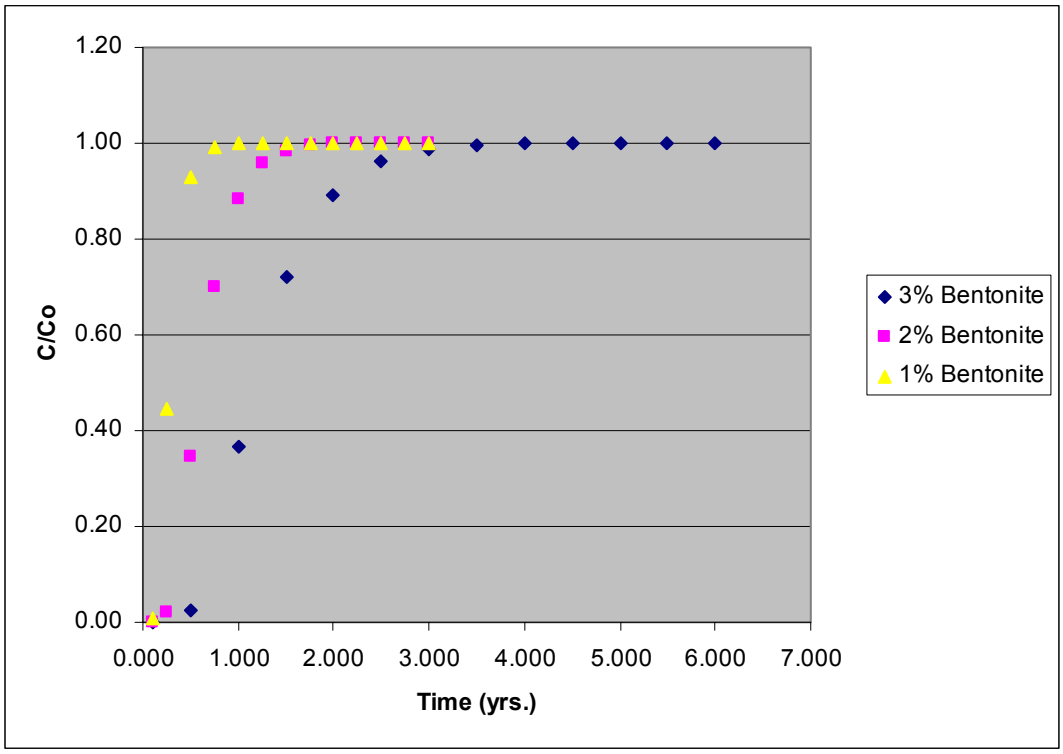

Fig 6.1(b) – Effect of Bentonite on Cadmium Adsorption

Table 6.2 (a) – Adsorption of Chromium

1% BENTONITE

Time (yrs.)	Time Factor	C/Co
0.100	0.593	1.60E-01
0.250	1.482	8.69E-01
0.500	2.965	9.97E-01
0.750	4.447	1.00E+00
1.000	5.930	1.00E+00
1.250	7.412	1.00E+00
1.500	8.895	1.00E+00
1.750	10.377	1.00E+00
2.000	11.860	1.00E+00
2.250	13.342	1.00E+00
2.500	14.825	1.00E+00
2.750	16.307	1.00E+00
3.000	17.790	1.00E+00

(b)

2% BENTONITE

Time (yrs.)	Time Factor	C/Co
0.100	0.192	3.48E-05
0.250	0.481	6.78E-02
0.500	0.962	5.51E-01
0.750	1.442	8.54E-01
1.000	1.923	9.58E-01
1.250	2.404	9.88E-01
1.500	2.885	9.97E-01
1.750	3.366	9.99E-01
2.000	3.846	1.00E+00
2.250	4.327	1.00E+00
2.500	4.808	1.00E+00
2.750	5.289	1.00E+00
3.000	5.770	1.00E+00

(c)

3% BENTONITE		
Time (yrs.)	**Time Factor**	**C/Co**
0.100	0.016	0.00E+00
2.500	0.401	2.74E-02
5.000	0.801	3.89E-01
7.500	1.202	7.37E-01
10.000	1.603	9.01E-01
12.500	2.003	9.65E-01
15.000	2.404	9.88E-01
17.500	2.805	9.96E-01
20.000	3.205	9.99E-01
22.500	3.606	9.99E-01
25.000	4.007	1.00E+00
27.500	4.407	1.00E+00
30.000	4.808	1.00E+00

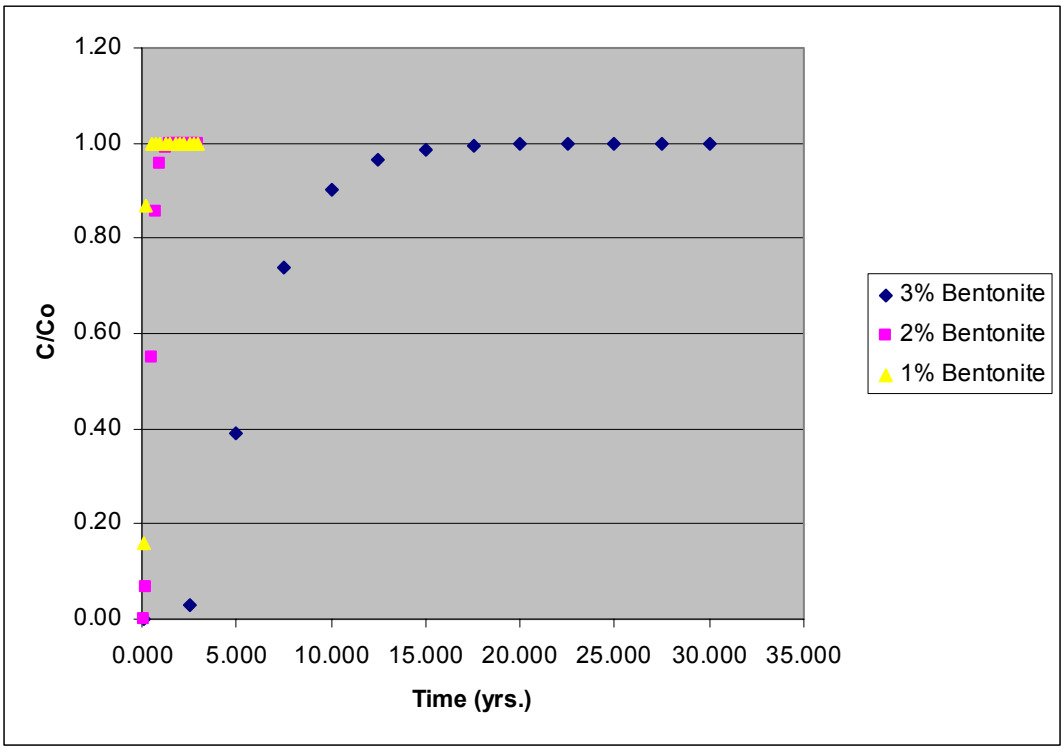

Fig 6.2 – Effect of Bentonite on Chromium Adsorption

Table 6.3 (a) – Adsorption of Lead

1% BENTONITE

Time (yrs.)	Time Factor	C/Co
0.100	0.120	1.38E-08
0.250	0.301	3.51E-03
0.500	0.602	1.69E-01
0.750	0.903	4.93E-01
1.000	1.205	7.39E-01
1.250	1.506	8.76E-01
1.500	1.807	9.43E-01
1.750	2.108	9.75E-01
2.000	2.409	9.89E-01
2.250	2.710	9.95E-01
2.500	3.011	9.98E-01
2.750	3.312	9.99E-01
3.000	3.614	1.00E+00

(b)

2% BENTONITE

Time (yrs.)	Time Factor	C/Co
0.100	0.035	0.00E+00
1.000	0.348	1.06E-02
2.000	0.697	2.70E-01
3.000	1.045	6.24E-01
4.000	1.393	8.35E-01
5.000	1.741	9.32E-01
6.000	2.090	9.73E-01
7.000	2.438	9.89E-01
8.000	2.786	9.96E-01
9.000	3.134	9.98E-01
10.000	3.483	9.99E-01
11.000	3.831	1.00E+00
12.000	4.179	1.00E+00

(c)

3% BENTONITE		
Time (yrs.)	**Time Factor**	**C/Co**
0.100	0.005	0.00E+00
8.000	0.383	2.09E-02
16.000	0.765	3.49E-01
24.000	1.148	7.02E-01
32.000	1.531	8.82E-01
40.000	1.913	9.56E-01
48.000	2.296	9.84E-01
56.000	2.679	9.94E-01
64.000	3.061	9.98E-01
72.000	3.444	9.99E-01
80.000	3.827	1.00E+00
88.000	4.209	1.00E+00
96.000	4.592	1.00E+00

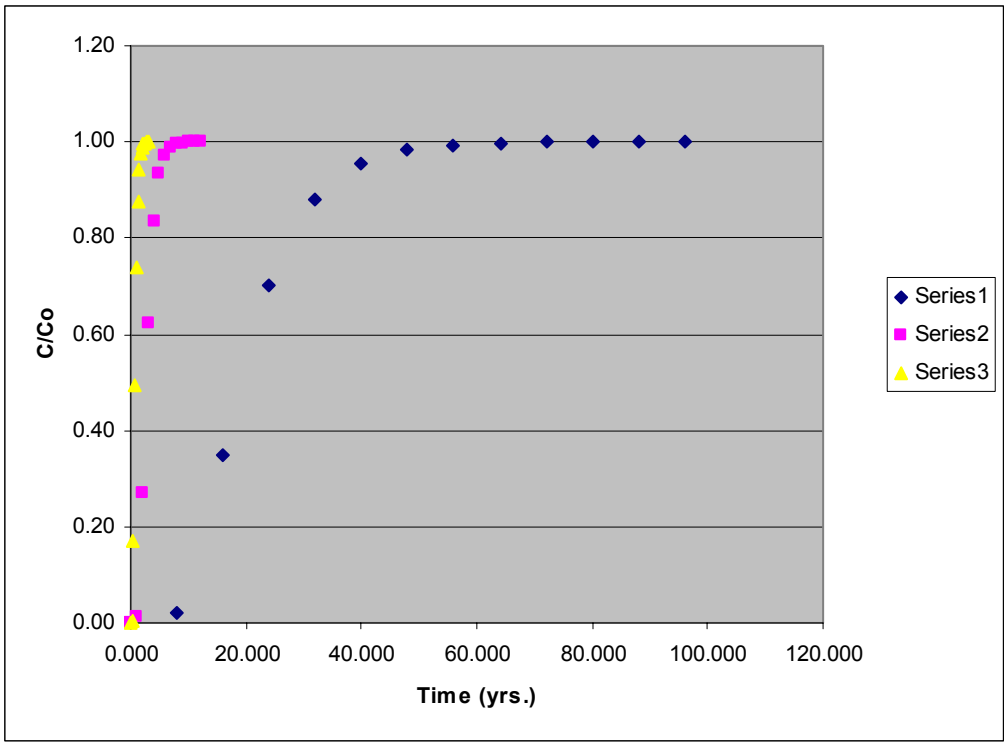

Fig 6.3 – Effect of Bentonite on Lead Adsorption

Table 6.3 (a) – Adsorption of Zinc

1% BENTONITE

Time (yrs.)	Time Factor	C/Co
0.100	0.120	1.38E-08
0.250	0.301	3.51E-03
0.500	0.602	1.69E-01
0.750	0.903	4.93E-01
1.000	1.205	7.39E-01
1.250	1.506	8.76E-01
1.500	1.807	9.43E-01
1.750	2.108	9.75E-01
2.000	2.409	9.89E-01
2.250	2.710	9.95E-01
2.500	3.011	9.98E-01
2.750	3.312	9.99E-01
3.000	3.614	1.00E+00

(b)

2% BENTONITE

Time (yrs.)	Time Factor	C/Co
0.100	0.035	0.00E+00
1.000	0.348	1.06E-02
2.000	0.697	2.70E-01
3.000	1.045	6.24E-01
4.000	1.393	8.35E-01
5.000	1.741	9.32E-01
6.000	2.090	9.73E-01
7.000	2.438	9.89E-01
8.000	2.786	9.96E-01
9.000	3.134	9.98E-01
10.000	3.483	9.99E-01
11.000	3.831	1.00E+00
12.000	4.179	1.00E+00

(c)

3% BENTONITE		
Time (yrs.)	**Time Factor**	**C/Co**
0.100	0.005	0.00E+00
8.000	0.383	2.09E-02
16.000	0.765	3.49E-01
24.000	1.148	7.02E-01
32.000	1.531	8.82E-01
40.000	1.913	9.56E-01
48.000	2.296	9.84E-01
56.000	2.679	9.94E-01
64.000	3.061	9.98E-01
72.000	3.444	9.99E-01
80.000	3.827	1.00E+00
88.000	4.209	1.00E+00
96.000	4.592	1.00E+00

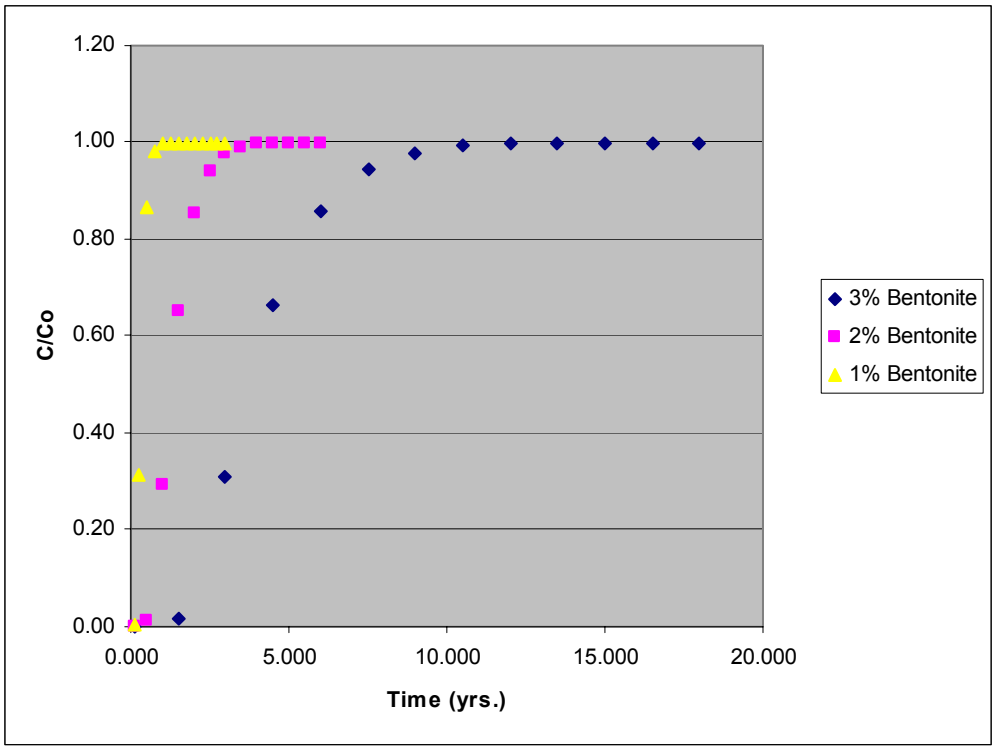

Fig 6.4 – Effect of Bentonite on Zinc Adsorption

6.1.2 – Effect of Fly ash Content on Adsorption

In using the metals tested, it was found that the corresponding breakthrough time decreased with increasing fly ash content. It was expected that the carbon content in the fly ash would enhance the adsorption capacity of the mix. However, the increased hydraulic conductivity of the mix (which leads to lower adsorption capacity) may have outweighed the beneficial adsorptive effects of the carbon in the fly ash. In the case of cadmium, 5% and 8% fly ash content gave corresponding breakthrough times of approximately 110 and 36 days respectively. Table 6.5 and Figure 6.5 show the behavior of cadmium. Figure 6.5(a) shows C/C_o versus the dimensionless time factor, T_r. To more clearly show the time effects, Figure 6.5(b) shows C/C_o versus time in years. In the case of chromium, 5% and 8% fly ash content gave corresponding breakthrough times of approximately 90 and 40 days respectively. Table 6.6 and Figure 6.6 show the behavior of chromium.

In the case of lead, 5% and 8% fly ash content gave corresponding breakthrough times of approximately 275 and 135 days respectively. Table 6.7 and Figure 6.7 show the behavior of lead. In the case of zinc, 5% and 8% fly ash content gave corresponding breakthrough times of approximately 220 and 100 days respectively. Table 6.8 and Figure 6.8 show this behavior trend.

6.1.3 – Effect of Varying Field Conditions on Adsorption

Under the circumstances tested, typical field condition values for hydraulic gradient in the field, effective porosity and thickness of barrier were varied to see the

effect they would have on the breakthrough time. This was analyzed using Equation 6.1 and the associated breakthrough curve plots.

In all cases, an increase in the thickness of barrier from 0.8 m to 1.1 m leads to a moderate increase in the breakthrough time. For the mix containing 3% bentonite that was being used to adsorb zinc, the breakthrough time increased from approximately 12 years to 16.5 years. Similar trends were obtained for the other metals tested with different design mixes, the trend is shown in Figure 6.9. This could be theoretically explained in that there is a larger specific surface area of the material that has the capacity to adsorb the respective metal. This theory has been seconded in a study by Moo-Young et al (2000).

An increase in the hydraulic from 0.02 to 0.08 lead to a substantial decrease in the breakthrough time. For the mix containing 3% bentonite that was being used to adsorb zinc, the breakthrough time decreased from approximately 36 years to 9 years. Similar trends were obtained for the other metals tested, the trend is shown in Figure 6.10. This can be explained in that an increased hydraulic gradient causes ground water or contaminant solution to flow faster and therefore drives the contaminants (metals) through the barrier mix at a faster rate.

An increase in the effective porosity from 0.27 to 0.37, lead to no significant change in the breakthrough time. For the mix containing 2% bentonite that was being used to adsorb zinc, the breakthrough time remained at approximately 5 years. Similar results were obtained for the other metals tested, the trend is shown in Figure 6.11. It would be theoretically expected that there would be a decrease in the breakthrough time. This is because an increased effective porosity means greater pore space for the

Table 6.5(a) – Adsorption of Cadmium

1%BENTONITE & 5%FLY ASH		
Time (days)	**Time Factor**	**C/Co**
0.100	0.003	0.00E-00
10.000	0.306	4.00E-03
20.000	0.613	1.79E-01
30.000	0.919	5.09E-01
40.000	1.225	7.52E-01
50.000	1.532	8.84E-01
60.000	1.838	9.48E-01
70.000	2.145	9.77E-01
80.000	2.451	9.90E-01
90.000	2.757	9.96E-01
100.000	3.064	9.98E-01
110.000	3.370	9.99E-01
120.000	3.676	1.00E+00

(b)

1%BENTONITE & 5%FLY ASH		
Time (days)	**Time Factor**	**C/Co**
0.100	0.010	0.00E+00
3.000	0.298	3.15E-03
6.000	0.595	1.62E-01
9.000	0.893	4.82E-01
12.000	1.191	7.31E-01
15.000	1.488	8.71E-01
18.000	1.786	9.40E-01
21.000	2.084	9.73E-01
24.000	2.381	9.88E-01
27.000	2.679	9.95E-01
30.000	2.976	9.98E-01
33.000	3.274	9.99E-01
36.000	3.572	1.00E+00

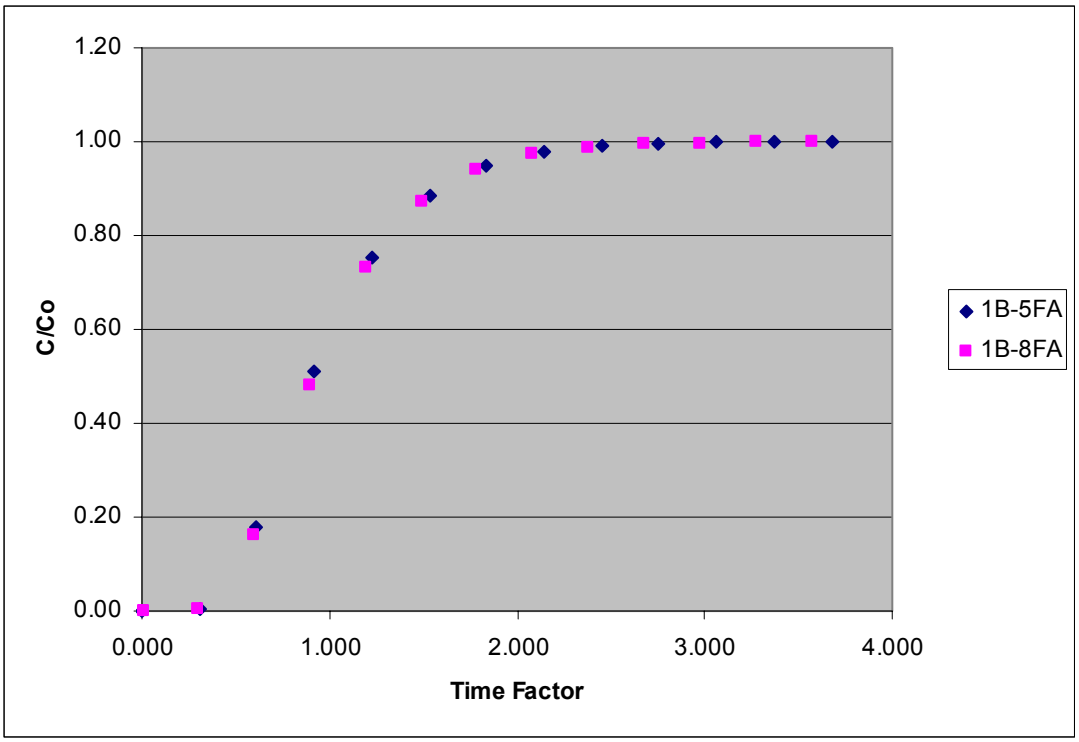

Fig 6.5(a) – Effect of Bentonite on Cadmium Adsorption

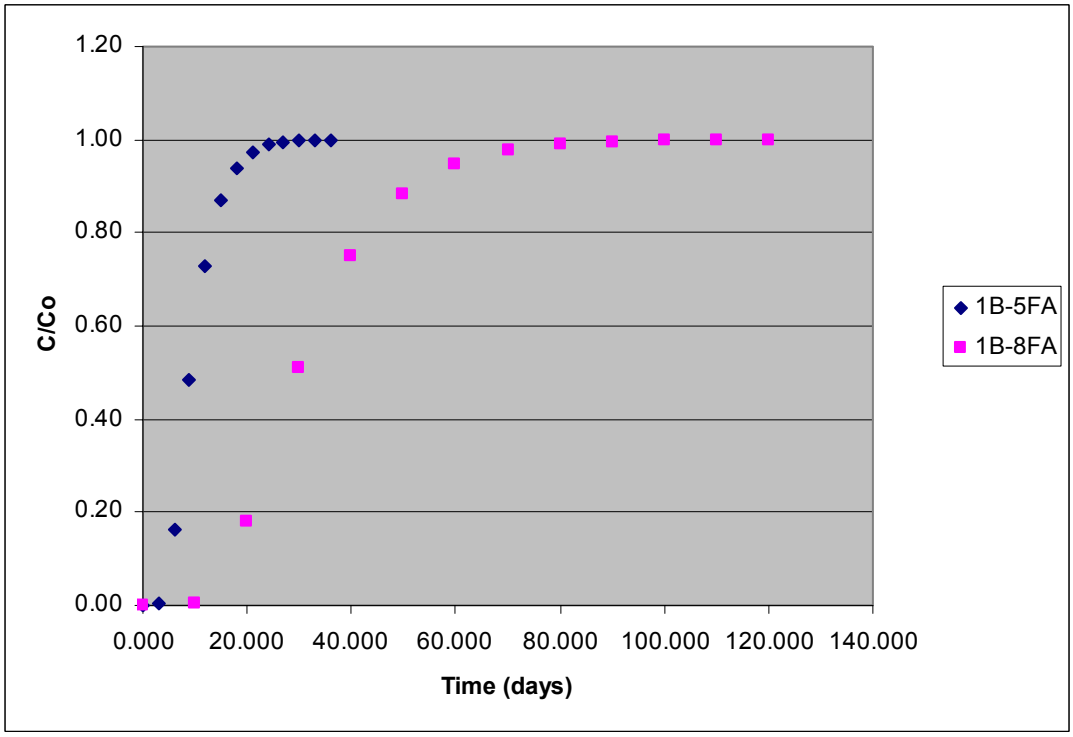

Fig 6.5(b) – Effect of Bentonite on Cadmium Adsorption

Table 6.6(a) – Adsorption of Chromium

1%BENTONITE & 5%FLY ASH

Time (days)	Time Factor	C/Co
0.100	0.004	0.00E+00
10.000	0.391	2.19E-02
20.000	0.782	3.63E-01
30.000	1.172	7.19E-01
40.000	1.563	8.93E-01
50.000	1.954	9.62E-01
60.000	2.345	9.87E-01
70.000	2.736	9.95E-01
80.000	3.127	9.98E-01
90.000	3.517	9.99E-01
100.000	3.908	1.00E+00
110.000	4.299	1.00E+00
120.000	4.690	1.00E+00

(b)

1% BENTONITE & 8% FLY ASH

Time (days)	Time Factor	C/Co
0.100	0.008	0.00E+00
4.000	0.330	7.09E-03
8.000	0.661	2.29E-01
12.000	0.991	5.77E-01
16.000	1.321	8.03E-01
20.000	1.651	9.15E-01
24.000	1.982	9.65E-01
28.000	2.312	9.85E-01
32.000	2.642	9.94E-01
36.000	2.973	9.98E-01
40.000	3.303	9.99E-01
44.000	3.633	1.00E+00
48.000	3.963	1.00E+00

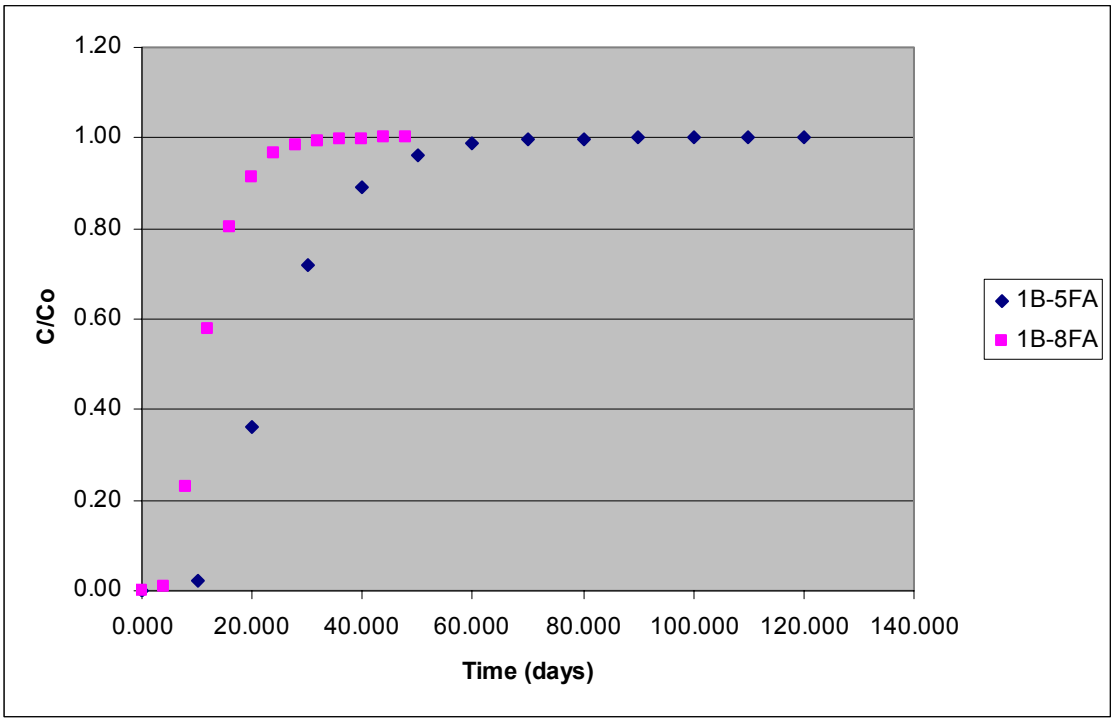

Fig 6.6 – Effect of Bentonite on Chromium Adsorption

Table 6.7(a) – Adsorption of Lead

1%BENTONITE & 5%FLY ASH		
Time (days)	**Time Factor**	**C/Co**
0.100	0.001	0.00E+00
25.000	0.288	2.42E-03
50.000	0.577	1.44E-01
75.000	0.865	4.53E-01
100.000	1.153	7.06E-01
125.000	1.441	8.54E-01
150.000	1.730	9.31E-01
175.000	2.018	9.68E-01
200.000	2.306	9.85E-01
225.000	2.595	9.93E-01
250.000	2.883	9.97E-01
275.000	3.171	9.99E-01
300.000	3.459	9.99E-01

(b)

1% BENTONITE & 8% FLY ASH		
Time (days)	**Time Factor**	**C/Co**
0.100	0.002	0.00E+00
15.000	0.370	1.55E-02
30.000	0.740	3.16E-01
45.000	1.110	6.75E-01
60.000	1.479	8.68E-01
75.000	1.849	9.50E-01
90.000	2.219	9.81E-01
105.000	2.589	9.93E-01
120.000	2.959	9.97E-01
135.000	3.329	9.99E-01
150.000	3.699	1.00E+00
165.000	4.069	1.00E+00
180.000	4.438	1.00E+00

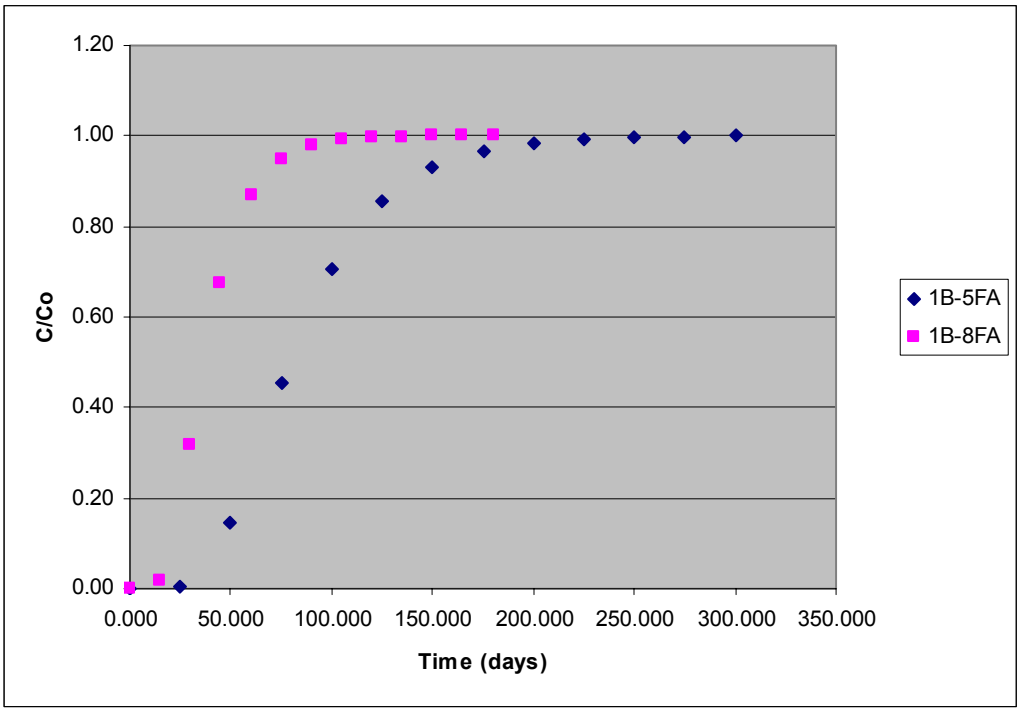

Fig 6.7 – Effect of Bentonite on Lead Adsorption

Table 6.8(a) – Adsorption of Zinc

Time (days)	1%BENTONITE & 5%FLY ASH Time Factor	C/Co
0.100	0.002	0.00E+00
20.000	0.305	3.86E-03
40.000	0.610	1.77E-01
60.000	0.915	5.05E-01
80.000	1.220	7.49E-01
100.000	1.525	8.82E-01
120.000	1.830	9.47E-01
140.000	2.136	9.76E-01
160.000	2.441	9.90E-01
180.000	2.746	9.95E-01
200.000	3.051	9.98E-01
220.000	3.356	9.99E-01
240.000	3.661	1.00E+00

(b)

Time (days)	1% BENTONITE & 8% FLY ASH Time Factor	C/Co
0.100	0.004	0.00E+00
10.000	0.361	1.32E-02
20.000	0.722	2.97E-01
30.000	1.084	6.55E-01
40.000	1.445	8.56E-01
50.000	1.806	9.43E-01
60.000	2.167	9.78E-01
70.000	2.528	9.92E-01
80.000	2.889	9.97E-01
90.000	3.251	9.99E-01
100.000	3.612	1.00E+00
110.000	3.973	1.00E+00
120.000	4.334	1.00E+00

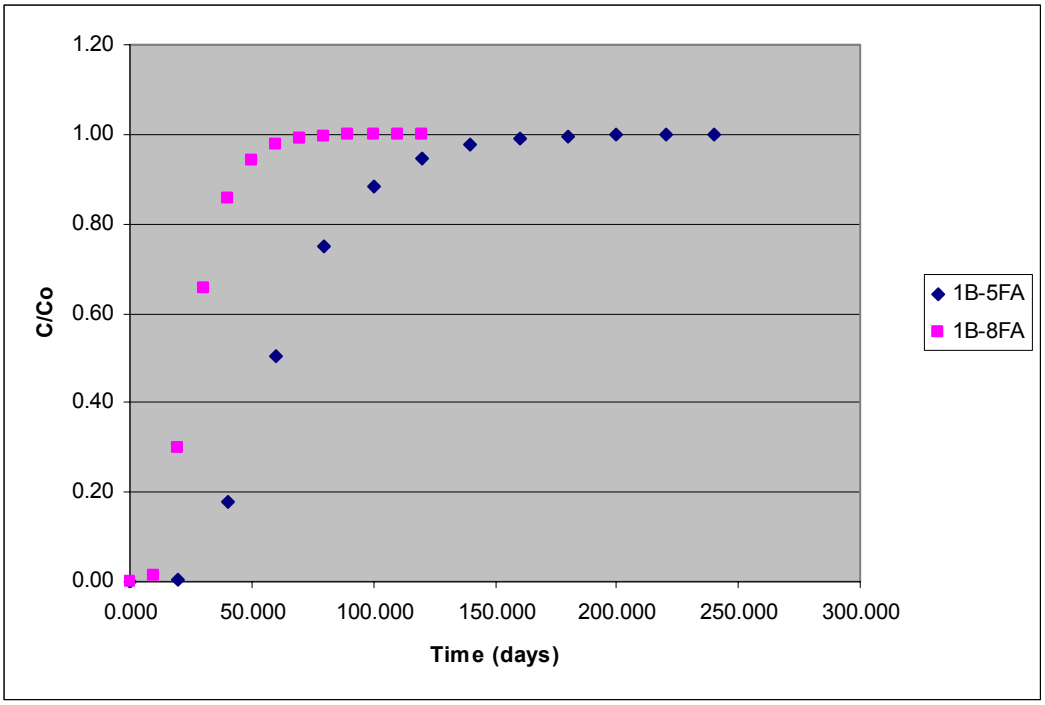

Fig 6.8 – Effect of Bentonite on Zinc Adsorption

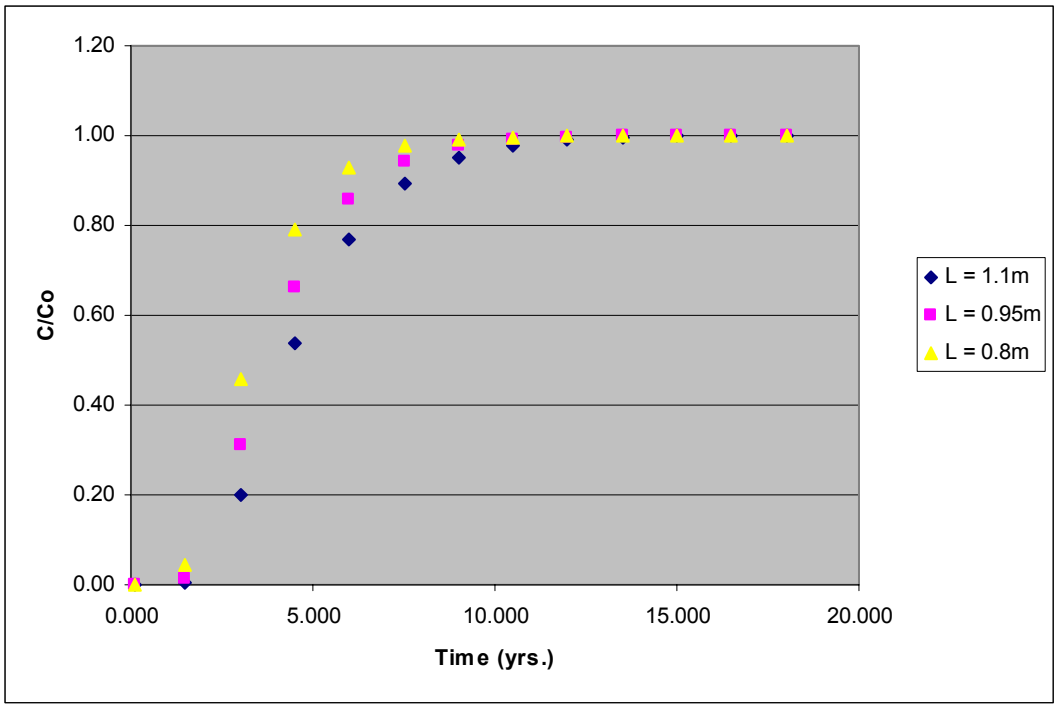

Fig. 6.9 – Effect of Barrier Thickness on Adsorption

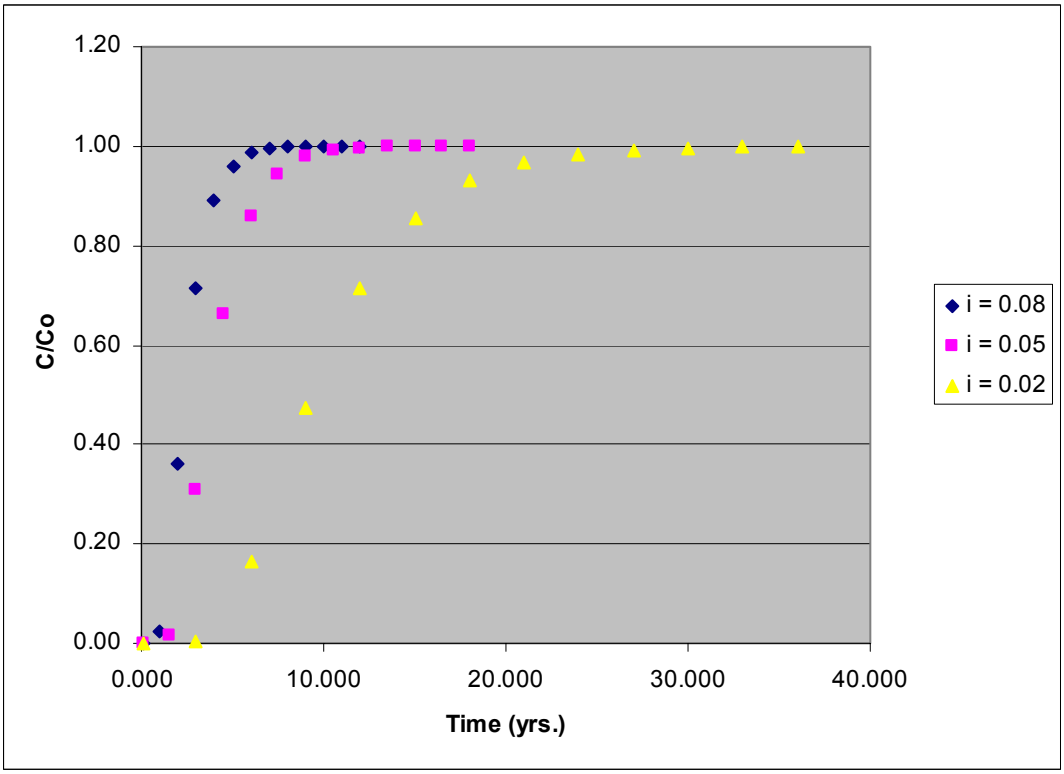

Fig 6.10 – Effect of Hydraulic Gradient on Adsorption

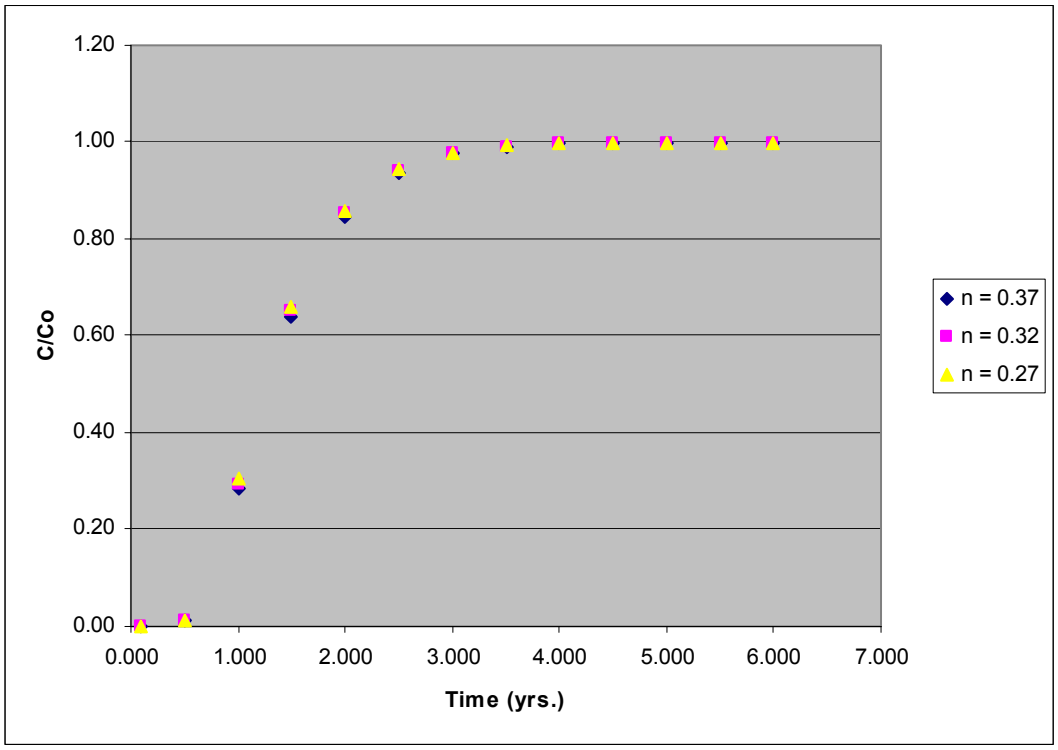

Fig 6.11 – Effect of Porosity on Adsorption

respective metal to pass through the barrier material, hence the breakthrough time would be reduced. The minimal variation in porosity values in the field that were used in the analysis might explain the lack of change in the breakthrough time.

6.1.4 Summary of Values

Table 6.9 shows a summary of the partitioning coefficient (K_d) values obtained for the metals tested using the different design mixes. Table 6.10 shows a summary of the estimated breakthrough time for the dredged sediment mixes. These values show that lead tends to be attenuated for the longest time before reaching its breakthrough time, hence the most threatening, followed by zinc, cadmium then chromium. These values compare well with the values obtained from the study by Moo-Young et al, (2000), in testing the adsorption characteristics of paper mill sludge and comparing it to the adsorption potential of materials in use today. As the values obtained in this study compare well with the adsorptive materials in use today, it can be said that dredged sediment barriers can serve as an effective containment as well as remediation system.

Table 6.9 – Summary of Partitioning Coefficient (K_d) Values

	Average Kd Values (L/kg)			
Mix Type	**Cadmium**	**Chromuim**	**Lead**	**Zinc**
1% BENTONITE+5% FLY ASH	12.00	9.00	35.00	26.00
1% BENTONITE+8% FLY ASH	13.00	16.00	58.00	39.00
1% BENTONITE	10.00	5.00	32.00	12.00
2% BENTONITE	8.00	6.00	41.00	19.00
3% BENTONITE	3.22	22.05	77.85	13.98

Table 6.10a – Summary of Estimated Breakthrough Times with Fly Ash Mixes

	Estimated Breakthrough Times (days)			
Mix Type	**Cadmium**	**Chromuim**	**Lead**	**Zinc**
1% BENTONITE+5% FLY ASH	110	90	275	220
1% BENTONITE+8% FLY ASH	36	40	135	100

Table 6.10b – Summary of Estimated Breakthrough Times with Bentonite Mixes

	Estimated Breakthrough Times (years)			
Mix Type	**Cadmium**	**Chromuim**	**Lead**	**Zinc**
1% BENTONITE	1	0.75	2.75	1.25
2% BENTONITE	2.25	1.75	10	5
3% BENTONITE	4.5	20	72	13.5

6.2 - SYNTHESIS

The mixes containing 1%, 2% and 3% bentonite were tested for their adsorption properties. The mix containing 1% bentonite was additionally modified by the addition of 5% and 8% fly ash by weight to test the effects of fly ash on adsorption. Typical field values for thickness of barrier, hydraulic gradient and effective porosity were varied to determine their effects on adsorption capacity. The metals tested include cadmium, chromium, lead and zinc.

The conclusions that can be drawn are as follows:

- For all metals tested, increased bentonite content lead to an increase in the adsorption capacity of the mix.
- For all the metals tested, increased fly ash content lead to a decrease in the adsorption capacity of the mix.
- A larger barrier thickness resulted in a longer breakthrough time, hence greater adsorption capacity.
- An increased hydraulic gradient resulted in a shorter breakthrough time, hence less adsorption capacity.
- An increased effective porosity lead to minimal to no change in the breakthrough time and adsorption capacity.
- It can be said that dredged sediment barriers can serve as an effective containment and remediation system under appropriate conditions.

SECTION 7

CONCLUSIONS AND RECOMMENDATIONS

7.1 SUMMARY AND CONCLUSIONS

The intention of the testing plan is to find an appropriate mix of sediment and bentonite that will be able to function as a vertical cut-off wall backfill material. The preliminary tests on the bentonite were carried out for screening purposes and to find an appropriate water content that will satisfy the desired viscosity range.

Bentonite was then added to the dredged sediment in ratios of 1%, 2% and 3% of the total dredged sediment weight. The preliminary tests were repeated for each of these mixes to determine applicable trends and at what percentages of bentonite, the viscosity of the mixture was still in the workable range. The 1% bentonite mix was additionally modified with the addition of 5% and 8% fly ash by weight. These mixtures were then subjected to API filter press tests (used as a rigid wall permeameter) to determine the effect these mixes would have on the hydraulic conductivity. Adsorption testing was also carried out on all the sediment mixes and aqueous solutions containing heavy metals to determine the adsorption capacities of the sediment mix. The metals used include cadmium, chromium, lead and zinc.

Detailed conclusions of the study can be found at the end of Sections 5 and 6. They are summarized as follows:

- The mud weight density of the dredged sediments was 10.77 kN/m³ (68.49 pcf) and this value falls within the range of bentonite slurries 10.06 - 12.58 kN/m3 (64-80 pcf).

- A suitable moisture content and viscosity of the dredged sediments can be attained that will make it usable in the mix design. It is workable and pumpable.
- Increasing bentonite content leads to an increase in mud weight density. This is helpful as the backfill material must be denser than the slurry in order to displace it in the construction process.
- An increase in bentonite content allows for decreased moisture content and correspondingly increased viscosity.
- Increasing bentonite content, to the percent tested (3%), resulted in a decrease in hydraulic conductivity. The optimum range to serve the purpose of use as a vertical cutoff wall ($1x10^{-7}$ to $1x10^{-8}$ cm/s) was near realized ($4.48x10^{-7}$ cm/s) at 3% bentonite and an applied pressure of 48.3kPa.
- Increasing the flyash content to the percent tested (8%), (with the base as dredged sediments and 1% bentonite by weight), increased the hydraulic conductivity.
- The filtrate loss results did not show any distinct trends. The filtrate loss on the bentonite specimens tested ranged from 2.27 mL/s to 0.04 mL/s. The filtrate loss on the fly ash specimens tested ranged from 14.29 mL/s to 1.54 mL/s.
- For all metals tested, increased bentonite content lead to an increase in the adsorption capacity of the mix.
- For all the metals tested, increased fly ash content lead to a decrease in the adsorption capacity of the mix. It was expected that the carbon content in the flyash would enhance the adsorption capacity of the mix. However, the increased hydraulic conductivity of the mix (which leads to lower adsorption capacity) may have outweighed the beneficial adsorptive effects of the carbon in fly ash.

- A larger barrier thickness resulted in a longer breakthrough time, hence greater adsorption capacity.
- An increased hydraulic gradient resulted in a shorter breakthrough time, hence less adsorption capacity.
- An increased effective porosity lead to minimal to no change in the breakthrough time and adsorption capacity.
- It can be said that dredged sediment barriers can serve as an effective inhibitor to the flow of ground water and serve as an effective containment and remediation system under appropriate conditions.

7.2 PRACTICAL APPLICATIONS

The dredged sediments can be manipulated to a moisture content, viscosity (32 - 40s) and density that satisfy the appropriate range of corresponding slurry values used in field practice today. The optimum mix design of the mixes tested was the mix of dredged sediments and 3% bentonite by weight which gave desirable properties and a hydraulic conductivity of 4.48×10^{-7} cm/s at an applied pressure of 48.3 kPa. Increased bentonite content decreases the hydraulic conductivity and increases the breakthrough time for the relevant metal, which is the desired effect in the performance of a vertical cut-off wall. Increasing fly ash content had the opposite expected effect, that is, it increases the hydraulic conductivity and decreases the breakthrough time for the relevant metal.

7.3 RECOMMENDATIONS FOR FUTURE RESEARCH

The main requirements of a good vertical barrier system are its ability to limit the flow of groundwater and contain and remove or attenuate contaminants. In performing the literature review relative to this topic, very few detailed technical studies were found to specifically address the beneficial re-use of dredged sediments. More studies need to be undertaken on this topic –(specifically their use as a vertical cut-off wall material)– in order to have a larger comparative base. More design mixes can be explored to determine possibly a more optimum design mix. In addition, the behavior of these walls in the field (as discussed in Chapter 4), should be explored further to better understand the stresses they experience in the field and, hence, lead to better design work in terms of applied pressures.

A great deal of dredging operations is carried out in harbors in industrial areas where the dredged sediments are already contaminanted with certain metals. The remediation and use of these sediments can be explored to see if their use is still more economical than the alternative of substituting natural soil resources. As dredged sediments are the by-product of the dredging industry, cost savings will be realized through its use. The use of dredged sediments is also appealing from an environmental and social point of view, since the beneficial reuse applications reduce landfilling costs.

REFERENCES

1. Palmero, Michael R.; Wilson, Joseph R., 1997, *Dredging and Management of Dredged Material, Geotechnical Special Publication No. 65, ASCE, 1-11*, Dredging State of the Practice: Corps of Engineers Perspective.

2. Snyder, Gary W.; Ponton, John R.; Deming, Peter W., 1997, *Dredging and Managemen*t *of Dredged Material, Geotechnical Special Publication No. 65, ASCE, 23-33*, Dredging with Environmental Controls – Baltimore, Maryland, Inner Harbor.

3. Daniel, David E., 1993, Geotechnical Practice for Waste Disposal.

4. Jones, K.W.; Stern, E.A.; Donato, K.; Clesceri, N.L., 1997, *Dredging and Management of Dredged Material, Geotechnical Special Publication No. 65, ASCE, 49-66*, Processing of NY/NJ Harbor Estuarine Dredged Material.

5. Vaghar, S.; Donovan, J.; Dobosz, K.; Clary, J., 1997, *Dredging and Management of Dredged Material, Geotechnical Special Publication No. 65, ASCE, 105 –121*, Treatment and Stabilization of Dredged Harbor Bottom Sediments, Central Artery/ Tunnel Project, Boston, Massachusetts.

6. Verhoeven, F.A.; de Jong, A.J.; Lubkin, P., 1988, *Hydraulic Fill Structures, Geotechnical special Publication No. 21, ASCE, 1033 - 1064,* The Essence of Soil Properties in Today's Dredging Technology.

7. Poindexter, Marian E.; Walker, James E. Jr., 1988, *Hydraulic Fill Structures, Geotechnical special Publication No. 21, ASCE, 676 – 692,* Dredged Fill Performance: South Blakeley Island.

8. Yamasaki, S.; Yasui, H.; Fukue, M., 1995, *Dredging, Remediation, and Containment of Contaminated Sediments, ASTM Special Technical Publication No. 1293, ASTM, 136 - 142,* Development of Solidification Technique for Dredged Sediments.

9. De Silva M.S.; Fleming G.; Smith P.G., 1991, *Water Science and Technology, v 24, no. 10, 9-17,* Alternative strategies for the disposal of UK estuarine dredgings.

10. Kayyal, M.K.; Hassen M., 1998, *ASCE Journal of Geotechnical and Geoenvironmental Engineering, v 124, no. 11,* Case Study of Slope Failures at Spilmans Island.

11. Krizek, R.J.; Casteleiro M.; Edil, T.B., 1977, *Journal of the Geotechnical Engineering Division, v 13, no. 12, 1399-1418,* Dessication and Consolidation of Dredged Materials.

12. Evans J.C., 1994, *Hydraulic Conductivity and Waste Contaminant Transport in Soil, ASTM STP 1142,* Daniel, David E; Trautwein, Stephen J., Eds., Hydraulic Conductivity of Vertical Cutoff Walls.

13. D' Appolonia, David J., 1980, *Journal of the Geotechnical Engineering Division, ASCE, 399-417*, Soil-Bentonite Slurry Trench Cutoffs.

14. Rad N. S.; Bachus R.C.; Jacobson B.D., 1995, *Dredging, Remediation, and Containment of Contaminated Sediments, ASTM Special Technical Publication, no. 1293, 239-251,* Soil-Bentonite Design Mix for Slurry Cutoff Walls Used as Containment Barriers.

15. Martinenghi L., 1995, *Dredging, Remediation, and Containment of Contaminated Sediments, ASTM Special Technical Publication, no. 1293, 271-286,* Design and Performance Verification of a Soil-Bentonite Slurry Wall for the Hydraulic Isolation of Contaminated Sites.

16. Zamojski L.D.; Perkins S.W.; Reinknect D., , Design and Construction Evaluation of a Slurry Wall at FLR Landfill Superfund Site.

17. Moo-Young H.; Ochola C.; Gallagher M., 2000, *Environmental geotechnics : proceedings of sessions of Geo-Denver 2000, ASCE, no. 105, 168 p.*, Laboratory Determination of Slurry Wall Construction with Paper Clay.

18. Suthersan S.S., 1997, Remediation Engineering Design Concepts.

19. Filz G. M.; Henry L.B.; Heslin G.M.; Davidson R.R., 2001, *Geotechnical Testing Journal, GTJODJ, v 24, no. 1, 61-71*, Determining Hydraulic Conductivity of Soil-Bentonite Using the API Filter Press.

20. Kutay M.E.; Aydilek A.H., 2003, *Environmental Geotechnics Report # 03-2, University of Maryland, College Park, MD, 130p.*, Hydraulic Conductivity of Geotextile Containers Confining Geomaterials.

21. Abichou T.; Benson C. H.; Edil T.B.; Freber B.W., 1998, *Recycled Materials in Geotechnical Applications, Geotechnical Special Publication No. 79, ASCE, 86-99,* Using Waste Foundry Sand for Hydraulic Barriers.

22. Abichou T.; Benson C. H.; Edil T.B., 1998, *Recycled Materials in Geotechnical Applications, Geotechnical Special Publication No. 79, ASCE, 210-223,* Database on Beneficial Reuse of Foundry By-Products.

23. Wilson J., 1999, *WisDOT Study # 99-05, 29p.,* Flowable Fill as Backfill for Bridge Abutments.

24. Bhat, S.T.; Lovell, C.W., 1997, *Transportation Research Record No. 1589, 26-28,* Mix Design for Flowable Fill.

25. Sayeed, J.; Lovell, C.W., 1995, *Transportation Research Record No. 1486, 109-113,* Use of Waste Foundry Sands in Civil Engineering.

26. Xanthakos P. P.; Abramson L. W.; Bruce D. A., 1994, Ground Control and Improvement.

27. Evans J. C.; Costa M. J.; Cooley B., 2000, *Geoenvironment 2000, 1173-1191,* The State-of-Stress in Soil Bentonite Slurry Trench Cutoff Walls.

28. Gill S. A., 1980, *Journal of the Construction Division, ASCE, v. 106, no. CO2., 155-167,* Applications of Slurry Walls in Civil Engineering.

29. Britto A. M.; Kusakabe O., 1984, *Canadian Geotechnical Journal, v. 21, no. 2*, On the Stability of Supported Excavations.

30. Nash K. L., 1974, *Journal of the Construction Division, ASCE, v. 100, No. CO4., 533-541,* Stability of Trenches Filled with Fluids.

31. Wong, G. C. Y., 1984, *Journal of Geotechnical Engineering, v. 110, no. 11, 1577-1590*, Stability Analysis of Slurry Trenches.

32. Tsai, J.; Chang C.; Jou L., 1998, *Journal of Geotechnical and Geoenvironmental Engineering, v. 124, no. 11*, Lateral Extrusion Analysis of Sandwiched Weak Soil in Slurry Trench.

Using Bioaugmentation to Improve the Biodegradation of Chlorinated Compounds in Wetlands -- Summer Fellowship

Basic Information

Title:	Using Bioaugmentation to Improve the Biodegradation of Chlorinated Compounds in Wetlands -- Summer Fellowship
Project Number:	2004MD68B
Start Date:	6/1/2004
End Date:	10/1/2004
Funding Source:	104B
Congressional District:	5th District of Maryland
Research Category:	None
Focus Category:	Toxic Substances, Wetlands, Treatment
Descriptors:	None
Principal Investigators:	Allen Davis, Philip Kearney

Publication

Evaluation of the Use of Bioaugmentation and Biostimulation to Improve the Degradation of Chlorinated Compounds in Natural Freshwater Tidal Wetlands

Emily N. Devillier

2004 Maryland Water Resources Research Center Summer Assistantship Report

Contamination of groundwater with chlorinated solvents, specifically, 1,1,2,2-tetrachloroethane (TeCA), tetrachloroethene (PCE), trichloroethene (TCE), trichloromethane (chloroform, CF), and carbon tetrachloride (CT), is a serious problem at Aberdeen Proving Grounds (APG). Of particular concern are numerous seep sites at APG where groundwater is presumably discharging to the surface water at a relatively high rate and, more importantly, significant levels of the above parent chlorinated compounds and/or daughter degradation products are detected in the surface waters.

The objectives for Summer 2004 were to test the hypothesis that contaminant-degrading bacteria are absent from, or present in insufficient numbers, at seeps, and to evaluate the use of bioaugmentation to improve the degradation of chlorinated compounds. The culture used for the bioaugmentation experiment, WBC2, was obtained from another West Branch Creek site where successful degradation has been observed. Reductive dehalogenation can only be sustained if sufficient electron donors are present. In addition, in past studies, it has been shown that chlorinated compounds, such as TeCA and TCE, degrade more quickly in the presence of methanogenic conditions, rather than under nitrate or sulfate-reducing conditions. Therefore, in addition to bioaugmentation, it was also hypothesized that biostimulation through the addition of limiting growth substrates, i.e., electron donors, might also be necessary to promote biodegradation of the chlorinated solvents at the seep sites.

A preliminary methane experiment, conducted for 23 days, evaluated the availability of methanogenic substrates in the unamended seep site sediment and groundwater. The results showed that low concentrations of methane (less than 0.05 uM) were present, suggesting that the levels of endogenous degradable substrates were low and addition of electron donors to the seep site samples would be needed to sustain reductive dechlorination. Therefore, the bioaugmentation experiments included treatments that were designed to evaluate the effect of exogenous electron donors on chlorinated solvent biodegradation. Ethanol and lactate were the exogenous donors selected for use in various bioaugmentation experiment treatments because previous studies conducted with batch and column studies have shown that these compounds are effective at sustaining reductive dechlorination of the parent compounds and potential daughter products in APG sediments.

The effectiveness of bioaugmentation and biostimulation at enhancing chlorinated solvent biodegradation at a single seep site, 3-4W, is being evaluated in two experiments, which are referred to as the small-scale and large-scale experiments and are described below.

Small-Scale Experiment

In the small-scale microcosm experiment, the concentrations of the parent chlorinated solvents and their daughter products were monitored using gas chromatographic analysis of headspace samples. This precluded the use of TeCA, which is much less volatile compared to the other parent chlorinated compounds, but it meant that the same microcosms could be repeatedly sampled at each sampling interval and limited the number of microcosms that had to be prepared. Four anaerobic microcosms were prepared in serum bottles. Each contained a slurry of sediment collected from site 3-4W and groundwater and a headspace of N_2/CO_2. Since PCE, TCE, CT, and CF are soluble in ethanol, an ethanol stock solution of PCE, TCE, CT, and CF was added to each microcosm to provide the appropriate concentration of ethanol (as an electron donor) and chlorinated solvents. Lactate was also added to each microcosm. To two of the microcosms, the bacterial culture, WBC2, was added, in addition to the electron donors. Two water controls were also prepared to monitor abiotic losses. The results of this experiment collected to date appear in Figures 1 and 2.

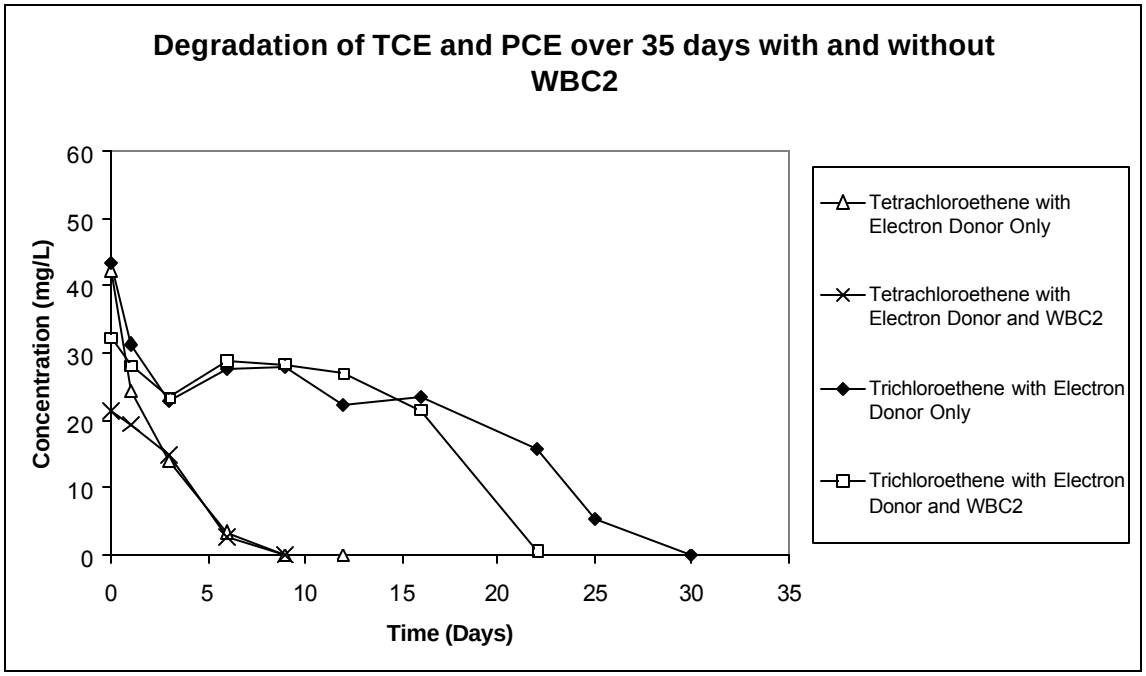

Figure 1. Concentrations of TCE and PCE in seep site (3-4W) sediment slurries with and without addition of WBC2 culture. Each data point represents the average concentration for the sampling day.

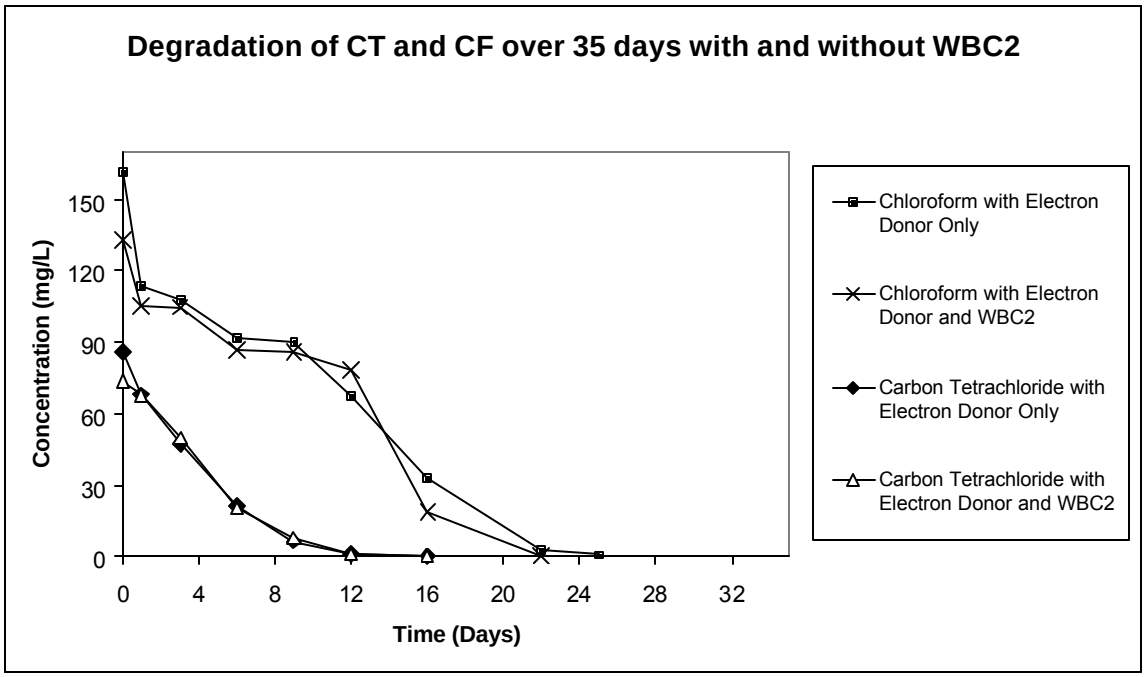

Figure 2. Concentrations of CF and CT in seep site (3-4W) sediment slurries with and without addition of WBC2 culture. Each data point represents the average concentration for the sampling day.

In particular, removal of TCE appeared to be significantly enhanced by the addition of WBC2 (Fig.1). CF in WBC2 augmented samples also appeared to occur at slightly faster rates compared to unaugmented samples (Fig. 2). CT and PCE displayed no change in its degradation rate between augmented and unaugmented samples. Additional analyses will evaluate the effect of WBC2 on the accumulation and biodegradation of daughter products, in order to determine whether bioaugmentation or biostimulation improves the complete degradation of the parent compounds.

At the conclusion of the experiment, the community DNA in each microcosm will be extracted and analyzed using a fingerprinting technique, to observe significant differences in the structures of the bacterial communities due to the addition of WBC2 and/or the biodegradation of the chlorinated solvents.

A larger-scale experiment was also conducted in order to evaluate the effectiveness of biostimulation, with and without bioaugmentation, at enhancing the removal of TeCA, as well as the other parent chlorinated solvents, in the seep sediment.

Large-Scale Experiment

Because of the need to analyze TeCA in the large-scale experiment, it differed in several respects compared to the small-scale experiment. Specifically, the chlorinated solvents had to be extracted from the sediment slurry before being quantified using gas chromatography. This meant that individual microcosms could not be repeatedly sampled, and, instead, duplicate microcosms were sacrificed at each sampling event. All

microcosms were amended with a mixture of chlorinated solvents. One set of viable microcosms did not receive any other amendments. In addition to the chlorinated solvents, three other sets of viable microcosms were amended with electron donors only, WBC2 culture only, or electron donors plus WBC2 culture. Several different types of abiotic controls were also prepared for sacrificing at different time points. Therefore, a very large number of microcosms were established for this experiment.

In addition to observing the removal of chlorinated compounds, other tests are being done to observe the changes in the microcosm biogeochemistry over time. A colorimetric method using bipyridine is used to monitor iron reduction by detecting the change in ferrous iron concentration. The amount of methane produced in the microcosms is being tested using gas chromatography. At the conclusion of this experiment, we should have a better understanding of how biostimulation through the addition of electron donors and bioaugmentation with the enrichment culture affects biodegradation of the chlorinated solvents in the seep sediment.

Information Transfer Program

Student Support

Student Support					
Category	**Section 104 Base Grant**	**Section 104 RCGP Award**	**NIWR-USGS Internship**	**Supplemental Awards**	**Total**
Undergraduate	2	0	0	0	2
Masters	1	0	1	0	2
Ph.D.	2	0	0	0	2
Post-Doc.	0	0	0	0	0
Total	5	0	1	0	6

Notable Awards and Achievements

Publications from Prior Projects

1. 2002MD4B ("Sustainable Oil and Grease Removal from Stormwater Runoff Hotspots using Bioretention ") - Articles in Refereed Scientific Journals - Hong, E., Seagren, E.A., and Davis, A.P. Sustainable Oil and Grease Removal from Synthetic Storm Water Runoff Using Bench-Scale Bioretention Studies, Water Environ. Res., in press